Primary Metabolic Chemistry

A thesis submitted in
partial fulfilment of the
requirements for the degree of

Doctor of Philosophy in Chemistry

at the

University of Canterbury

by

Susie J. Meade

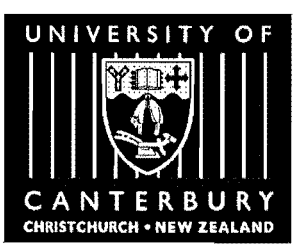

University of Canterbury

Christchurch, New Zealand

1999

In science the credit goes to the man who convinces the world,
not to the man to whom the idea first occurs.

F. Darwin 1914

Table of contents

Acknowledgments

First, I would like to thank Mum and Dad for encouraging me to leave country life for university and for welcoming me home when it all got too much.

I'd like to thank all those people who helped make my time in the Chemistry Department an experience to remember, particularly those who have "shared" glassware, solvents and lab-space with me.

Thanks also goes to my supervisor Dr Andy Pratt for his enthusiasm, which convinced me to begin this endeavour and for his continuing help throughout the journey that is my Ph.D.

Thank you to all the technical staff and academic staff in the Chemistry department without whose help this project would not have been possible. In particular, I would like to acknowledge Wayne for his friendship and speedy electrical repairs, Rewi for his patience when providing NMR help, John Davis for fixing my computer problems, Bruce Clark for managing to get mass spectometry results on some very nasty samples, John Blunt for being understanding no matter how many times I phoned him at home with NMR problems and "the glassblowers" (Rob and Dave) for their expertise in dealing with my sealed tube reactions. .

Thankyou Sian, Juliet, Peter, Phil, Rachel, Elizabeth, Alison (aka "The Dwarf"), Andy, Wallace and Gromit for being there in times of crisis and generally for your continuing friendship.

The biggest thankyou goes to Richard for his help and support throughout my Ph.D., including his jobs as consultant inorganic chemist, proof reader and financial provider.

Last but not least, I'd like to thank junior for being considerate enough to allow me to submit before choosing to make an appearance.

Abstract

Thioesters and acyl phosphates are important metabolites throughout the biosphere. This may imply that they were involved in prebiotic chemistry. The study of the reactivity of thioesters and acyl phosphates may therefore provide some insights into the possible roles for these molecules in prebiotic chemistry.

The work described in this thesis demonstrates that acetyl phosphate and inorganic phosphate react to form pyrophosphate in the presence of salts of some divalent metals. Divalent metal ions and nitrogen containing compounds act in synergy to promote pyrophosphate formation in some cases. Ferrous salts were much more efficient at promoting the formation of pyrophosphate than similar reactions containing magnesium ions. Addition of pyridine, or a variety of other nitrogen containing compounds, did not enhance the pyrophosphate yield. The promotion of pyrophosphate formation at near neutral pH by ubiquitous metal salts is considered to be a feasible route for prebiotic production of pyrophosphate.

One chemoautotrophic origin of life theory concentrates on the oxidative formation of pyrite (FeS_2) from ferrous sulfide and hydrogen as a possible source of prebiotic reductive power. *N*-Phenyl acetamide can be prepared from mercaptoacetic acid and aniline in water using FeS/H_2S as a reagent system. We have established that one possible intermediate, *N*-phenyl mercaptoacetamide does react to give the product, and that this reaction is fast.

Ferrous ions were observed to promote the formation of *N*-acetyl alanine from alanine and thioacetic acid. Zinc and cadmium ions on the other hand, promote the hydrolysis of thioacetic acid to acetic acid in preference to the *N*-acylation reaction. Both ferrous ions and ferrocyanide ions were observed to promote the peptide bond formation between protected amino acid derivatives.

The results described in this thesis are consistent with the proposal that iron chemistry may have been important in prebiotic chemistry.

Abbreviations

AcPi	acetyl phosphate
ADP	adenosine 5'-diphosphate
AMP	adenosine 5'-monophosphate
ATP	adenosine 5'-triphosphate
bs	broad singlet
d	doublet
DCC	1,3-dicyclohexylcarbodiimde
DMAP	4-dimethylaminopyridine
DMF	*N,N*-dimethylformamide
EDCI	1-(3-dimethylaminopropyl)-3ethylcarbodiimide
EDTA	ethylenediaminetetraacetic acid
GDP	guanosine 5'-diphosphate
GTP	guanosine 5'-triphosphate
HEPES	4-(*N*-2-hydroxyethyl)-1-piperazine-*N*-2'-ethane-sulphonic acid
HOBT	1-hydroxybenzotriazole hydrate
HPLC	high pressure liquid chromatography
Im	imidazole
ImPi	*N*-phosphoryl imidazole
kg	kilogram
Ksp	Solubility product
M	moles per litre

MES	4-(*N*-morpholine)ethane-sulphonic acid
min	minute
mL	millilitre
μL	microlitre
mM	millimole per litre
μm	micrometre
mmol	millimole
μmol	micromole
mol	mole
mRNA	messenger RNA
mV	millivolt
nm	nanometre
NMR	nuclear magnetic resonance
Nu	nucleophile
OFN	oxygen free nitrogen
Pi	inorganic phosphate
PIPES	1,4-piperazine-*N*,*N'*-bis(2-ethanesulphonic acid)
PPi	pyrophosphate
ppm	parts per million
PPPi	tripolyphosphate
Pyr	pyridine
r.p.m.	revolutions per minute
s	singlet
sec	second
t	triplet

TFA	trifloroacetic acid
THF	tetrahydrofuran
tRNA	transport RNA
UV	ultraviolet
V	volt
v/v	volume per volume
w/v	weight per volume
Z	benzyloxycarbonyl

Chapter 1

Introduction

1.1 The origins of life

The origin of life on earth has been the subject of much discussion in both the scientific and non-scientific communities. Various theories have been put forward, ranging from creation and spontaneous generation, to evolution of life in a series of small steps. This thesis will address only scientifically testable conjectures. The concept of creation, in particular, does not lend itself to scientific examination and will not be discussed further. Early experiments seemed to support the theory of spontaneous generation: for example, in the mid 17th century, Van Helmont, a Flemish physician reported that mice could be generated from wheat grains and a sweat-stained shirt[1]: however as scientific experimentation became more rigorous this theory was discredited. The controversy of spontaneous generation continued until 1864 when Pasteur described experiments using nutrient broth in open and closed jars, in which microbial life grew in the open jar but not in the closed jar[1,2]. These and later experiments led to the widespread acceptance

that current life on earth is perpetuated exclusively by replication and evolution of existing organisms. This still leaves open the question of the emergence of the original forms of life on earth. To shed light on this issue it is necessary to establish information about the history of the earth and of life and possible connections with contemporary biochemistry.

1.1.1 Geological records

Modern theories of the origins of life are widely varied, not least because the conditions under which life emerged are far from certain. Evidence about past conditions on earth is provided by fossil and rock deposits. The date of the formation of the earth gives us an upper limit to the time taken for life on earth to evolve. Radiometric dating estimates the formation of the earth and solar system to have occurred 4.6 billion years ago[3]. For the first billion years of its existence the earth is thought to have undergone a heavy bombardment by solar matter[4]. The oldest known unmodified sedimentary rocks are estimated to be ~3.45 billion years old[5]. Older sedimentary rocks, originating between 3.8–4 billion years ago, have been found but they have been heavily modified during their geological history. It is to these rocks, that we have to turn to look for the oldest evidence of life on earth.

1.1.2 Fossils and the tree of life

Fossils of primitive life-forms have provided much evidence for the timescale of evolution. Cell-like structures have been found in ancient fossils. The age of these fossils is estimated by the geological record provided by the rock layers above and below the fossils. At best this type of research can only provide a record of the first detected occurrence of a type of organism

Some of the most ancient fossils widely accepted as records of life on earth are of cyanobacteria-like organisms found in sedimentary rock formations in Western Australia. These fossils have been dated at 3.5 billion years old[6,7,8]. Objects which have been interpreted as fossil micro-organisms have been found in Greenland rocks which are 3.8–4 billion years old but the rocks are too metamorphosed for universal acceptance of their biogenic origin[9].

Whilst more evidence must be accumulated about early life on earth, it is clear that life emerged within the first billion years of the earth's history. Organisms present today are likely to be vastly different from the earliest organisms, as they have had a long time to develop. The details of the biochemical pathways employed by cells may also have evolved significantly, but some of the basics are likely to have remained relatively unchanged. All known life-forms are related to common ancestors based on lipid-encapsulated cells with proteins playing a key role in structure and catalysis and nucleic acids being associated with genetic information. In addition, all life carries out a range

of metabolic reactions on small molecules such as amino acids, and the common ancestor may have been no exception.

The widespread use of linear macromolecules (proteins and nucleic acids) in biochemistry provides a molecular equivalent of a fossil record. Comparative sequencing of nucleic acids and the proteins they code for has been used to infer relationships between different life-forms. This technique assumes that sequence similarities in genes or proteins of different organisms reflects some common ancestry. The basis of this technique is widely accepted, but the details of the tree-like branching structure, a phylogenetic tree, are still being developed as more sequence information becomes available. It is, however, generally agreed that all life on earth today evolved from a common unicellular ancestor[9].

The biochemistry of cells today may contain clues to the initial biochemical reactions of primitive cells. The chemistry that led to the evolution of life is likely to be a lot more primitive and simple than the complex array of enzyme catalysed reactions known to occur in cells today. Today we can observe a common core of metabolism in cells, for example, the citric acid cycle, which, in some form, is a ubiquitous feature of metabolism. Likewise ATP, and related polyphosphates are commonly used to drive chemical reactions[10]. This core metabolism provides the foundation for all life and is likely to be more ancient than other cellular reactions. Therefore there is much interest in how these core metabolic processes could have evolved.

1.2 Sources of Organic Compounds

The current theories of the origins of life differ widely in the conditions they assume to have been prevalent when life was getting started. However, it is accepted that for life to come into being, "essential" compounds, such as amino acids, must have been available. The first organisms could either have made use of available chemicals, such as amino acids, or made these chemicals themselves. That is, the origin of life could have been either heterotrophic or autotrophic. In the succeeding discussion of heterotrophy and autotrophy, we will focus on amino acids as a representative example of essential organic metabolites.

1.2.1 Heterotrophic Origin of Life

A heterotrophic origin of life implies a source of complex organic molecules as a feedstock for the original organisms. There are two possible sources of essential compounds such as amino acids: extraterrestrial formation; or terrestrial formation.

Extraterrestrial formation of amino acids

Amino acids and other metabolic building blocks may have been deposited on the earth by the impact of extraterrestrial objects, such as comets and meteorites. Although the environment on earth is known to have changed radically since the evolution of life the interstellar environment is thought to have remained essentially unchanged. Therefore

it is presumed that much can be inferred about the organic compounds that may have been delivered to the Earth's surface during the period when life was beginning from studying the composition of extra-terrestrial bodies. Information can be gleaned by examining meteorites that are found on earth. Radioastronomy has also been used to identify molecules present in the interstellar medium. Almost one hundred different molecules have detected, ranging from simple diatomic molecules such as H_2, CN and CO to polyatomic molecules like HCN, NH_3, CH_3OH and CH_3CN. A number of unsaturated organic molecules and charged species have also been identified[11]. Some of the molecules of possible relevance to the origin of life are listed in *Table 1.1*.

H_2	CO	H_2CCHCN
CH_4	CH_2O	H_2CNH
HCN	NH_3	H_3CNH_2
HCO_2H	HCCCN	H_3CCN

Table 1.1 A range of molecules observed by radioastronomy

The remains of many meteorites can be found on earth. Some meteorites (particularly the carbonaceous chondrites) have been found to contain ~2-4% total carbon content[12]; the Murchison meteorite, that crashed into the Murchison Desert, Australia, in 1969, is a typical example. With efforts made to minimise potential contamination, it was found that approximately 2% of this meteorite was carbon. 10-20% of this total carbon was present as organic compounds. The types and the concentrations of compounds found are shown in *Table 1.2*[11]. As can been seen, amino acids are among the compounds detected in these and other meteorite samples.

Compound	Concentration (ppm)
Aliphatic hydrocarbons	12 – 35
Aromatic hydrocarbons	15 - 28
Monocarboxylic acids ($C_2 - C_8$)	~ 170
Aldehydes ($C_2 - C_4$)	> 10
Ketones ($C_3 - C_5$)	~ 10
Alcohols ($C_1 - C_4$)	> 10
Amino acids	10 - 20
Amines ($C_1 - C_4$)	~ 2
Ureas	~ 20
N-Heterocycles (Purines, pyrimidines etc)	> 2

Table 1.2 Type of organic compounds detected in Murchison Meteorite

By extrapolating from this data it has been estimated that comets and meteorites could have delivered up to 10^6-10^7 kg of intact organic compounds per year, 4.5 billion years ago[13,14]. The amounts would have declined slowly after this time, so that there may have been significantly less than this amount of material arriving by the time that the conditions on earth were such that life could have evolved.

It is possible that extraterrestrial sources of amino acids were viable for the evolution of life. However, this theory has its problems. The flux of organic compounds falling to the earth's surface was probably not constant. The stocks of amino acids must be

constantly replenished as a variety of processes, including degradation by ultraviolet light, would have resulted in degradation of organic molecules. This would greatly limit the development and multiplication of organisms, at least until they developed the ability to make amino acids for themselves.

Terrestrial formation of amino acids

The alternative to extraterrestrial sources of organic compounds is terrestrial synthesis of amino acids. Two main phases were available in which chemical reactions could occur, the atmosphere and water. The viability of these two phases for synthesis of amino acids is very dependent on the environment of the early Earth.

It was thought at one time that the primitive Earth had an atmosphere of mainly methane and ammonia and hydrogen. This was based on observation of the high cosmic abundance of hydrogen, the composition of the atmospheres of Jupiter and Saturn, and the expectation that in an atmosphere high in hydrogen, the carbon and nitrogen that could be a possible source of organic molecules would exist as methane and ammonia[15].

Using reactants consistent with the prevailing views of the prebiotic atmosphere at that time, Miller conducted an experiment to assess the viability of amino acid synthesis[16]. An electrical discharge was passed through vapour containing methane, ammonia and hydrogen over a solution of boiling water. The electrical discharges were meant to mimic lightning. A range of amino acids were detected in the reaction mixture[16].

It is thought that the amino acids were not formed directly in the electrical discharge but they were produced as the result of solution chemistry of molecules produced in the electrical discharge such as hydrogen cyanide and aldehydes[17]. A possible mechanism for the formation of amino acids in Miller's experiments is shown in *Figure 1.1*[18,19]. It has since been shown that hydrolysis of hydrogen cyanide oligomers produces glycine and alanine[18]. Hydrogen cyanide is observed in volcanic emissions and in the interstellar medium.

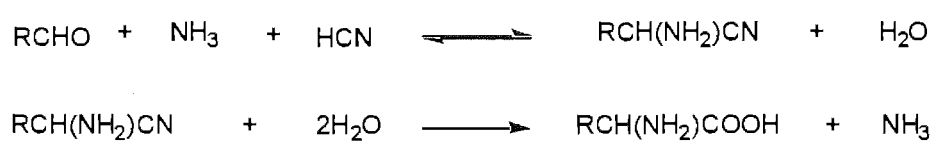

Figure 1.1 Possible mechanism for amino acid synthesis in Miller's experiment

However, it is now thought that cosmic abundances of elements, as used in the above theory and Miller's experiment, may not represent the composition of the atmosphere of the early earth[4,20,21]. It is now considered likely that volatile elements such as hydrogen would be depleted in the early, high temperature, stages of the Earth's formation. Therefore the composition of the atmosphere was probably significantly lower in ammonia and methane than the conditions used for Miller's experiments. The atmosphere was likely to have been formed mainly from volcanic gases[22]. Modern volcanic gases are low in hydrogen and ammonia.

Currently the most widely held view of the composition of the prebiotic atmosphere is that it was a mixture of nitrogen, carbon dioxide and water, with a little carbon monoxide and hydrogen[4,23,24,25]. Geological evidence has been used to infer that atmospheric oxygen levels were low until after life evolved. Banded iron formations were formed up until about 2 billion years ago but not after[4,26]. These formations are indicative of the availability of large amounts of ferric ions at the point of deposition; deposition of banded iron formations is thought to require an anoxic deep ocean. This is inconsistent with the presence of high levels of oxygen in the atmosphere. Therefore it is believed that oxygen built up in the atmosphere after life developed, as a result of the evolution of photosynthetic bacteria.

Amino acids may have been produced in an aqueous environment. Water is essential to all life and is abundant on the earth's surface. Therefore water may well have been intimately involved in the environment in which life evolved. Water is only liquid between the temperatures of 0°C and 100°C at one atmosphere pressure. It is unlikely that the temperature in the bulk of the oceans was at the extremes of this range.

Prebiotic soup

Whether the abiotic synthesis of amino acids was extraterrestrial or terrestrial, their presence in the "prebiotic soup" is probable. The concentrations of organic compounds, in particular amino acids in this soup are a subject of much conjecture. The concentrations may have been significant, provided the destructive processes did not overwhelm the rates of formation. The conditions in the prebiotic soup are uncertain. A variety of conjectures have been made for these conditions, ranging from small warm

ponds with relatively high concentrations of organic compounds and high levels of solar radiation to vast oceans containing organic compounds at very low concentrations. Whatever the situation, it is clear that life had to evolve the capability to catalyse the formation of organic compounds from inorganic materials. The nature of such chemistry will now be considered.

1.2.2 Autotrophic Origins of Life

The heterotrophic evolution of life with its implied primordial soup is not the only option; the origin of life could have been autotrophic. Autotrophs live off mineral resources, they build up small organic molecules which they further assemble into macromolecules. Autotrophs can use carbon dioxide as their carbon source from which they construct all their organic compounds. Autotrophic organisms can also assimilate inorganic nitrogen species, such as nitrate or molecular nitrogen, to generate nitrogen containing compounds.

An autotrophic origin of life requires the development of chemistry for the synthesis of organic compounds from inorganic carbon compounds, notably carbon monoxide or carbon dioxide. Such groups of chemical reactions could mimic catalytic pathways of biological carbon fixation such as the reductive citric acid cycle found in extant organisms. These pathways are made up of simple chemical reactions which may have originated with more primitive catalysts than enzymes. Chemical pathways of this kind may have provided a means by which the first autotrophic organisms could synthesise

complex molecules. Autotrophic organisms may therefore have retained these chemical cycles but modified them over time to form the biochemical cycles which are now found in cells.

A chemoautotrophic theory of the evolution of life has been put forward by Wächtershäuser. In a chemoautotrophic origin of life the starting material for organic compounds is carbon dioxide or some other inorganic one-carbon equivalent. This essentially means that a reductive carbon fixation process is required. One such pathway from contemporary biochemistry, which has been examined as a possible prebiotic process, is anaerobic carbon fixation *via* the acetyl Co-A synthetase pathway (*Figure 1.2*)[27].

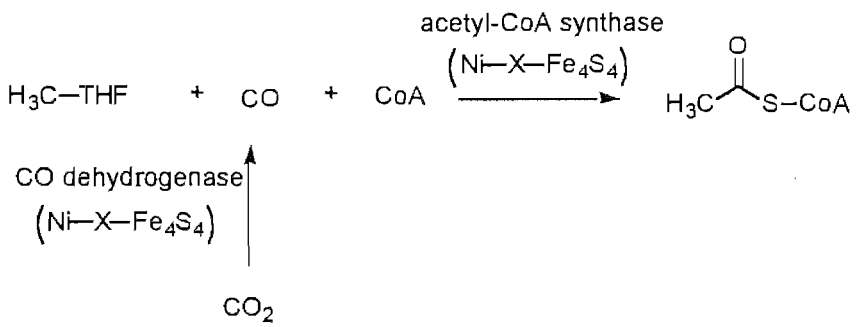

Figure 1.2 *Synthesis of acetyl Co-A in autotrophic anaerobes*

The active site of the acetyl CoA synthetase enzyme is based around a nickel-iron-sulfur cluster. A plausible prebiotic mimic of the acyl-CoA synthetase reaction was discovered by Huber and Wächtershäuser. A carboxylic acid and a thioester can be produced from a mixture containing carbon monoxide and thiol in the presence of

nickel sulfide and ferrous sulfide *(Figure 1.3)*[28]. The intermediate in this reaction is thought to be the corresponding metal-bound thiocarboxylic acid. The reactants are produced at hydrothermal vents; sites at mid-ocean ridges where minerals, especially metal sulfides, are released into the sea. Such vents have been proposed as possible sites for the origin of life.

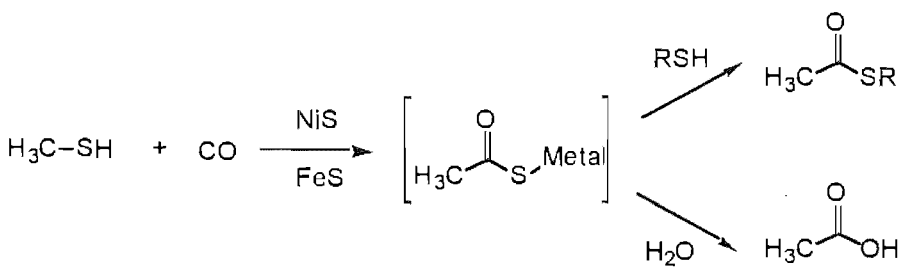

Figure 1.3 Carbon fixation mediated by nickel and ferrous sulfide

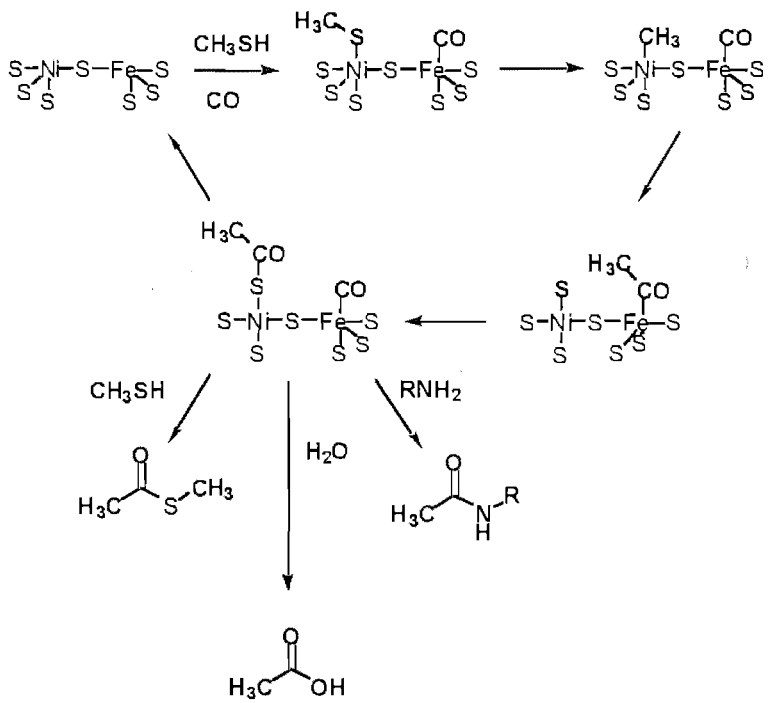

Figure 1.4 Possible biomimetic carbon fixation mediated by nickel and ferrous sulfide

A mechanism for this reaction has been put forward that involves a series of chemical group migrations on a nickel-iron sulfide surface (*Figure 1.4*). This parallels the chemistry of the nickel-iron-sulfur cluster at the active site of acetyl CoA synthetase.

Thioesters are key intermediates in a range of carbon fixation reactions. For example, thioesters are involved in reductive carbon fixation to form α-keto acids. An illustrative example is the reductive carbon dioxide fixation of acetyl-CoA to produce pyruvate, an α-keto acid (*Figure 1.5*).

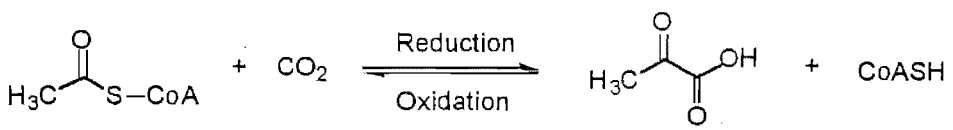

Figure 1.5 Reductive carbon dioxide fixation to form pyruvate

A plausible prebiotic model of this reaction has been developed (*Figure 1.6*)[29]. In the presence of carbon dioxide and an iron-sulfur complex, thioesters are thought to give rise to α-keto acids. The products of this process have been trapped by conversion to the corresponding α-amino acids[29].

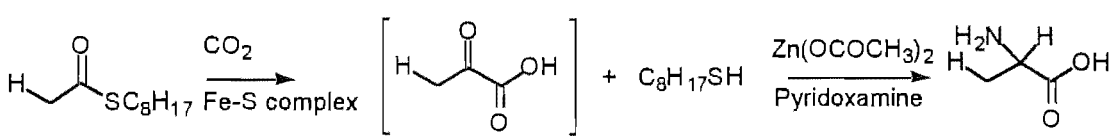

Figure 1.6 Possible biomimetic formation of α-keto acids

Furthermore, recent studies have reported that α-amino acids can be produced by reductive amination of α-keto acids mediated by a combination of iron sulfide, carbon dioxide and ammonia (*Figure 1.7*)[30].

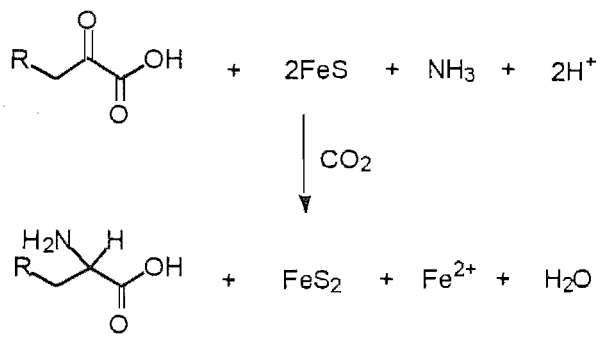

Figure 1.7 Formation of α-amino acids from α-keto acids

1.2.3 Summary

Thioesters have been formed from thiols and carbon monoxide in the presence of metal sulfides. Thioesters and carbon dioxide are reported to produce α-keto acids in the presence of an iron-sulfur complex. α-Keto acids can be reductively aminated to form α-amino acids in reaction mixtures containing iron-sulfide, ammonia and carbon dioxide. These biomimetic reactions provide a plausible prebiotic source of α-amino acids. Hence a combination of iron, nickel and sulfur appears to be capable of catalysing the generation of α-amino acids *via* reductive carbon fixation. Not only do the key reactions mimic contemporary biochemical processes, but also the mineral catalysts are closely related to metal-sulfur clusters which are common co-enzymes in enzyme-catalysed reactions (*Figure 1.8*).

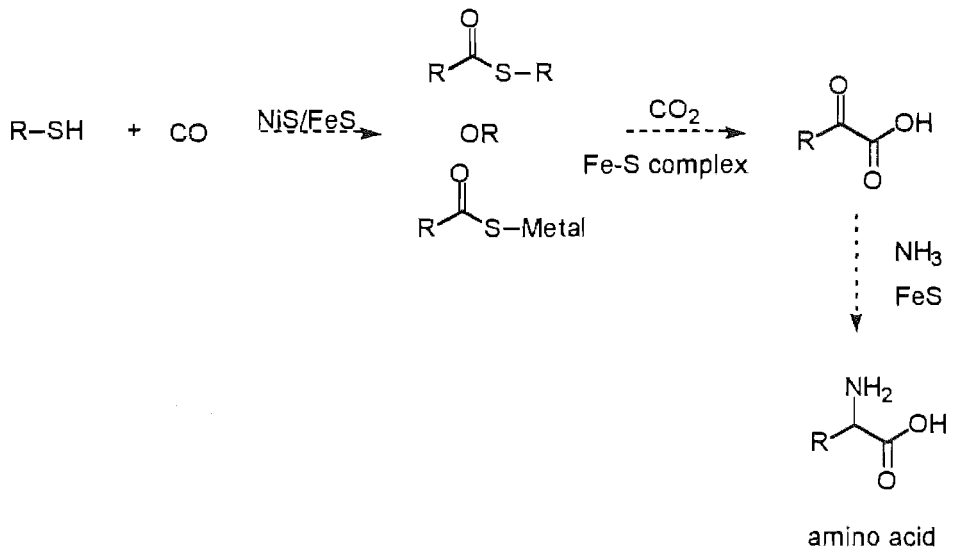

Figure 1.8 Possible reaction sequence to form α-amino acids

Thioesters play a key role in the synthesis of α-amino acids *via* this route. Metal-bound thiocarboxylic acids have been implicated as intermediates in this chemistry. These metal-bound thiocarboxylic acids may have been prebiotic precursors to thioesters, in the presence of metal sulfides. Mineral surfaces, metal sulfides in particular, may therefore have played an important role in prebiotic chemistry. Mineral surfaces have many features which may be attractive from an evolutionary point of view[31]. Surfaces are capable of adsorbing molecules; this can result in higher concentrations of reactants (and products) being found on the mineral surfaces. Iron sulfides are potentially interesting in this regard because of their connections to both geochemistry and biochemistry. These iron sulfide surfaces are the subject of several chemoautotrophic origin of life theories. This is discussed in more detail in Chapter Three, which describes some of the reductive chemistry of iron sulfides which may be relevant to these theories on the origins of life.

1.3 Thioesters and the origins of life

Thioesters are important metabolites, in a wide range of biochemical processes. It seems likely that they were important in the early evolution of metabolism. The functions of thioesters in the prebiotic world may have included participating in the generation of macromolecules, and involvement in redox chemistry.

1.3.1 Formation of amide bonds from thioesters

Amino acids are likely to have been present when life evolved, as has been discussed in earlier sections. They are ubiquitous in life, forming the building blocks for peptides and proteins. Condensation reactions that allow the formation of peptide polymers from amino acid monomers were essential in the development of a protein-dependant metabolism. Condensation reactions of amines and acids are unfavourable in an aqueous environment; a means of making these dehydration reactions favourable in an aqueous environment was required for the evolution of metabolism.

A number of bacterial peptides are formed *via* non-ribosomal peptide syntheses, in this case the activated carboxylic acids derivatives are amino acid thioesters (*Figure 1.9*)[32,33,34]. Wieland and coworkers report that peptides can spontaneously form from aminoacyl thioesters when incubated in alkaline aqueous solutions[35].

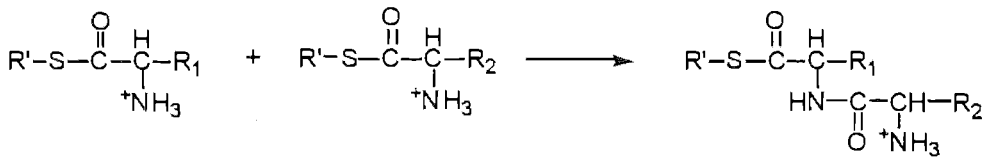

Figure 1.9 Non-ribosomal peptide synthesis

A more recent study of a possible biomimetic prebiotic synthesis of amide bonds showed that peptides were produced when aqueous solutions of amino acids were heated with ferrous sulfide, nickel sulfide, carbon monoxide and a thiol (or hydrogen sulfide) (*Figure 1.10*)[36].

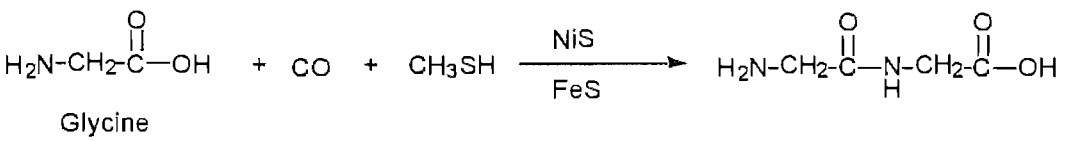

Figure 1.10 Biomimetic non-ribosomal peptide synthesis

The reaction conditions are similar to those which give rise to thioesters or metal-bound thiocarboxylic acids in the biomimetic carbon fixation process described in section 1.2. Therefore amide bond formation may be occurring *via* a sulfur derivative of a carboxylic acid, such as thiocarboxylic acid. This theory is supported by the observation that, when carboxylic acids were heated with thiols, carbon monoxide, nickel sulfide and ferrous sulfide, thioesters were detected (*Figure 1.3*).

1.3.2 Thiocarboxylic acids and amide bond formation

There has been limited study of amide bond formation from thiocarboxylic acids and amines in aqueous solution. The original report of these reactions was published in 1952 by Sheehan and Johnson[37]. Liu and Orgel report acylation of phenylalanine using thiocarboxylic acids in the presence of oxidants[38]. They propose that the initial step is oxidation of the thiocarboxylic acid to the corresponding disulfide; reaction of this intermediate with an amine produces an amide(*Figure 1.11*).

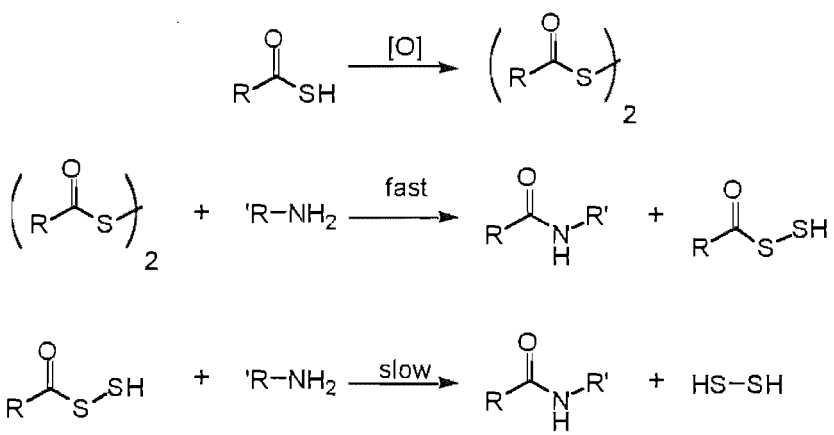

Figure 1.11 Proposed oxidative acylation chemistry of thiocarboxylic acids

For this mechanism of acylation to be plausible in prebiotic chemistry (where the atmosphere was oxygen free) a suitable oxidising agent is required. Liu and Orgel used ferric ions as the oxidant in their system. Ferric ions may have been available in prebiotic times *via* photooxidation of ferrous ions. The importance of the oxidation of

thiocarboxylic acids and/or the possible role of thiocarboxylic acids and metal-bound thiocarboxylic acids in prebiotic amide bond formation is an area that requires more investigation. Studies of this kind are outlined in Chapter Four.

1.3.3 Interconversion of thioesters and polyphosphates

The generation and interconversion of thioesters and polyphosphates plays a key role in metabolism. The citric acid cycle includes an example of this chemistry: the conversion of succinyl-CoA, guanosine 5'-diphosphate (GDP) to succinate and guanosine 5'-triphosphate (GTP) (*Figure 1.12*)[10]. In this reaction, inorganic phosphate attacks the thioester, succinyl-CoA, to form an acyl phosphate. The acyl phosphate undergoes phosphoryl transfer to GDP to form GTP, which contains an additional anhydride linkage.

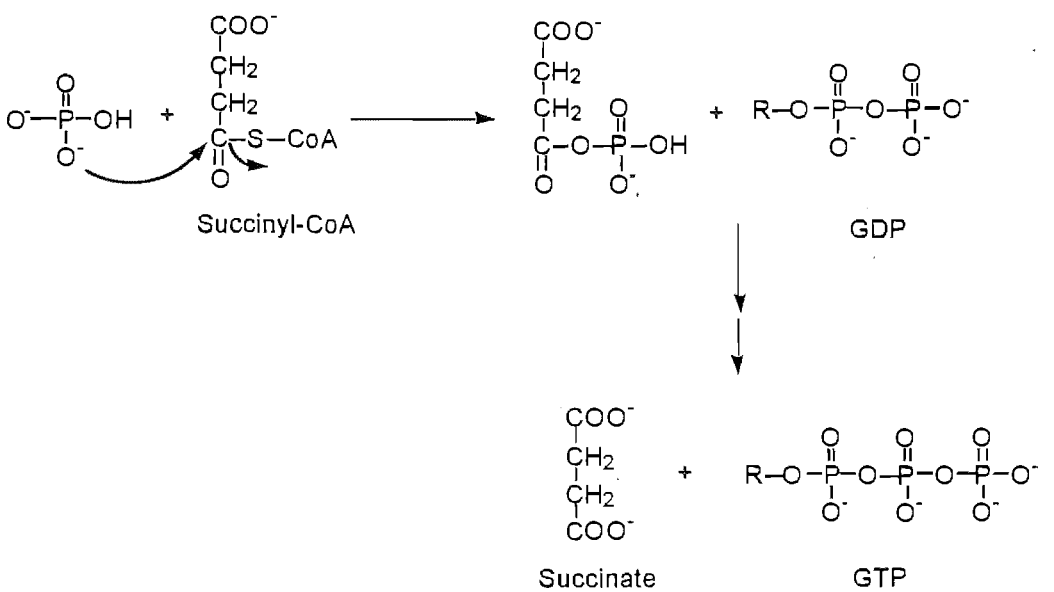

Figure 1.12 Formation of GTP from GDP

Investigation of these types of reactions (acyl and phosphoryl transfer to phosphate) may provide an insight into the prebiotic interconversion of thioesters and polyphosphates. Weber[39] has undertaken studies of this kind and reported the production of polyphosphates when *N,S*-diacetylcysteamine, imidazole and orthophosphate were reacted by drying reaction mixtures at 50°C (*Figure 1.13*).

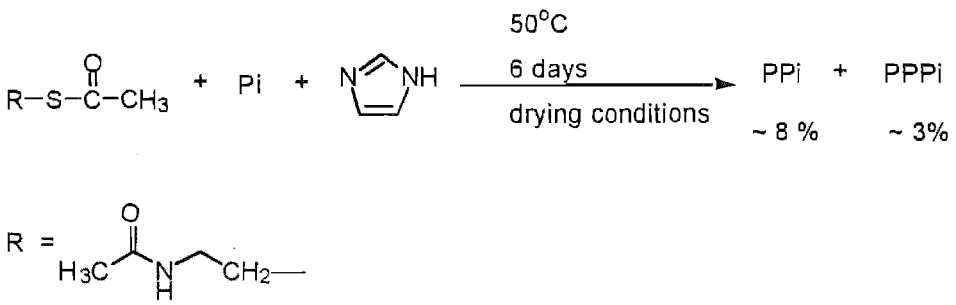

Figure 1.13 Formation of polyphosphates from a thioester

Weber[39] extended the study to aqueous solutions. Pyrophosphate was detected when the reaction was performed in the presence of metal ions. Weber has proposed the reaction mechanism shown in *Figure 1.14*, in which the thioester is in equilibrium with acyl phosphate, which in turn can form pyrophosphate[40,41,42].

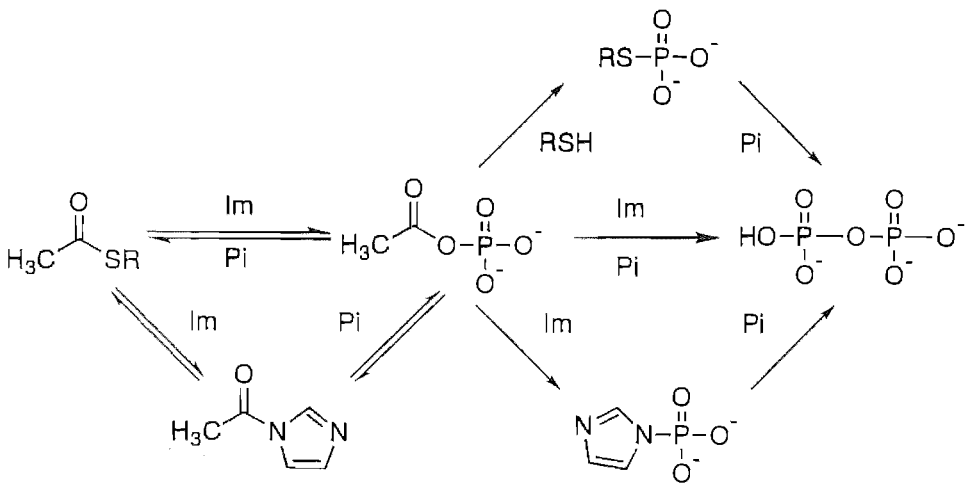

Figure 1.14 Possible reactions in the interconversion of thioester and pyrophosphate

Pyrophosphate may have preceded ATP as a source of biochemical energy. In fact pyrophosphate is still used as a phosphoryl donor for certain reactions in several bacterial species[43]. In summary, it can be seen that acyl phosphates and thioesters are used, as activated carboxylic acid derivatives, in a variety of different biochemical reactions. The widespread use of thioesters, acyl phosphates and polyphosphates highlights their likely importance as prebiotic molecules.

1.4 Polyphosphates and the origins of life

1.4.1 Introduction

Biosynthesis of peptides involves the activation of the carboxylic group of the amino acids followed by reaction to form the amide bond. Acyl phosphates are key intermediates in some of this chemistry. An illustrative example of this is the chemistry

involved in ribosomal biosynthesis of peptides. This is shown in simplified form in *Figure 1.15* and *Figure 1.16*[10].

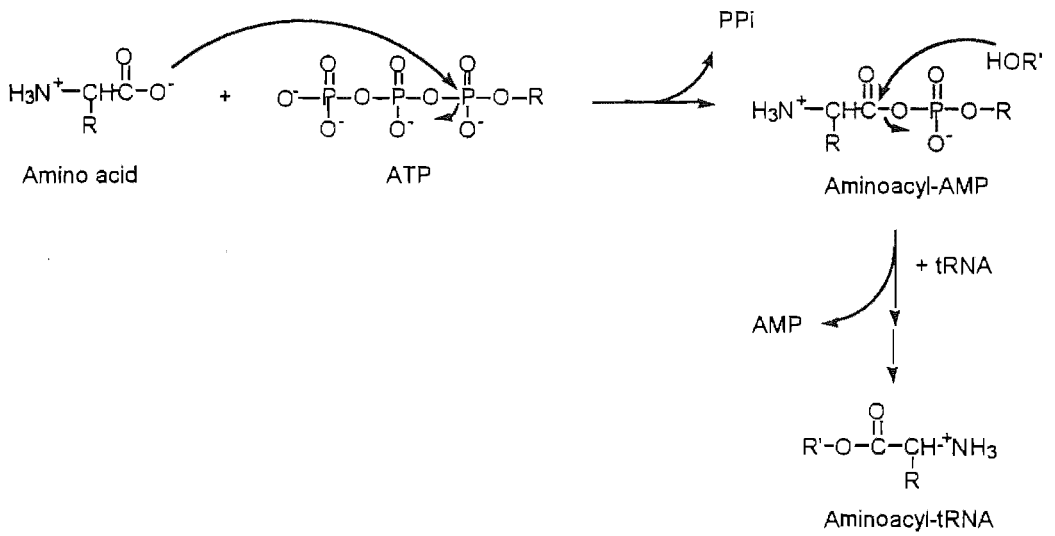

Figure 1.15 *Formation of aminoacyl-tRNA in ribosomal peptide synthesis*

The carboxylate group of an amino acid attacks a triphosphate to form an acyl phosphate which, in turn, reacts with an alcohol group on tRNA to generate aminoacyl-tRNA. Two aminoacyl-tRNA species bind to mRNA at adjacent sites. The amine group and ester group are held in close proximity and therefore react readily to form an amide bond (*Figure 1.16*)[10].

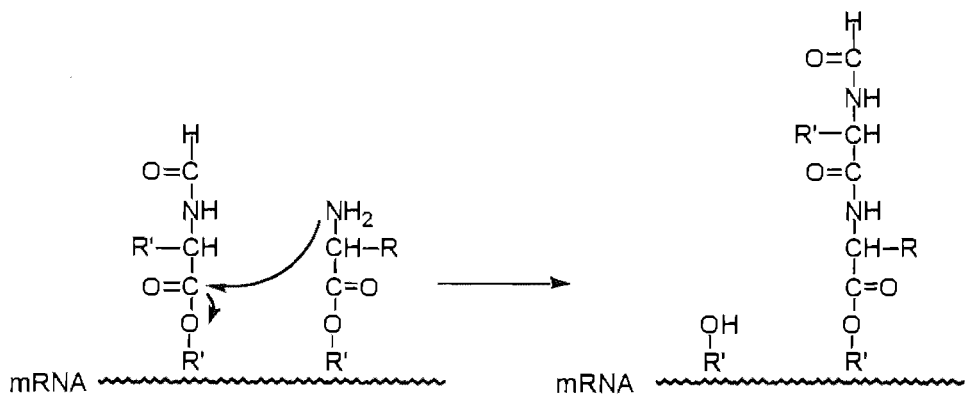

Figure 1.16 *Ribosomal peptide synthesis*

Polyphosphates, as acid anhydrides, are used in cells to bring about dehydration chemistry which would otherwise be unfavourable. In current biochemistry the high energy phosphoryl bonds of ATP are widely used as a chemical energy source in cells. Related compounds, such as pyrophosphate, the simplest polyphosphate may have played an important role in early metabolism.

1.4.2 Reactions of acyl phosphates

Acyl phosphates are key intermediates in the biochemical production of polyphosphates. Conversion of an acyl phosphate and inorganic phosphate to pyrophosphate is a thermodynamically favourable reaction (*Figure 1.17*)[44]. As has been mentioned previously, pyrophosphate may have been the original polyphosphate used in metabolism.

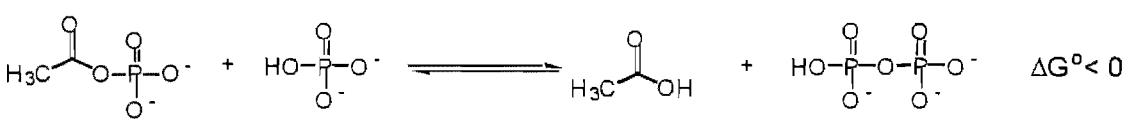

Figure 1.17 The formation of pyrophosphate from acetyl phosphate

Pyrophosphate formation from aqueous acetyl phosphate has been reported with a conversion of 0.5%[44]. The yield of the reaction was pH dependent with a maximum at near neutral pH. The mechanism of nucleophilic substitution of phosphate esters at the phosphorus centre has been studied extensively in an effort to determine if it is a concerted or stepwise mechanism[45,46,47]. No clear evidence for the mechanism has been

established. Reactions of acyl phosphates are further complicated by the fact that the acyl phosphate function contains two electrophilic centres, the carbonyl carbon and the phosphoryl group. There are two possible reaction pathways; nucleophiles can attack acyl phosphates at either the carbonyl group or the phosphoryl group (*Figure 1.18*).

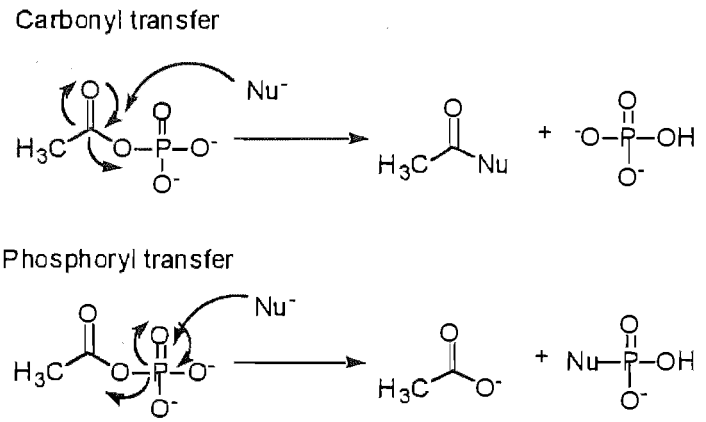

Figure 1.18 Two possible reaction pathways for acetyl phosphate

The carbonyl carbon is generally more reactive towards nucleophiles than the phosphoryl group, due to electrostatic repulsion. Nucleophiles, especially anions, approaching the phosphoryl centre are repelled by the anionic phosphate. This electrostatic repulsion can be reduced in the presence of cations, such as protons or metal ions.

Hydrolysis of acyl phosphates to form a carboxylic acid and inorganic phosphate is reported to be catalysed by a range of metal ions, for example Fife and Pujari[48] report that divalent metal ions significantly catalyse this class of hydrolysis reaction. High concentrations of Ni^{2+}, Co^{2+} or Zn^{2+} ions catalyse the reaction of hydroxide with 1,10-phenanthroline-2-carbonyl phosphate by a factor of $>10^7$ at 30°C. The hydrolysis of

acetyl phosphate in the presence of metal ions has also been investigated. Lipmann and Tuttle showed that hydrolysis of acetyl phosphate was catalysed by calcium ions[49]. The catalysis of hydrolysis of acetyl phosphate by metal ions is reported to be pH dependent[50]. Magnesium ions were found to catalyse hydrolysis of the acetyl phosphate dianion, while no effect on the rate of hydrolysis observed for the corresponding monoanion or uncharged acetyl phosphate. The mode of catalysis may be due to complexation of the metal ions with the acetyl phosphate[50], charge neutralisation[51] or generation of metal-bound hydroxide[52,53].

High concentrations of monovalent ions have been reported to catalyse phosphoryl transfer reactions in which pyrophosphate is produced from acetyl phosphate and inorganic phosphate[45]. Sodium ions are thought to catalyse this process by charge neutralisation. Formation of pyrophosphate results from the nucleophilic attack by inorganic phosphate at the phosphorus centre of the acetyl phosphate. However, the acetyl phosphate is a dianion at near neutral pH and thus is not a very good electrophile. The sodium ions can complex with the acetyl phosphate and reduce the electrostatic repulsion between the electrophile and nucleophile. The high concentration of sodium ions required is consistent with the requirement for several cations to complex the negatively charged phosphate group in the transition state.

The location of the nucleophilic attack, at either the carbonyl centre or the phosphorus centre, is nucleophile dependent. Acetyl phosphate has been reported to undergo predominantly acyl transfer in the presence of organic nucleophiles including imidazole[54,55]. However there have been conflicting reports about the location of attack

by imidazole on acetyl phosphate. Acetyl phosphate has been reported to react with imidazole to form imidazole phosphate[56,42]. By contrast, the majority of the literature reports seem to indicate imidazole attacks acyl phosphates at the carbonyl carbon centre[55].

Nucleophilic reactions of acyl phosphates, which occur at the carbonyl carbon, are affected by steric factors. For instance, imidazole is reported to react at the carbonyl centre of acetyl phosphate, but there was no observable reaction of imidazole with trimethylacetyl phosphate or with 3,3-di-methylbutyryl phosphate[57]. This steric effect is also observed for the hydrolysis of the acyl phosphates. Acetyl phosphate dianions hydrolyse more rapidly than the more sterically hindered trimethylacetyl phosphate and 3,3-di-methylbutyryl phosphate[57].

Catalysis of the phosphoryl transfer from acetyl phosphate to inorganic phosphate is reported by some organic nucleophiles such as pyridine[58]. Similarly, macrocyclic polyamines are found to catalyse pyrophosphate formation from acetyl phosphate[59,60]. The postulated intermediate, *N*-phosphorylated polyamine macrocycle (*Figure 1.19*) was detected by ^{31}P NMR spectroscopy in these reaction mixtures. Metal ions (calcium and magnesium ions) have been observed to promote this phosphoryl transfer[61].

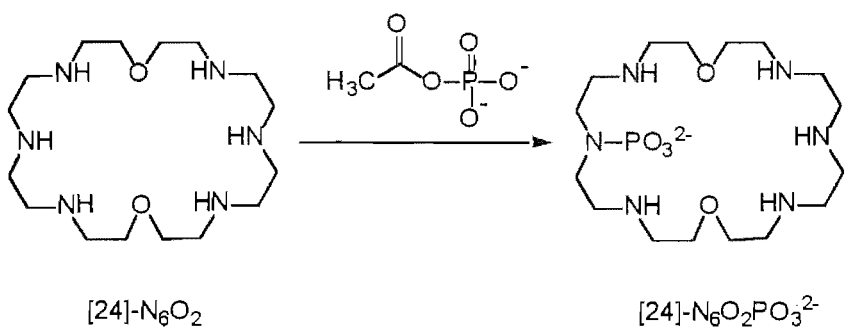

Figure 1.19 Formation of N-phosphoryl macrocyclic polyamine

Herschlag and Jencks[45] have studied the formation of pyrophosphate from acetyl phosphate. They report the yield of pyrophosphate was improved with the addition of pyridine in the presence of sodium ions. This increase in the production of pyrophosphate was thought to be due to the intermediacy of *N*-phosphoryl pyridine (*Figure 1.20*).

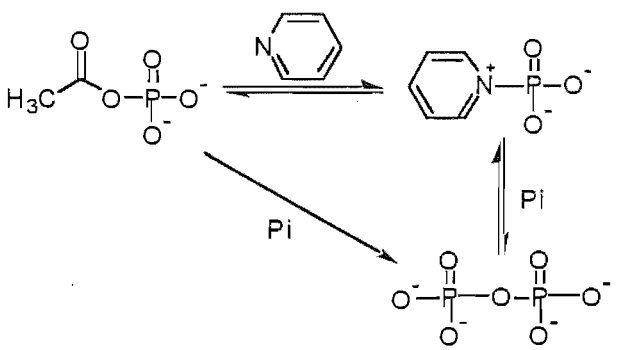

Figure 1.20 Formation of pyrophosphate in the presence of pyridine

The prevalence of phosphoryl transfer was rationalised through the proposal that pyridine, being uncharged, undergoes more facile reaction than anionic phosphate. The *N*-phosphoryl pyridine, in turn, is more electrophilic than acetyl phosphate and therefore the reaction with inorganic phosphate is faster than for acetyl phosphate.

The formation of polyphosphates from acyl phosphates in the presence of amines and/or metal ions may provide a plausible prebiotic synthesis of energy rich polyphosphates. The results of investigating this possibility will be described in Chapter Two. It is the starting point of our efforts to shed light on the possible origins of metabolism.

1.5 References

1 A. Brack, in *The Molecular Origins of Life*, A. Brack (ed), Cambridge University Press, 1-10 (1998).

2 L. Pasteur, Oeuvres de Pasteur, Masson & Cie (1992).

3 F. A. Podosek, *Science*, **283**, 1863 (1999).

4 J. F. Kasting, *Science*, **259**, 920 (1993).

5 E. S. Barghoorn, *Life: Origin and evolution*, Freeman, Scientific American Inc, C. E. Folsome (ed), 66-78 (1979).

6 S. M. Awramik, J. W. Schopf & M. R. Walter, *Precambrain Res.*, **20**, 357 (1983).

7 J. W. Schopf & B. M. Packer, *Science*, **237**, 70 (1987).

8 J. W. Schopf, *Science*, **260**, 640 (1993).

9 J. W. Schopf, in *The Molecular Origins of Life*, A. Brack (ed), Cambridge University Press, 336-362 (1998).

10 A. L. Lehninger, D. L. Nelson & M. M. Cox, *Principles of Biochemistry*, Worth Publishers (1993).

11 M. S. Chadha, in *Chemical Evolution: Physics of the Origin and Evolution of Life*, J. Chela-Flores & R. Raulin (eds), Kluwer Academic Publishers, 107-122 (1996).

12 J. R. Cronin, in *The Molecular Origins of Life*, A. Brack (ed), Cambridge University Press, 119-146 (1998).

13 E. Anders, *Nature*, **342**, 255 (1989).

14 C. F. Chyba, P. J. Thomas, L. Brookshaw & C. Sagan, *Science*, **249**, 366 (1990).

15 J. F. Kasting & L. Brown, in *The Molecular Origins of Life*, A. Brack (ed), Cambridge University Press, 35-56 (1998).

16 S. L. Miller, *Science*, **117**, 528 (1953).

17 S. L. Miller, *Biochem. & Biophys. Acta.*, **23**, 480 (1957).

18 J. P. Ferris, P. C. Joshi, E. H. Edelson & J. G. Lawless, *J. Mol. Evol.*, **11,** 293 (1978).

19 S. L. Miller, in *The Molecular Origins of Life*, A. Brack (ed), Cambridge University Press, 59-85 (1998).

20 D. M. Hunten, *Science*, **259**, 915 (1993).

21 J. F. Kasting & L. Brown, in *The Molecular Origins of Life*, A. Brack (ed), Cambridge University Press, 35-56 (1998).

22 A. Poldervaart, *Crust of the Earth*, Geol. Soc. Am. (1955).

23 J. C. G. Walker, *Evolution of the Atmosphere*, Macmillan (1977).

24 J. W. Schopf, *Earth's Earliest Biosphere: Its Origin and Evolution*, Princeton University Press (1983).

25 H. D. Holland, *The Chemical Evolution of the Atmosphere and Oceans*, Princeton University Press (1984).

26 P. E. Cloud, *Am. J. Sci.*, **272**, 537 (1972)

27 S. W. Ragsdale & M. Kumar, *Chem. Rev.*, **96**, 2515 (1996).

28 C. Huber & G. Wächtershäuser, *Science*, **276**, 245 (1997).

29 T. Nakajima, Y. Yabushita & I. Tasbushi, *Nature*, **256**, 60 (1975).

30 D. Hafenbradl, M. Keller, G. Wächtershäuser & K. O. Stetter, *Tet. Let.*, **36**, 5179 (1995).

31 G. Wächtershäuser, *Microbiol. Rev.*, **52**, 452 (1988).

32 W. Gevers, H. Kleinkauf & F. Lipmann, *Proc. Natl. Acad. Sci. USA*, **63**, 1335 (1964).

33 H. Kleinkauf & H. von Dohren, *Annu. Rev. Microbiol.*, **41**, 259 (1987).

34 F. Lipmann, *Science*, **173**, 875 (1971).

35 T. Weiland, in *The roots of modern biochemistry: Fritz Lipmann's squiggle and its consequences*, H. Kleinkauf, H. von Dohren & L. Jaenicke (eds), Walter de Grayter 212-221 (1988).

36 C. Huber & G. Wächtershäuser, *Science*, **281**, 670 (1998).

37 J. C. Sheehan & D. A. Johnson, *J. Am. Chem. Soc.*, **74**, 4726 (1952).

38 R. Lui & L. E. Orgel, *Nature*, **389**, 52 (1997).

39 A. L. Weber, *J. Mol. Evol.*, **18**, 24 (1981).

40 M. J. Heller, J. A. Walder & I. M. Klotz, *J. Am. Chem. Soc.*, **99**, 2780 (1977).

41 G. DiSabato & W. P. Jencks, *J. Am. Chem. Soc.*, **83**, 4400 (1961).

42 D. Gibbs, R. Lohrmann & L. E. Orgel, *J. Mol. Evol.*, **15**, 347 (1980).

43 F. H. Westheimer, *Science*, **235**, 1173 (1987) and references therein.

44 E. Etaix & R. Buvet, *Origins of Life*, **6**, 175 (1975).

45 D. Herschlag & W. P. Jencks, *J. Am. Chem. Soc.*, **108**, 7938 (1986).

46 D. Herschlag & W. P. Jencks, *J. Am. Chem. Soc.*, **109**, 4665 (1987).

47 D. Herschlag & W. P. Jencks, *J. Am. Chem. Soc.*, **112**, 1942 (1990).

48 T. J. Fife & M. P. Pujari, *J. Am. Chem. Soc.*, **112**, 5551 (1990).

49 F. Lipmann & L. C. Tuttle, *J. Biol. Chem.*, **153**, 571 (1944).

50 D. E. Koshland, *J. Am. Chem. Soc.*, **74**, 2286 (1952).

51 C. H. Oestreich & M. M. Jones, *Biochemistry*, **6**, 1515 (1967).

52 P. J. Briggs, D. P. N. Satchell & G. F. White, *J. Chem. Soc. B.*, 1008 (1970).

53 D. A. Buckingham & C. R. Clark, *Aust. J. Chem.*, **34**, 1769 (1981).

54 D. E. Koshland, *J. Am. Chem. Soc* , **73**, 4103 (1951).

55 W. P. Jencks & J. Carriuolo, *J. Biol. Chem.*, **234**, 1272 (1959).

56 A. L. Weber, *J. Mol. Evol.*, **18**, 24 (1981).

57 D. R. Phillips, *J. Org. Chem.*, **34**, 2710 (1969).

58 G. Di Sabato & W. P. Jencks, *J. Am. Chem. Soc.*, **83**, 4393 (1961).

59 M. W. Hosseini & J-M Lehn, *J. Chem. Soc., Chem. Commun.*, 1155 (1985).

60 M. W. Hosseini & J-M Lehn, *J. Chem. Soc., Chem. Commun.*, 397 (1988).

61 M. W. Hosseini & J-M Lehn, *J. Chem. Soc., Chem. Commun.*, 451 (1991).

Chapter 2

Acetyl phosphate Chemistry

2.1 Introduction

Acyl phosphates are high energy intermediates in the biochemical thioester-polyphosphate interconversion (*Figure 2.1*), as previously discussed in section 1.3. This means that the formation of either thioesters or polyphosphates from acyl phosphates is thermodynamically favourable. Studying the reactions of acetyl phosphate therefore provides a means of analysing these equilibria.

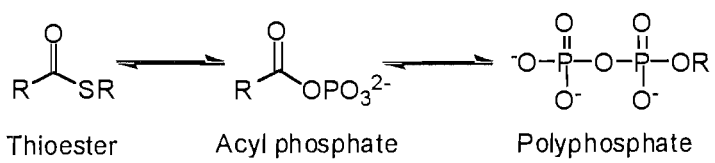

Figure 2.1 *Thioester-polyphosphate interconversion*

The acyl phosphate functional group contains two electrophilic centres, the carbonyl carbon and the phosphoryl group. Therefore, there are two possible reaction pathways for nucleophilic substitution; nucleophiles can attack acyl phosphates at either the

carbonyl group or the phosphoryl group (*Figure 2.2*). The carbonyl carbon is generally more reactive with nucleophiles than the phosphoryl group due to electrostatic repulsion as nucleophiles approach the phosphoryl centre.

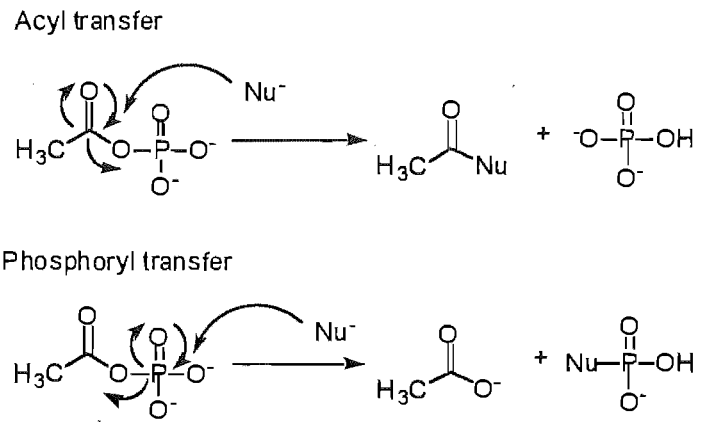

Figure 2.2 *Nucleophilic substitution at acetyl phosphate*

Acetyl phosphate has been reported to undergo predominantly acyl transfer in the presence of organic nucleophiles including imidazole[1,2,3]. However, acetyl phosphate has been shown to undergo a certain degree of phosphoryl transfer chemistry in the presence of cations. Phosphoryl transfer is made more favourable when neutral, rather than anionic, nucleophiles and cations are present. Both of these conditions decrease electrostatic repulsion between the electrophile and nucleophile. The phosphoryl transfer pathway is reportedly catalysed by some organic nucleophiles such as pyridine[2,4].

The ultimate aim of the work described in this chapter was to assess the ability of acetyl phosphate to act as a phosphoryl transfer agent. The studies of acetyl phosphate

chemistry described in Chapter two of this thesis are divided into four parts. These studies require a source of pure acetyl phosphate. The first part, section 2.2, describes the assessment of various sources of acetyl phosphate (commercially available material and synthetic samples from a number of different preparations) as well as purification procedures.

High concentrations of sodium ions have been reported to catalyse phosphoryl transfer reactions in which pyrophosphate is produced from acetyl phosphate and inorganic phosphate both in the presence and absence of nitrogen-containing compounds[5]. Phosphoryl transfer reactions of acetyl phosphate and inorganic phosphate were carried out in the presence of imidazole and pyridine. Possible intermediates of these reactions are *N*-phosphoryl imidazole and *N*-phosphoryl pyridine respectively. Our attempts to detect the formation of the proposed intermediates and to reproduce the formation of pyrophosphate are discussed in section 2.3.

There are numerous literature reports describing catalysis of acyl phosphate hydrolysis by divalent metal ions[6,7,8]. The reactions of acetyl phosphate with inorganic phosphate in the presence of magnesium ions or ferrous ions, with and without organic nucleophiles, are described in sections 2.3 and 2.4. The study of phosphoryl transfer reactions was further extended in order to assess whether ferrous sulfide was a catalyst for this reaction. The results of this study may be important in light of the proposals, discussed in Chapter 1, that ferrous ions and/or ferrous sulfide may act as prebiotic catalysts.

2.2 Acetyl phosphate

2.2.1 Silver salts and related chemistry

Our study of the reactions of acetyl phosphate with inorganic phosphate to form pyrophosphate required access to pure acetyl phosphate and inorganic phosphate. Aldrich supplies the lithium potassium salt of acetyl phosphate with a stated purity of 97%. A ^{31}P NMR spectrum obtained from a sample of this material contained multiple resonances, which indicated the presence of several phosphorus containing compounds. The chemical shifts and assignments of the resonances observed in the lithium potassium acetyl phosphate are shown in *Table 2.1*. Significant amounts of inorganic phosphate, pyrophosphate and tripolyphosphate were detected. Less than 40% of the phosphate present was acetyl phosphate. The impurities, particularly pyrophosphate and tripolyphosphate, are undesirable in the study of phosphoryl transfer reactions, as they are possible products of these reactions. Two possible strategies to provide acetyl phosphate suitable for the desired experiments were investigated, they are purification of the commercially acetyl phosphate and synthesis of acetyl phosphate.

^{31}P δ ppm	Multiplicity	Species
1.85	s	Inorganic phosphate
-0.91	s	Acetyl phosphate
-6.52	d	Tripolyphosphate
-7.07	s	Pyrophosphate
-19.60	t	Tripolyphosphate

Table 2.1 *^{31}P NMR data for commercial lithium potassium acetyl phosphate*

The silver salts of inorganic phosphates are less soluble in water than those of organic phosphates[9]. We explored the possibility of selective precipitation of silver salts of inorganic phosphate, pyrophosphate and tripolyphosphate. The K_{sp} values for silver phosphate[10] and silver pyrophosphate[9] are 8.88×10^{-17} and 6.75×10^{-24} respectively. By contrast silver acetyl phosphate is reported to be slightly more soluble[9].

A solution of silver ions was added to the aqueous acetyl phosphate solution and the resulting insoluble silver salts were removed by centrifugation. The integrations of the resonances of the phosphorus containing species observed were measured in order to enable approximate quantification of the phosphorous containing species present.

The results are shown graphically in *Figure 2.3*, expressed as a percentage of the total phosphate. The observed trends indicate that inorganic phosphate, pyrophosphate and

tripolyphosphate are selectively precipitated. However due to the low purity of the original sample it was not possible to remove all the impurities. Synthesis of acetyl phosphate was therefore explored in an effort to produce purer material.

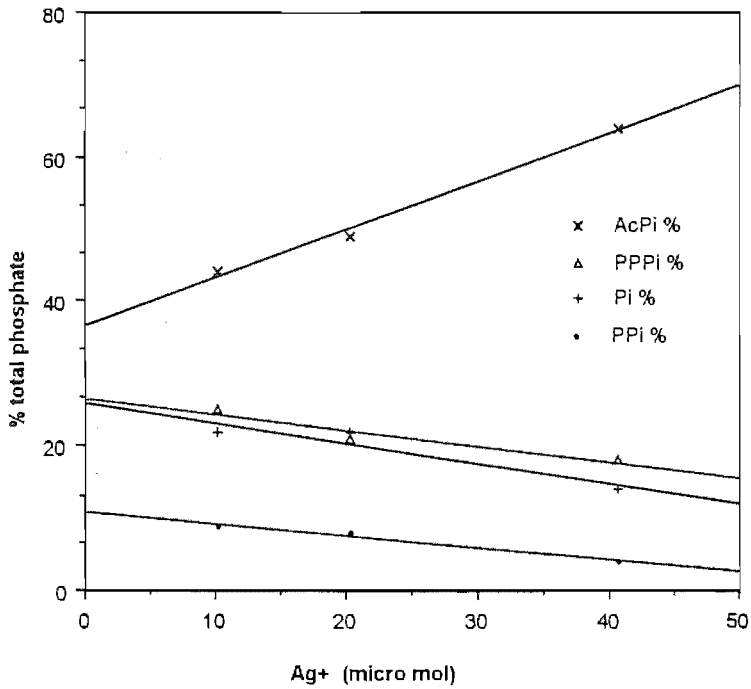

Figure 2.3 Attempted purification of acetyl phosphate by addition of silver ions

2.2.2 Synthesis of acetyl phosphate

The silver salt of acetyl phosphate was initially prepared by the method of Lipmann and Tuttle as shown in *Figure 2.4*[9]. Trisilver phosphate is converted to silver dihydrogen phosphate in order to prevent multiple acetylation and formation of polyacetyl phosphate species. The acetyl phosphate was precipitated as the silver salt.

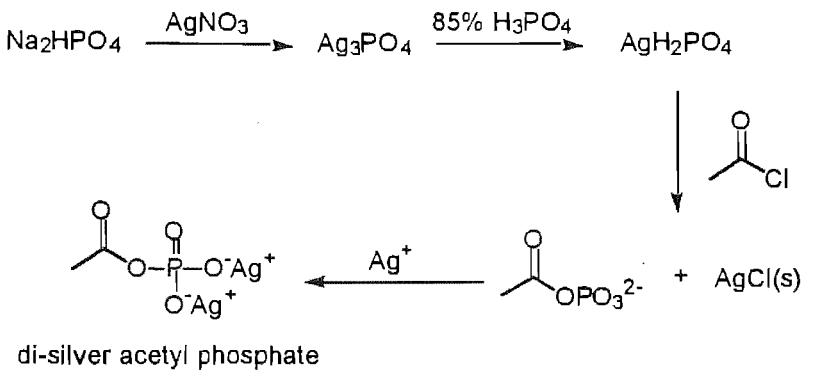

Figure 2.4 Synthesis of di-silver acetyl phosphate

Di-silver acetyl phosphate has only modest solubility in water. Di-silver acetyl phosphate was redissolved in aqueous sodium chloride solutions to enable analysis by ^{31}P NMR spectroscopy. In order to facilitate the efficient dissolution of acetyl phosphate, high concentrations of sodium chloride were added. Silver ions are precipitated as silver chloride in the presence of chloride ions. The removal of the silver ions, produced from dissolving a small amount of di-silver acetyl phosphate, shifts the solubility equilibrium and thus more di-silver acetyl phosphate can be dissolved

The ^{31}P NMR spectrum of the acetyl phosphate solution, prepared as described above, contained 4 resonances. Two components were readily identifiable; the resonances at 4.57 ppm and -1.03 ppm were consistent with the presence of inorganic phosphate and acetyl phosphate. The other two resonances at -4.61 and -42.49 ppm could not be readily assigned. Analysis of solutions of acetyl phosphate indicated that both acetyl phosphate and the compound giving rise to a resonance at -4.61 ppm were hydrolytically unstable.

The synthesis failed to produce acetyl phosphate in a form suitable for the desired phosphoryl transfer experiments. In particular the presence of undesired impurities, high concentrations of sodium ions and especially unidentified phosphorus containing compounds rendered these samples of acetyl phosphate inappropriate for the phosphoryl transfer experiments. An alternative synthesis of acetyl phosphate was therefore investigated.

The second synthetic approach involved reacting an aqueous solution of potassium dihydrogen phosphate and potassium monohydrogen phosphate with acetic anhydride in the presence of pyridine (*Figure 2.5*)[5,11]. On completion of the reaction the pyridine was removed by extraction into ether. Analysis of the resulting aqueous solution by ^{31}P NMR spectroscopy revealed two singlet resonances at 1.37 ppm and -1.45 ppm that could be assigned to inorganic phosphate and acetyl phosphate respectively. No pyrophosphate or tripolyphosphate was detected.

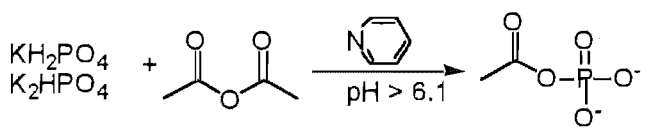

Figure 2.5 Synthesis of an aqueous solution of acetyl phosphate

The aqueous solutions contained acetyl phosphate and inorganic phosphate, these are the reactants required for the phosphoryl transfer reactions. Therefore, provided we can quantify the composition of the solution, it is possible to use this aqueous solution directly.

Although the relative amounts of inorganic phosphate and acetyl phosphate can be estimated from integrations of signals in the ^{31}P NMR spectra, we needed to augment this methodology with a method to measure the absolute concentrations of inorganic phosphate and acetyl phosphate in the aqueous solutions.

2.2.3 Quantification of acetyl phosphate

Three methods of quantification of acetyl phosphate and/or inorganic phosphate were carried out to give independent determinations of the amount each of these species. The first method of measuring the acetyl phosphate concentration was that of Lipmann and Tuttle[12], as modified by Herschlag and Jencks[13]. In this method acetyl phosphate is converted to acetohydroxamic acid by reaction with hydroxylamine. The concentration of the purple-red complex of the resulting acetohydroxamate and ferric ions was determined colorimetrically through measurement of absorbance at 540 nm (*Figure 2.6*).

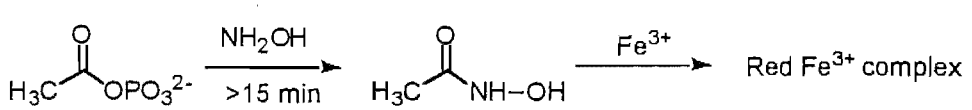

Figure 2.6 Colorimetric assay for acetyl phosphate

The calibration curve was determined using 98% acetohydroxamic acid supplied by Aldrich, the purity of which was confirmed by ^{1}H NMR spectroscopy. The colorimetric assay was performed on solutions of acetohydroxamic acid and the results were used to establish the relationship between acetohydroxamic acid and absorbance at 540 nm. The graphical representation of the data clearly shows a linear relationship between absorbance measured at 540 nm and concentration of acetohydroxamic acid, even up to absorbances approaching 2 (*Figure 2.7*).

The calibration curve was used to determine the concentration of the aqueous solutions of acetyl phosphate. The acetyl phosphate solution was assayed, diluted and reassayed until the absorbance was within the range 0-1. The concentration was calculated from the calibration curve relationship described above. The acetyl phosphate concentration for the aqueous solution we prepared was generally in the range of 0.3 - 0.7 M.

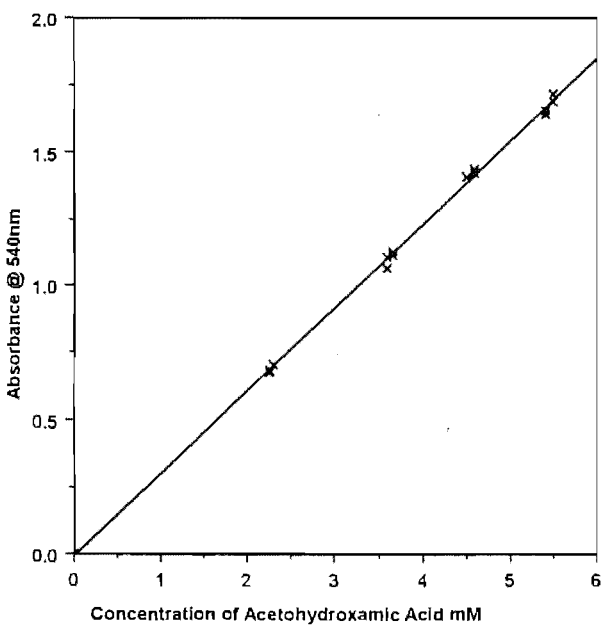

Figure 2.7 *Relationship between absorbance and acetohydroxamic acid concentration*

The second method quantifies the total amount of phosphate containing species. Therefore the inorganic phosphate concentrations can be calculated by difference from the colorimetric assays of acetyl phosphate (described above) and this total phosphate assay. The total phosphate assay was developed by Fiske and Subbarrow in 1925 (*Figure 2.8*)[14]. It is carried out under acidic conditions that hydrolyse acetyl phosphate to inorganic phosphate. In this assay, all the inorganic phosphate present in solution after treatment with acid, reacts with ammonium molybdate to form phosphomolybdic acid. The phosphomolybdic acid produced is then reduced by 4-(*N*-methylamino)phenol sulfate, thereby generating a blue pigment.

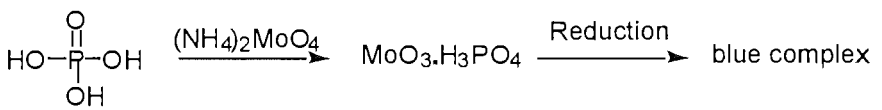

Figure 2.8 *Colorimetric assay for inorganic phosphate*

The intensity of absorbance of the blue chromophore is determined by measuring the absorbance at 660 nm and provides a measure of the concentration of phosphate species in solution. A calibration curve was determined and is shown in *Figure 2.9*. The graphical representation of the data clearly shows a linear relationship between absorbance measured at 660 nm and concentration of phosphate concentration (mM).

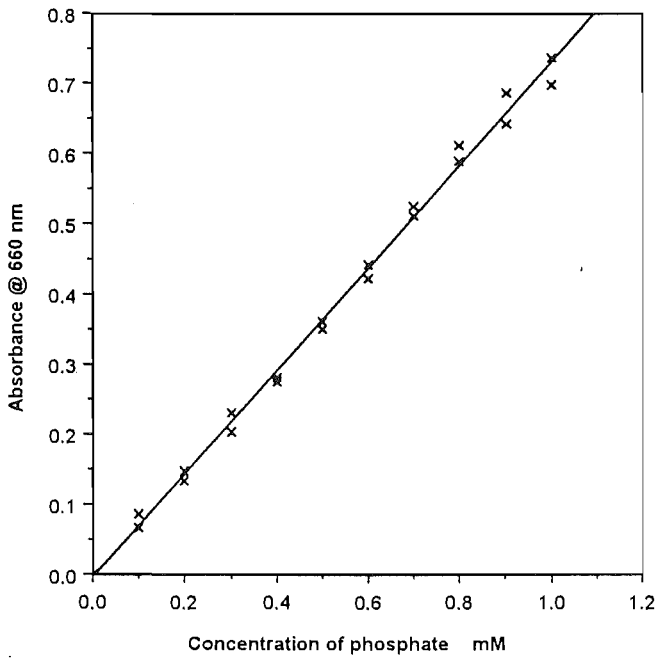

Figure 2.9 Relationship between absorbance and inorganic phosphate concentration

This method was employed to analyse for total phosphate concentration in aqueous solutions of acetyl phosphate. The total phosphate concentration calculated from assaying the aqueous solution of acetyl phosphate was generally in the range of 0.8-1.2 M. The inorganic phosphate concentration could be determined from the acetyl phosphate and total phosphate concentration. The inorganic phosphate concentration was generally similar to the acetyl phosphate concentration.

These two colorimetric assays combined give absolute measures of acetyl phosphate and inorganic phosphate concentrations. However ^{31}P NMR spectroscopy gives the relative amounts of phosphorus containing species. Therefore the colorimetric assays can be used as an external calibration for ^{31}P NMR spectroscopy, and as a check on the integration data.

2.2.4 Optimised ^{31}P NMR method

The most convenient method for analysing reaction mixtures is ^{31}P NMR spectroscopy. ^{31}P NMR spectroscopy provides a method for direct, non-destructive measurement of the relative concentrations of phosphorus containing species. For this to be reliable the signal integrations for acetyl phosphate and inorganic phosphate must be proportional to the quantities present. This will be true provided that the radio frequency pulses are sufficiently separate in time to allow the nuclear magnetisation to relax fully with respect the applied external magnetic field before the next pulse is applied. If relaxation of a nucleus is not complete then the observed signal intensity for that nucleus will be reduced. A sufficient delay in the pulse sequence must therefore be allowed for the relaxation to occur. Measurement of the longitudinal relaxation times, T_1, allowed calculation of an appropriate delay. Generally, delays greater than three times the relaxation time are required in order to obtain accurate integrations[15].

An experiment was carried out to determine the longitudinal relaxation times T_1, of acetyl phosphate and inorganic phosphate. This showed the T_1 of acetyl phosphate to be 2.441 seconds and the T_1 of inorganic phosphate to be 0.54 seconds. Therefore all phosphate NMR spectra were subsequently run with a delay (D_1) of 10 seconds in order to allow complete relaxation of the acetyl phosphate magnetisation[16].

We can colorimetrically assay aqueous solutions of acetyl phosphate to determine the absolute concentrations of acetyl phosphate and inorganic phosphate using the methods described in section 2.2.3. These assays can be correlated with the relative concentrations provided by ^{31}P NMR spectroscopy. The ^{31}P NMR spectroscopy can therefore be used to monitor reactions in a non-destructive manner. The percentage of acetyl phosphate, inorganic phosphate and pyrophosphate were calculated from the integrations of the signals in the ^{31}P NMR spectra that had been assigned to the acetyl phosphate, inorganic phosphate and pyrophosphate.

2.3 Attempts to catalyse phosphoryl transfer in solution

2.3.1 Introduction

Two types of catalysis have been reported for the phosphoryl transfer reaction to produce pyrophosphate from inorganic phosphate and acetyl phosphate. Some nucleophiles, such as nitrogen containing compounds, are reported to catalyse the reaction of acyl phosphate with inorganic phosphate to form pyrophosphate. Metal ions, both monovalent and divalent have also been reported to catalyse this transformation.

Nitrogen-containing compounds are known to react with acyl phosphates in a nucleophilic manner. Acyl phosphates contain two electrophilic centres and thus phosphoryl transfer is in competition with acyl transfer. The phosphoryl transfer is encouraged by neutral nucleophiles, which minimise the electrostatic repulsion between the nucleophile and the anionic phosphate group.

Large macrocyclic polyamines are known to catalyse the formation of pyrophosphate from acetyl phosphate. Analysis of the NMR studies of these reactions has shown the accumulation of an *N*-phosphoryl intermediate which is lost with time. An amine group of the macrocyclic polyamine is thought to act as a nucleophile and react with the phosphorus of acetyl phosphate. Detection of the *N*-phosphoryl species seems to support this mechanism for catalysis of pyrophosphate *via* the *N*-phosphoryl species.

Weber reported the reaction of thioester with imidazole and inorganic phosphate to form acetyl phosphate[17]. The thioester was proposed to react with imidazole to give *N*-acetylimidazole, which subsequently reacts with inorganic phosphate to give acetyl phosphate. This acetyl phosphate can then react with imidazole and inorganic phosphate to yield pyrophosphate (*Figure 2.10*)[17]. This reaction is thought to proceed *via N*-phosphoryl imidazole. Fife and Pujari contradicted this by reporting that imidazole attacks exclusively at the carbonyl group of acetyl phosphate[7]. Weber also reports that *N*-phosphoryl imidazole reacts with inorganic phosphate to give pyrophosphate[18].

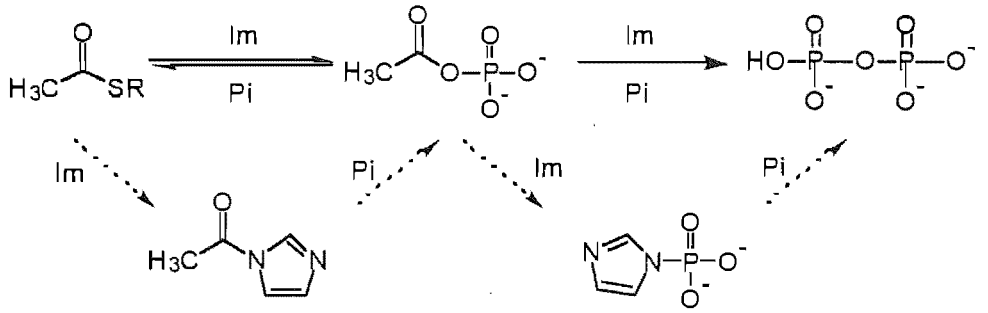

Figure 2.10 *Reaction of thioesters to from pyrophosphate in the presence of imidazole*

Herschlag and Jencks[5] reported the conversion of acetyl phosphate into pyrophosphate in the presence of pyridine and high concentrations of monovalent ions. The increase in the production of pyrophosphate was thought to be due to nucleophilic catalysis and the associated intermediacy of *N*-phosphoryl pyridine (*Figure 2.11*).

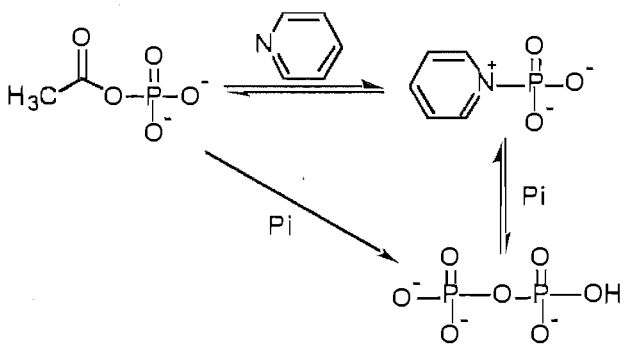

Figure 2.11 *Proposed conversion of acetyl phosphate to pyrophosphate in the presence of pyridine*

Pyridine acts as a catalyst for polyphosphate formation; it is a better nucleophile than inorganic phosphate as it is not negatively charged and thus experiences less repulsion from the negatively charged phosphate group. The *N*-phosphoryl pyridine is more

electrophilic than acetyl phosphate and therefore the reaction with inorganic phosphate is faster than in the case of acetyl phosphate[5].

The catalysis of phosphoryl transfer by nitrogen containing compounds, from acyl phosphate *via* *N*-phosphoryl intermediates, may be relevant to the study of prebiotic chemistry. Nitrogen-containing compounds were present in the prebiotic soup and thus this type of chemistry may have played a role in catalysis of formation of polyphosphates.

In addition, monovalent ions have been reported to catalyse the reaction of acetyl phosphate and inorganic phosphate to form pyrophosphate, in the absence of nitrogen-containing compounds. Herschlag and Jencks found the optimum conditions (7 M sodium ions, 0.16 M AcPi & 0.4 M Pi) produced 9.7% pyrophosphate[5]. The catalysis of formation of pyrophosphate in the presence of sodium ions is thought to be due to complex formation. The formation of pyrophosphate results from the nucleophilic attack by inorganic phosphate at the phosphorus centre of the acetyl phosphate. However, the phosphate portion of the acetyl phosphate is negatively charged and thus is not a very good electrophile. The sodium ions can complex with the acetyl phosphate and reduce the electrostatic repulsion between the electrophile and nucleophile. Multiple sodium ions would be required to complex the negatively charged phosphate group in the transition state. This is consistent with the high concentrations required to catalyse the reaction.

Divalent metal ions are also reported to catalyse the phosphoryl transfer reaction to form pyrophosphate. They are often used in concert with nitrogen containing nucleophiles.

We sought to investigate catalysis of pyrophosphate formation with combinations of the two types of catalysis, nucleophilic and metal ion catalysis, with attendant controls. In addition, we wished to study the effect of addition of nitrogen containing compounds such as pyridine and imidazole on the reaction of acetyl phosphate and inorganic phosphate, with a view to detecting any accumulation of *N*-phosphoryl pyridine or *N*-phosphoryl imidazole. We needed to synthesis authentic samples of these compounds in order to assist us in the detection of *N*-phosphoryl pyridine or imidazole through identification of their resonances by ^{31}P NMR spectroscopy.

2.3.2 Synthesis of *N*-Phosphoryl intermediates

An authentic sample of *N*-phosphoryl pyridine was needed as a standard in order to determine the chemical shift of its ^{31}P NMR resonance. This would allow us to attempt to detect *N*-phosphoryl pyridine in the aqueous reaction mixtures. Attempts to prepare (and measure the ^{31}P NMR spectrum of *N*-phosphoryl pyridine) by the method of Skoog and Jencks proved to be unsuccessful[19]. A solution of pyridine and potassium hydroxide was prepared and mixed with cold phosphoryl chloride. Skoog and Jencks report the half life of hydrolysis for *N*-phosphoryl pyridine to be 1.73×10^{-4} sec, at pH = 0.35[19]. The rate was not measured at higher pH. Other substituted pyridines with slower rates of hydrolysis were measured and the half lives became smaller at higher pH. In our case

it is likely the rate of hydrolysis for *N*-phosphoryl pyridine could not be measured as it is too fast. This is consistent with *N*-phosphoryl pyridine not being detected when ^{31}P NMR spectroscopy was performed on a sample of the reaction mixture. We were therefore unable to determine the chemical shift of the ^{31}P NMR resonance of *N*-phosphoryl pyridine.

Imidazole was another nitrogen containing nucleophile that we wished to investigate. In order to provide a standard for characterisation we synthesised a sample of *N*-phosphoryl imidazole. *N*-Phosphoryl imidazole was synthesised from phosphoric acid and *N,N'*-carbonyl-diimidazole by the method of Cramer, Schaller and Staab (*Figure 2.12*)[20].

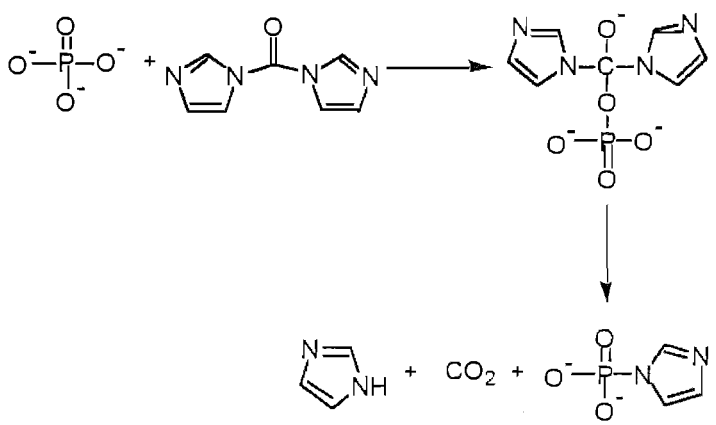

Figure 2.12 Synthesis of N*-phosphoryl imidazole*

When the sodium *N*-phosphoryl imidazole sample was analysed by ^{31}P NMR spectroscopy five resonances were observed. The chemical shifts and assignments are shown in *Table 2.2*, and are consistent with literature values[21,22].

^{31}P NMR δ ppm	Multiplicity	Species
3.50	s	Inorganic phosphate
-3.70	s	*N*-Phosphoryl imidazole
-4.46	d	Tripolyphosphate
-5.24	s	Pyrophosphate
-19.27	t	Tripolyphosphate

Table 2.2 *^{31}P NMR data from synthesis of N-phosphoryl imidazole*

N-Phosphoryl imidazole is reported to react with inorganic phosphate to produce pyrophosphate and tripolyphosphate[18]. Therefore, the pyrophosphate and tripolyphosphate detected in the synthesis of *N*-phosphoryl imidazole may be due to *N*-phosphoryl imidazole reacting with inorganic phosphate and pyrophosphate respectively *in situ* (*Figure 2.13*).

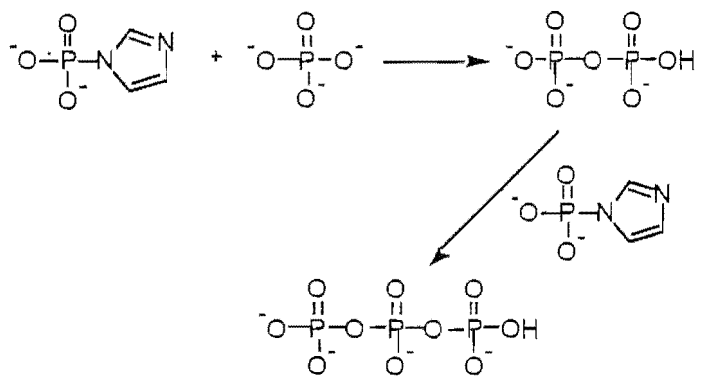

Figure 2.13 *Formation of pyrophosphate from N-phosphoryl imidazole*

The ^{31}P NMR chemical shift of *N*-phosphoryl imidazole was found to be –3.70 ppm. The authentic sample allowed us to test whether *N*-phosphoryl imidazole accumulates in phosphoryl transfer reactions containing imidazole. A series of experiments were performed using reaction mixtures containing acetyl phosphate and inorganic phosphate and metal ions in the presence and absence of imidazole and pyridine.

2.3.3 Sodium ions and imidazole or pyridine

Hershlag and Jencks report the formation of pyrophosphate from acetyl phosphate and inorganic phosphate in the presence of high concentrations of monovalent metal ions. They found the yield of pyrophosphate increased in the presence of pyridine.

Various experiments were performed in the presence and absence of sodium ions and pyridine in an effort to reproduce these results. Acetyl phosphate (0.10–0.13 M) and inorganic phosphate (0.16–0.25 M) were mixed with deuterium oxide in the presence of sodium ions (7 M) at pH ~7. No resonances consistent with pyrophosphate formation were detected in the ^{31}P NMR spectra obtained for these samples.

A number of reactions containing acetyl phosphate (0.10–0.13 M) and inorganic phosphate (0.16–0.25 M) in the presence of sodium ions (7 M) and pyridine (0.13–0.20 M) were performed. Again, no resonances consistent with pyrophosphate formation were detected by ^{31}P NMR spectroscopy. Using our different analytical methodology we were unable to reproduce the Herschlag and Jencks results.

The effect of sodium ions and imidazole was also investigated. A number of reactions containing acetyl phosphate (0.10–0.13 M) and inorganic phosphate (0.16–0.25 M) in the presence of sodium ions (7 M) and imidazole (0.13–0.20 M) were performed. However no resonances consistent with pyrophosphate or *N*-phosphoryl imidazole formation were detected by ^{31}P NMR spectroscopy.

Herschlag and Jencks reported a significant pH dependence on the yield of pyrophosphate. This could account for our failure to reproduce Hershlag and Jencks results. Alternatively, the difference in our methods for detection of pyrophosphate may account for the difference. Hershlag and Jencks quantified the pyrophosphate yields using the method of Kornberg[23], wherein manganese chloride was used to precipitate the pyrophosphate. However, since phosphate and pyrophosphate salts coprecipitate, they quantified the inorganic phosphate before and after hydrolysis. The amount of pyrophosphate present could be determined from the differences between these analyses. The detection method of Kornberg may result in catalysis of pyrophosphate formation during the quantification of pyrophosphate due to the presence of the manganese ions and/or as a result of surface reactions on the manganese phosphate precipitate. Whereas our method of analysis was non-destructive as we quantified the phosphate species by integration of ^{31}P NMR spectra.

We have been unable to produce pyrophosphate in the presence of sodium ions. However divalent metal ions were also reported to catalyse reactions of acyl phosphates[6,7,8]. This catalysis of hydrolysis in the presence of divalent metal ions is

thought to be due to complex formation. This theory was described previously in the section on sodium ions. Divalent metal ions including magnesium ions have been reported to catalyse the phosphoryl transfer reactions. This catalysis is even greater in the presence of both divalent metal ions and nitrogen nucleophiles.

2.3.4 Effect of magnesium ions and imidazole

We studied the effect of the combination of divalent metal ions and nitrogen nucleophiles on the reaction of acetyl phosphate with inorganic phosphate. A control reaction was performed without magnesium ions and nitrogen-containing compound, in order to provide a result that other reactions could be compared with. Acetyl phosphate was reacted with inorganic phosphate in deuterium oxide (pH = 6)[‡] at 30°C and analysed by ^{31}P NMR every hour for 13 hours. The results of these experiments are shown in *Figure 2.14*. No pyrophosphate was detected. The acetyl phosphate concentration decreased at the same rate as the inorganic phosphate increased, as would be expected for simple hydrolysis of acetyl phosphate.

---

‡ It should be noted that pH and pD are not the same when measured by glass electrode. The empirical relationship of pH (measured by glass electrode) and pD has been reported.

$$p[D^+] = pH_{measured} + 0.40$$

However, we measured the pD/pH with indicator paper. The effect of the deutrimum ions on indicator paper is not known. Therefore pD will be reported as the measured pH in this thesis.

The experiment was repeated in the presence of magnesium ions and the results were essentially identical to the result obtained in the absence of magnesium ions. Under these conditions magnesium ions do not appear to catalyse hydrolysis, or promote the formation of pyrophosphate.

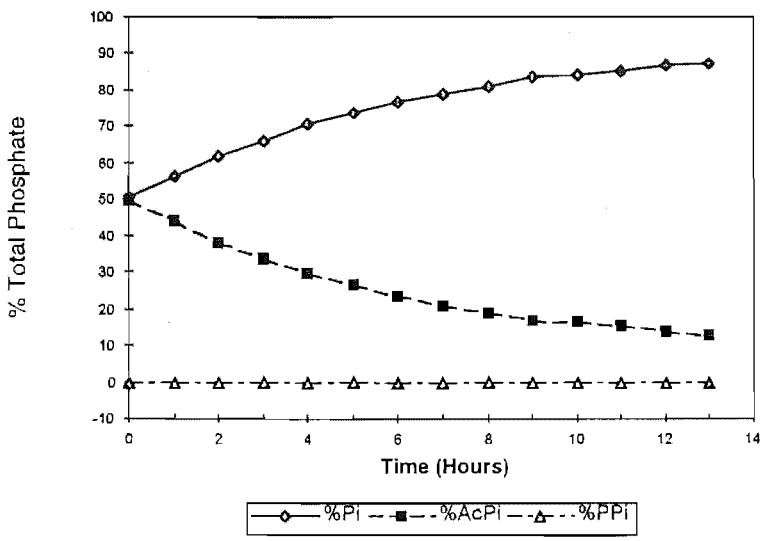

Figure 2.14 Reaction of acetyl phosphate and inorganic phosphate.

Performing the same reaction in the presence of imidazole led to the pH of the solution being slightly higher. Overall, the results obtained were not significantly different from those seen in the absence of imidazole. The combined results from these experiments are shown in *Figure 2.15*.

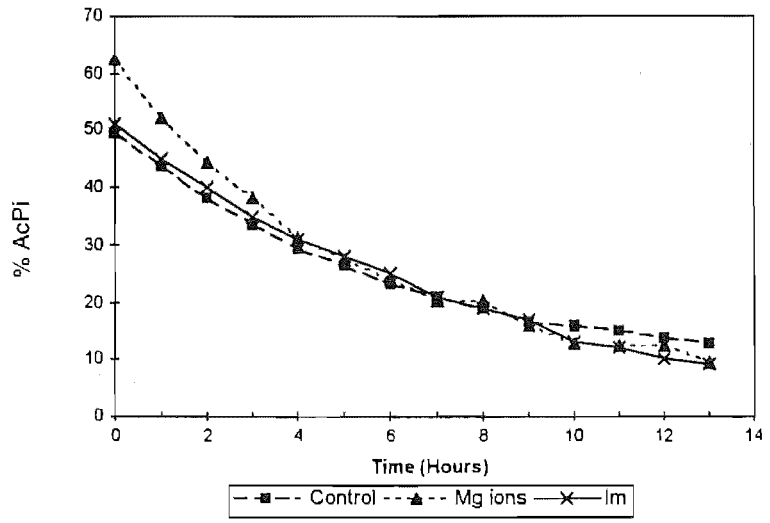

Figure 2.15 Comparison of loss of acetyl phosphate

A variety of different conditions were investigated in order to determine if a combination of magnesium and imidazole could catalyse the formation of soluble pyrophosphate from acetyl phosphate and inorganic phosphate. Only two experiments when analysed had levels of soluble pyrophosphate that could be quantified. The results of these reactions are shown in *Table 2.3*. No *N*-phosphoryl imidazole was detected in either reaction. In reaction 2.2, where a higher magnesium ion concentration was employed, a significant amount of white precipitate formed during the reaction. The magnesium concentrations were such that these reactions may have been at the limits of magnesium phosphate solubility. The solid magnesium phosphate salts may allow an alternative mechanism of catalysis on the surface of the precipitate.

Reaction	Temp °C	Time Hrs	% AcPi	% Pi	% PPi
2.1	23	48	14	84	2
2.2	30	3	21	77	2

Table 2.3 Experiments that produced pyrophosphate in the presence of imidazole

These reactions that produced pyrophosphate proved to be difficult to reproduce, possibly due to pH drift in the non-buffered reactions. pH has been shown to be important in similar reactions[5]. Therefore, buffers were investigated in an attempt to control the pH of the reaction mixture.

2.3.5 Buffers with magnesium ions and imidazole

Buffers provide a means of controlling the pH of reaction. It had been hoped that the inorganic phosphate and imidazole in the reaction mixtures would provide some natural buffer action close to neutral pH. Unfortunately, the concentration of these species was too low relative to the other reactants to prevent changes in pH occurring during the course of the reactions. Reaction mixtures were near neutral at the beginning of the experiment but the pH was much lower (3–4) by the end of the experiment.

Imidazole is a weak base and is therefore capable of acting as a buffer when the pH is close to the pK_a (pK_a = 6.95). Imidazole buffers (0.3–1 M) were prepared with pH of 6 & 7 respectively as the pH of interest is near neutral. Acetyl phosphate, inorganic phosphate and magnesium chloride were heated in the presence of these imidazole buffers at 30°C for 2 hours. The concentration of the magnesium ions and imidazole were varied between 0–500 mM and 0.3–1 M respectively. The results of these experiments are shown in *Table 2.4*. No pyrophosphate was detected in these reactions employing imidazole buffers.

Comparing reactions carried out in the presence and absence of magnesium ions indicated little difference between these reactions. Reactions containing a higher concentration of magnesium ions formed a white precipitate during the heating period. Given that inorganic phosphate is the phosphate species with the highest concentration in solution, and no pyrophosphate was seen by NMR, it is likely that the white precipitate is magnesium phosphate. There appeared to be no significant difference between the reactions at pH =6 and those at pH = 7. A slightly increased rate of hydrolysis was observed at the higher pH that may be due to the higher concentration of hydroxide ions.

$[Mg^{2+}]$ mM	[Im] mM	pH	% AcPi	% Pi	% PPi
0	300	6	41	59	0
150	300	6	32	68	0
150	300	7	30	70	0
500	1000	6	24	76	0
500	1000	7	22	78	0

Table 2.4 Experiments using imidazole buffers

An alternative buffer was investigated. The pH of interest is slightly more acidic than neutral therefore a phosphate buffer (0.3 M) was prepared with a pH=6.8. The second pK_a of phosphate is 7.21 thus phosphate is capable of buffering at pH= 6.8[24]. The reactions were run for 3.5 hours at 30°C, with varied magnesium and imidazole concentration. The results of these reactions are shown in *Table 2.5*. No soluble pyrophosphate or *N*-phosphoryl imidazole were detected by ^{31}P NMR spectroscopy. All reaction mixtures contained a white precipitate. This is probably due to the high concentration of phosphate which, with the magnesium ions, causes a precipitate to form. The formation of a precipitate renders the accuracy and reproducibility of these experiments doubtful. Previous experiments in non-buffered reactions show that pyrophosphate has some solubility in the presence of magnesium ions and imidazole; it is likely that, if this precipitate did contain pyrophosphate it would have been observed in solution.

$[Mg^{2+}]$ mM	[Im] mM	% AcPi	% Pi	% PPi
125	100	18.	82	0
250	100	20	80	0
500	25	5	95	0
500	50	17	83	0

Table 2.5 Experiments using phosphate as a buffer

Imidazole and magnesium ions appear only to catalyse the reaction of acetyl phosphate and inorganic phosphate under certain conditions. The reactions that lead to the successful production of pyrophosphate were incubated at different temperatures (23 & 30°C) for different times, and contained significantly different magnesium ion concentrations (*Table 2.3*). We were unable to identify the precise conditions which lead to the formation of pyrophosphate but magnesium ions concentration and pH may be important.

2.3.6 Magnesium ions and pyridine

The combination of pyridine and magnesium ions was investigated as a catalytic system for pyrophosphate formation from acetyl phosphate and inorganic phosphate. Acetyl phosphate was reacted with inorganic phosphate and pyridine (pH=6) at 30°C and analysed by ^{31}P NMR spectroscopy every hour for 10 hours. The results of this

experiment are shown in *Figure 2.16*. No pyrophosphate was detected. The acetyl phosphate concentration decreased at the same rate as the inorganic phosphate increased (*Figure 2.16*). Under these conditions pyridine does not appear to catalyse hydrolysis, or lead to formation of pyrophosphate.

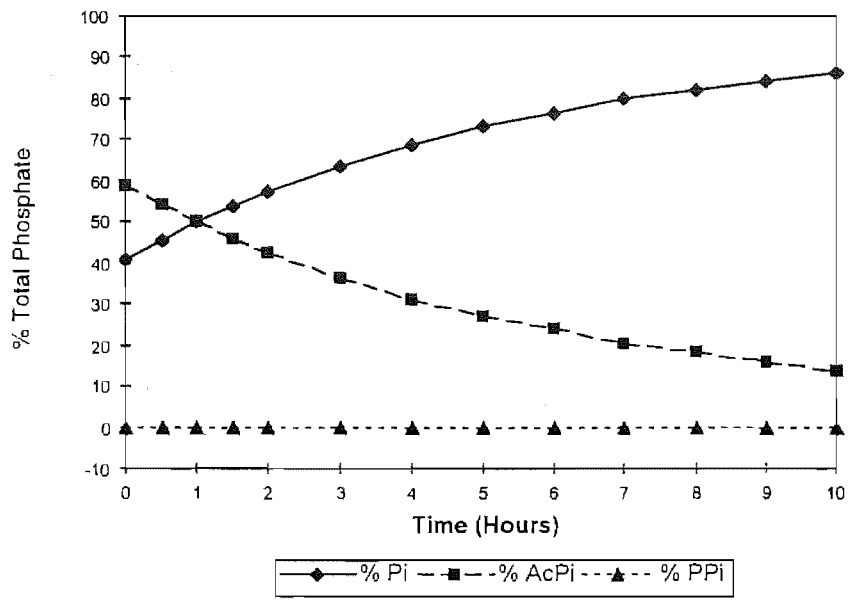

Figure 2.16 *Reaction of acetyl phosphate and inorganic phosphate in the presence of pyridine*

The other control reactions containing magnesium ions in the absence of pyridine were described in section 2.3.3

Reactions containing acetyl phosphate and inorganic phosphate in the presence of magnesium ions and pyridine were performed under a variety of different conditions. Various amounts of pyridine were added to the reaction mixtures that contained acetyl phosphate (25 mM), inorganic phosphate (25 mM) and magnesium ions (330 mM). The results of these reactions are shown in *Table 2.6*.

Pyridine mM	Temp °C	% AcPi	% Pi	% PPi
25	30	0	97	3
25	37	0	97	3
50	30	0	97	3
50	37	0	96	4
75	30	0	98	2
75	37	0	98	2
100	30	0	100	0
100	37	0	100	0

Table 2.6 Experiments using magnesium ions and various concentration of pyridine

The formation of soluble pyrophosphate reaches a maximum in the presence of 50 mM pyridine. A white precipitate formed during the reaction time when concentrations of pyridine greater than 75 mM were employed. A decrease in the yield of pyrophosphate coincides with the appearance of a white precipitate in the reaction mixtures. Therefore, the concentration of 50 mM pyridine was used in the following reactions, as it produced the largest yield of pyrophosphate without the associated problems of precipitation.

The effect of magnesium ion concentration on the yield of pyrophosphate was investigated. Various amounts of magnesium chloride were added to the reaction mixtures containing acetyl phosphate (25 mM), inorganic phosphate (25 mM), and pyridine (50 mM). These mixtures were heated at 20°C, 30°C, 40°C and 50°C respectively for 6 hours. The pyrophosphate formation results are shown in *Figure 2.17.*

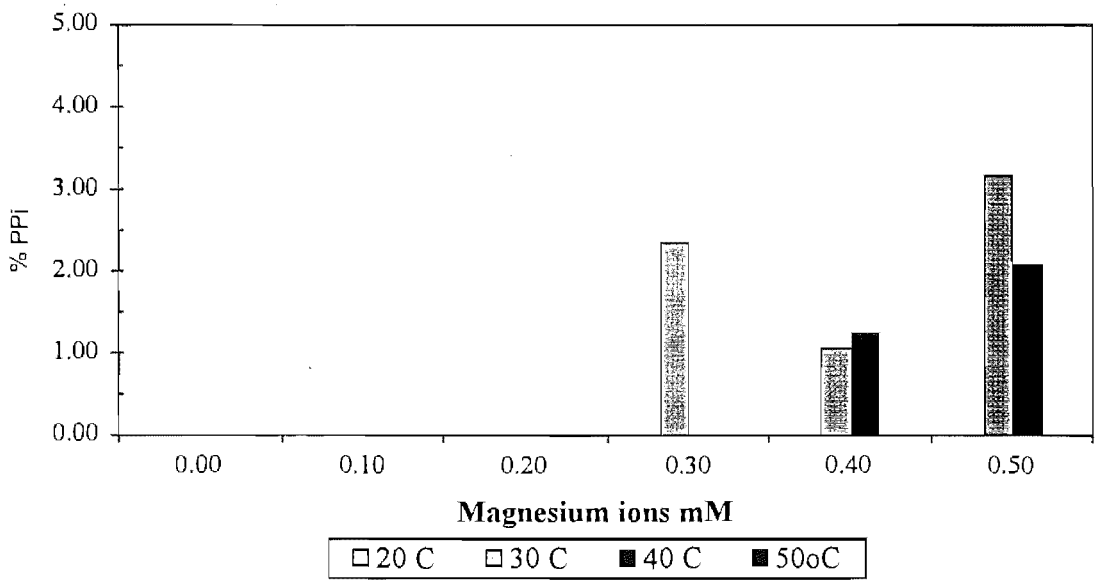

Figure 2.17 Percentage pyrophosphate formed at a range of magnesium ions concentrations and temperatures

At concentrations of 0.3 M magnesium ion and higher, a white precipitate formed during the reaction time. This precipitate may be responsible for the non-reproducibility of the yields of pyrophosphate. The pyrophosphate was only produced under these reaction conditions at concentrations of magnesium ions greater than 0.2 M and at temperature of 30°C and 40°C. When the reactions are heated at 50°C a white precipitate was formed with magnesium ion concentrations of 0.3 M and greater. The precipitate is probably mainly magnesium phosphate.

A graphical representation of these results shows the acetyl phosphate concentration to decrease with increasing temperature (*Figure 2.18*). The acetyl phosphate concentration decreases when magnesium ions are present. However, it appears to be relatively unaffected by increases in the magnesium ion concentration.

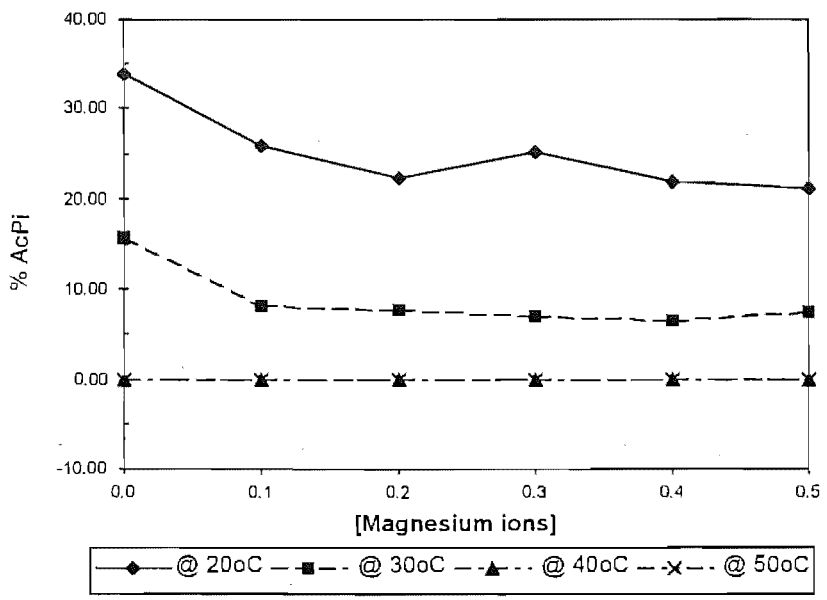

Figure 2.18 *Effect of magnesium ion concentration on percentage of acetyl phosphate*

No unidentified signals were detected in the ^{31}P NMR spectra of any of the reactions. The lack of a signal that could be assigned to *N*-phosphoryl pyridine in the ^{31}P NMR spectra does not imply it was not formed during the reaction. *N*-Phosphoryl pyridine has a very short half-life for hydrolysis[19]. Therefore if *N*-phosphoryl pyridine was a reaction intermediate, it would not be expected to accumulate in solution.

Many reactions were performed using both pyridine and magnesium ions under a variety of reaction conditions. The yields of pyrophosphate in these reactions were in the range

1–4%. The lack of reproducibility of the results implies uncertainty in quantification of pyrophosphate.

2.3.7 Buffers with magnesium ions and pyridine

Buffers were investigated in an attempt to control the pH during the reaction time. The pH was observed to drift downward during the reaction. It had been hoped that the phosphate and pyridine in the reaction mixtures would provide some natural buffer action, as the pK_a's of pyridinium ions and inorganic phosphate (pK_{a2}) are 5.25[10] and 7.21[24] respectively. However, the concentrations of these species appeared to be too low in the reaction mixtures to prevent changes in pH during the course of the reactions.

A phosphate buffer was our first choice as a buffer for this series of reactions. Phosphate was a reactant therefore there was little chance of the phosphate buffer altering the mechanism of reaction. Most buffers contain nucleophilic species which may react with the acetyl phosphate in competition with the inorganic phosphate. Phosphate can be used as a buffer when the pH is close to the pK_a. A phosphate buffer was prepared with pH = 6.8. Reactions containing acetyl phosphate, phosphate and magnesium chloride with the phosphate buffer were prepared and heated at 30°C for 3 hours. No pyrophosphate was detected following this reaction.

An alternative buffer was therefore investigated. We need a buffer that can not act as a catalyst in the way that has been proposed for some amines. Potassium hydrogen

phthalate with a pK_a of 4.82 was investigated (*Figure 2.19*). A phthalate buffer was prepared with pH = 5.8. Reactions containing acetyl phosphate, phosphate and magnesium chloride with phthalate buffer were prepared and heated at 30°C for 2 hours. Analysis of these reactions showed that no pyrophosphate was detected.

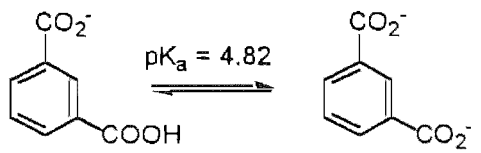

Figure 2.19 Acid dissociation of phthalate ions

Our attempt to investigate formation of pyrophosphate from reaction mixtures containing acetyl phosphate, inorganic phosphate, pyridine and magnesium ions in the presence of a buffer were unsuccessful.

2.3.8 Efforts to increase the solubility of magnesium phosphate and magnesium pyrophosphate

The formation of precipitates in some reaction mixtures containing acetyl phosphate, inorganic phosphate and magnesium ions in the presence or absence imidazole or pyridine was an ongoing problem. A precipitate formed if the concentrations of one or more reactants were increased too much. Our method of analysing these reactions is ^{31}P NMR spectroscopy. This method only detects soluble phosphorus containing species. Therefore care must be used in interpreting the results from reactions in which a precipitate formed.

The reactions with higher concentration of magnesium ions were of interest as, preliminary experiments indicated the yield of pyrophosphate increased with magnesium ion concentration. However, we needed a means of resolubilizing any precipitate before analysis by ^{31}P NMR spectroscopy, as both magnesium phosphate and magnesium pyrophosphate have low solubility.

Addition of hydrochloric acid was investigated. This treatment did resolubilize the precipitate. However, the chemical shifts of the ^{31}P NMR signals were changed markedly under these acidic conditions. Samples had to be spiked with authentic samples of compounds in order to identify the resonances. Acid treatment of reaction mixtures, that contained precipitates, did not result in pyrophosphate detection

Ethylenediaminetetracetate (EDTA) is a well known hexadentate ligand. EDTA forms water soluble complexes with a wide range of metal ions. Therefore the use of EDTA to resolubilize the magnesium salt was investigated. EDTA was not added prior to the reactions, as the EDTA may have sequestered the magnesium ions and interfered with their ability to catalyse the reaction. In addition, EDTA contains amine groups, which may affect the reaction. Therefore sodium EDTA was added after the reaction time in an effort to resolubilize the phosphate precipitates. ^{31}P NMR spectroscopy was employed in order to compare the results in the presence and absence of sodium EDTA. Reactions containing pyridine, magnesium ions, acetyl phosphate and inorganic phosphate were heated at 50°C, with and without addition of the disodium salt of EDTA after heating. The samples containing EDTA still contained some white precipitate.

Neither samples treated with EDTA nor those without produced any pyrophosphate. This is consistent with previously discussed experiments heated at 50°C.

2.3.9 Magnesium ions and other nitrogen containing compounds

Pyridine has been shown to catalyse the reaction of acetyl phosphate and inorganic phosphate in the presence of magnesium ions. Some limited evidence for imidazole catalysis was observed. Therefore, we investigated two other nitrogen-containing organic compounds for evidence of catalysis.

Adenine and adenosine are biologically important compounds. Adenine is the heterocyclic base found in adenosine which, in turn, forms the organic part of adenosine diphosphate (ADP) and adenosine triphosphate (ATP) (*Figure 2.20*).

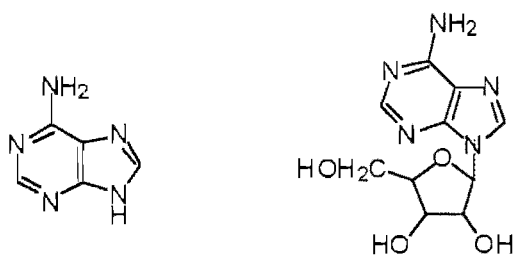

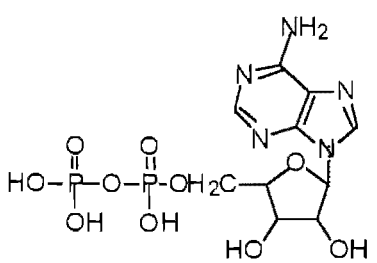

Figure 2.20 *Structures of adenine, adenosine and adenosine diphosphate*

Adenine is not very soluble in water. Reactions were carried out under similar conditions to those used in the optimised pyridine and magnesium ions experiments. A 2% yield of pyrophosphate was produced. This contrasts with the reaction of acetyl phosphate, inorganic phosphate, magnesium ions and adenosine in which no pyrophosphate was formed. This may be an indication that adenine could play a role in the evolution of phosphoryl transfer biochemistry. The efficiency of phosphoryl transfer was, however, still too low for definitive conclusions to be drawn.

2.3.10 Conclusions

Magnesium and nitrogen compounds (imidazole, pyridine and adenine) catalyse the formation of pyrophosphate from acetyl phosphate. The results from the study of these reactions demonstrate that the optimum conditions for pyrophosphate formation, are close to the solubility limits of magnesium phosphate species. The possible importance of the surface catalysis lead to the desire to study insoluble metal phosphate systems. The systems were chosen because they have possible prebiotic relevance.

2.4 Catalysis by iron(II) ions

2.4.1 Why iron(II)?

Iron is amongst the most abundant elements both cosmically and terrestrially. When the earth was formed most of the iron sank to form the earths core. The earth developed, life evolved, and, in time, photosynthesis began. Photosynthesis converts carbon dioxide and water into organic molecules and oxygen. This production of oxygen changed the atmosphere from a reducing environment to an oxidising one. Iron exists in number of different oxidation states, the most common are Fe(0), Fe(II) and Fe(III). Oxygen can oxidise ferrous ions to ferric ions. Evidence for this oxidation can be gleaned from the banded iron sediments found in geological samples. These are rich in ferric minerals in the rock layers. The occurrence of these bands, originating approximately 2 billion years ago is thought to coincide with the accumulation of oxygen in the atmosphere. Oxygen levels are thought to have been low before photosynthetic bacteria evolved. In this environment ferrous ions probably were more abundant in the hydrosphere than ferric ions.

In the present age, iron centres have been found in many proteins with varied functions. Many of these iron-containing proteins actually contain iron-sulfur clusters at their active sites. The importance of this has been discussed in chapter 1.

Ferrous ions have interesting chemical properties that may explain why nature evolved to use iron so extensively in biochemistry. Ferrous ions form complexes with many of the biologically important ligands which contain nitrogen, oxygen and sulfur groups. This coordination can effect the properties of both the cation and ligands.

Recently, a key evolutionary role has been proposed for mineral surfaces such as ferrous sulfide. The surface of minerals may catalyse reactions that lead to the formation of the compounds needed for the evolution of life. Early evolution of life is thought to have occurred in water, probably the ocean. Therefore dilution of compounds before they could react further would be a problem that evolution had to overcome. In particular, the low concentration of phosphate in seawater presents challenges to the evolution of phosphate-based biochemistry. Clearly surfaces could have a role in bringing reactants together. If reactions occur on a surface the reactants and products may remain adsorbed to the surface after the reaction has taken place. This means the compounds are held in close proximity and thus may react further. Many iron compounds are insoluble in water (e.g. ferrous phosphate). Therefore we wished to investigate ferrous ions as a potential promoter of pyrophosphate formation from acetyl phosphate and inorganic phosphate.

2.4.2 Resolubilizing ferrous phosphates

The K_{sp}'s of ferrous acetyl phosphate, ferrous phosphate and ferrous pyrophosphate are small. The low solubility of ferrous phosphate species introduces a problem for the

proposed detection method, ^{31}P NMR spectroscopy. The precipitate surface may adsorb some of the compounds we wished to quantify in solution. Indeed, this possibility is closely related to our reasons for performing the experiments. Thus, it was necessary to find a method of removing these compounds and any products from the solid surface.

Addition of cyanide ions was investigated as a means of removing any adsorbed phosphate species. Cyanide ions form a stable complex with the ferrous ions (the overall stability constant for $[Fe(CN)_6]^{4-}$, $\log \beta_6 = 24$). The large stability constant for formation of $[Fe(CN)_6]^{4-}$ indicates that cyanide ions will likely displace any other species bound to iron. The amount of cyanide required for complete desorption of phosphate ligands was determined by addition of varied molar equivalents of potassium cyanide to solutions containing ferrous ions, acetyl phosphate, inorganic phosphate and pyrophosphate. Analysis of the resulting supernatants was undertaken by ^{31}P NMR spectroscopy. The molar ratio of the phosphate species was restored when > 6 molar equivalents (relative to ferrous ions) of potassium cyanide was added to the reaction mixture. Any insoluble ferrous compounds were removed by centrifugation. This enabled us to detect, by ^{31}P NMR spectroscopy, any phosphate species that were originally adsorbed on the solid surface.

2.4.3 Reactions with ferrous ions added

Initial studies employed reaction conditions that were similar to those which provided the optimum yield of pyrophosphate in the presence of magnesium ions and pyridine.

Ferrous ions (330 mM) were added to the reaction mixture containing acetyl phosphate and inorganic phosphate. After the reaction time, the reaction was treated with cyanide ions as described above. The resulting precipitate was separated by centrifugation before analysis by ^{31}P NMR spectroscopy. The high concentration of ferrous ions in the small reaction volume lead to difficulties during analysis of the solution. At this concentration of ferrous ions the amount of precipitate formed upon addition of the cyanide ions made it difficult to obtain enough solution to enable a good lock to be obtained in the NMR spectrometer and thus the signal to noise ratio was poor.

We could increase the reaction volume while maintaining the concentrations, but this would require the use of greater volumes of deuterium oxide, which is relatively expensive. Alternatively, we could reduce the concentrations of the starting materials. This would reduce the concentration of pyrophosphate and hence the pyrophosphate ^{31}P NMR signal would be small. This was less than ideal, as weak signals give integrations which have a higher error associated with them. It was therefore decided to try reducing the concentration of the ferrous ions. Investigation of the effect of varying the amount of ferrous ions added to the reaction gave mixed results.

Further study showed that all reactions containing ferrous ions contained pyrophosphate but the yields were highly variable. The average yield was 15 % pyrophosphate. The precise reaction conditions were difficult to maintain and therefore the lack of reproducibility was not unexpected. The factors which may differ between reactions include the degree of oxidation of ferrous ions to ferric ions by trace oxidants (oxygen),

the heterogenous nature of the reaction mixture (with inherent variations in the surfaces formed between experiments), and the pH.

2.4.4 Oxidation of ferrous ions to ferric ions

Ferrous ions can be oxidised to ferric ions by oxygen. The standard reduction potentials of ferric ions and oxygen are 0.77 V and 1.23 V respectively. The E° for the oxidation of ferrous ions by oxygen is +0.46 V and is therefore spontaneous. This is at standard conditions which implies 1 M hydrogen ion concentration. Our reactions are performed close to pH=7. The Nernst equation can be used to calculate the reduction potential of oxygen at pH=7. It was calculated to be 0.817 V at 25°C. Therefore the E for the oxidation of ferrous ions by oxygen (25°C, pH=7) is 0.05 V and is spontaneous. However, +0.05 V does not provide the large overpotential required for rapid reaction. Therefore, ferrous ions in aqueous solution are slow to oxidise. The reduction potential is, however, affected by any change in the pH or the amount of oxygen present.

Methods for limiting the amount of oxygen were therefore required. Reaction mixtures were prepared in which different degassing procedures were performed on the solvent. The first method contained deuterium oxide straight from the bottle. The reactants were added and the vessel was allowed to stand open to the atmosphere for 10 mins before capping and heating for the appropriate time. The second method used deuterium oxide that had had oxygen-free nitrogen bubbled through the reaction mixture for 20 seconds before capping. Finally, a freeze-pump-thaw procedure was employed for the third

method. Oxygen free nitrogen was used to provide an atmosphere. This was repeated twice before the deuterium oxide was transferred by syringe to reaction vessels sealed with suba seals. The results of these reactions are shown in *Table 2.7*.

Method of deoxygenation		% Pi	% AcPi	% PPi
1	None	88	0	12
2	N_2 bubbling	83	0	17
3	Freeze/Pump/Thaw	81	0	19

Table 2.7 Comparison of deoxygenation of deuterium oxide

Although there appears to be a slight increase in yield of pyrophosphate as the degree of deoxygenation is increased, the difference is probably not significant given the level of reproducibility that is normally observed in these experiments. All the reaction mixtures contained rust, identified by its distinctive red-brown colour. The rust was concentrated at or above the solvent-atmosphere interface. All reactions henceforward were deoxygenated by bubbling oxygen-free nitrogen through the reaction mixture for approximately 20 seconds, before capping the reaction vessel with a wheaten vial cap.

2.4.5 Reproducibility issues

Examining the results for the reaction performed at the optimised conditions determined for ferrous ions we can see there is a spread of results as shown in *Table 2.8*.

Temp °C	pH	% Pi	% PPi
54	5	90	10
54	5	76	24
54	5	82	18
54	5	81	19
54	5	80	20
54	5	86	14
54	5	87	13
54	5	93	7
50	5	85	15
50	7	88	12
50	7	80	20
50	7	83	17

Table 2.8 *Formation of pyrophosphate in the presence of ferrous ions*

Averaging these results of those experiments shown at pH = 5 gives a yield of pyrophosphate of 15% compared with a yield of inorganic phosphate of 85%. The proportion of experiments with results in the various ranges is shown in *Table 2.9*.

Range	Number	% in this range
0 - 5% PPi	0	0
6 - 10% PPi	2	22
11 - 15% PPi	3	33
16 - 20% PPi	3	33
21 - 25% PPi	1	11

Table 2.9 Spread of % pyrophosphate formation in the presence of ferrous ions

This was compared to the results of reactions performed at pH = 7 where average yields of 16% pyrophosphate and of 84% inorganic phosphate were obtained. Comparison of the results from these experiments indicates that the pH is not very important. Therefore the lack of reproducibility observed in the reaction of acetyl phosphate with inorganic phosphate is probably not due to differences in pH between the less well buffered mixtures.

2.4.6 Reactions of acetyl phosphate with ferrous ions in the presence of nitrogen-containing compounds

Pyridine was investigated to see whether it complemented the catalysis of ferrous ions of the reaction of acetyl phosphate with inorganic phosphate, analogous to the synergy observed in the presence of magnesium ions. Reactions (pH=5) containing acetyl phosphate (25 mM), inorganic phosphate (25 mM) and ferrous ions (125 mM) with and

without pyridine (25 mM) were heated for 15, 60, 90 and 150 mins at 54°C. The results of these experiments are shown in *Table 2.10*.

Time	Pyridine			No Pyridine		
(mins)	% Pi	% AcPi	% PPi	% Pi	% AcPi	% PPi
15	64	27	9	63	30	7
60	81	3	16	80	6	14
90	88	0	12	86	0	14
150	91	0	9	87	0	13

Table 2.10 Comparison of reactions containing pyridine and no pyridine

Analysis of these results indicated that there was probably no significant difference between reactions containing pyridine and the controls. Any difference is small relative to the lack of reproducibility previously observed in these reactions containing ferrous ions.

A series of reaction mixtures that contained acetyl phosphate, inorganic phosphate, ferrous ions and pyridine were prepared in order to assess the reproducibility to this reaction. These reaction mixtures were heated at 54°C for 2 hours before potassium cyanide was added and ^{31}P NMR spectroscopy analysis undertaken. The results of these experiments are shown in *Table 2.11*.

% Pi	% PPi
88	12
91	9
86	14
74	26
81	19
83	17
92	8

Table 2.11 Comparison of a series of experiments containing ferrous ions and pyridine

The results at pH = 5 combine to give an average yield of pyrophosphate of 15%. The yield of inorganic phosphate was 85%. The results were again somewhat irreproducible. The proportion of experiments with results in the various ranges is shown in *Table 2.12*

Range	Number	% in this range
0 - 5% PPi	0	0
6 - 10% PPi	2	29
11 - 15% PPi	2	29
16 - 20% PPi	2	29
21 - 25% PPi	1	14

Table 2.12 Spread of % pyrophosphate yields

There is little difference between the reaction with pyridine and without pyridine. The amount of pyrophosphate formed was the same. There is a little more spread in the results but this is probably not significant.

A range of other nitrogen-containing compounds were screened in an effort to find compounds that significantly changed the amount of pyrophosphate formed. The averaged results of these experiments are shown in *Table 2.13*.

Compounds	pH	% Pi	% AcPi	% PPi
Imidazole	5	100	0	0
Imidazole	7	79	0	21
Glycine	5	93	0	7
Glycine	7	87	0	13
Histidine	6	91	0	9
Histidine	7	89	0	11
Imidazole dicarboxylic acid	5	100	0	0
Imidazole dicarboxylic acid	7	84	0	16
Pyridine dicarboxylic acid	7	92	2	6
Picolinic acid	7	87	0	13
Pyrozole 3,5-dicarboxyl acid	7	80	0	20
L-Aspartic acid	7	88	0	12
Adenosine	7	93	0	7

Table 2.13 *Effect of nitrogen-containing compounds on pyrophosphate formation*

The yields of pyrophosphate are probably not significantly different to those observed for reactions containing acetyl phosphate, inorganic phosphate and ferrous ions. Any difference is probably within the normal variation for these experiments.

2.5 Sulfur Chemistry

2.5.1 Why ferrous sulfide?

Iron-sulfur species are important in biochemistry. Iron-sulfur clusters are found in the active site of many proteins. Iron-sulfur centres have also been identified as sites for nonredox catalysis.

Ferrous sulfide is a geochemically abundant mineral. Iron sulfide has a low solubility in water. Iron sulfide salts appear in nature in various forms with different stoichiometries of iron and sulfur. Large deposits are found in deep ocean rifts where the hot magma is mixing with the cold ocean water. This causes the mineral to solidify. The production of large amount of black ferrous sulfide lead to the rifts being called black smokers. Many organisms live in and around these black smokers. These black smokers have been proposed as a region where life may have originated. There is considerable interest in the organisms that are found there, due to the novel biochemistry that they exhibit. Their metabolism is thought to be more dependent on metal ions for catalysis including metal-sulfur clusters. The potential catalytic properties and the abundance of prebiotic ferrous

sulfide lead us to assess ferrous sulfide as a catalyst for phosphoryl transfer reactions. Thus we investigated whether iron sulfide catalysed the formation of pyrophosphate from acetyl phosphate and inorganic phosphate.

2.5.2 Resolubilization of phosphate species in the presence of ferrous sulfide

Previously in reactions that contained ferrous ions, > 6 molar equivalents (relative to ferrous ions) of potassium cyanide was added to the reaction mixture to resolubilize the phosphate species. This concentration of cyanide ions was evaluated in trial reactions that contained ferrous sulfide, acetyl phosphate, inorganic phosphate and pyrophosphate. When this reaction mixture was analysed by ^{31}P NMR spectroscopy the molar ratio of the phosphate species was restored to the starting molar ratio. Therefore the same method of resolubilization was used for reactions that contained ferrous ions or ferrous sulfide.

2.5.3 Reaction of acetyl phosphate in the presence of ferrous sulfide

The ferrous sulfide used in these reactions was formed *in situ*. When ferrous ions are added to sulfide ions a black precipitate forms immediately. It has been postulated that any phosphate species present are adsorbed on the ferrous sulfide surface. The ordering of mixing of reagents in this system may therefore be important. We varied the order of addition of ferrous ions, sulfide ions and phosphate species in order to investigate this.

The results are shown in *Table 2.14*. When the ferrous ions and sulfide ions were mixed first, the colloidal suspension of ferrous sulfide was present prior to addition of the phosphate species. The experiments carried out under these mixing conditions produced 13% pyrophosphate. However when the phosphate species were added to a solution containing ferrous ions before the sulfide ions the yield was 10% pyrophosphate. For the reactions that had the sulfide ions and phosphate species added at the same time the pyrophosphate produced was 10%. Analysis of the results from these experiments showed no significant difference on changing the order of addition of the reagents.

Order of addition	Fe^{2+} M	S^{2-} M	pH	% Pi	% PPi
1. Fe^{2+} – 2. S^{2-} – 3. AcPi/Pi	0.1	0.1	7.0	87	13
1. Fe^{2+} – 2. AcPi/Pi – 3. S^{2-}	0.1	0.1	7.0	90	10
1. Fe^{2+} – 2. AcPi/Pi/S^{2-}	0.1	0.1	7.0	90	10

Table 2.14 Comparison of order of addition of starting materials

Although the order of addition appears irrelevant we chose to form the ferrous sulfide before addition of the phosphate species as this was experimentally more convenient. The effect of varying the amounts of ferrous ions and sulfide ions were investigated. The results are shown in *Table 2.15*.

Fe^{2+} M	S^{2-} M	pH	% Pi	% PPi
0.1	0.1	5.5	88	12
0.2	0.2	5.5	90	10
0.1	0.05	5.5	92	8

Table 2.15 Comparison of amounts of ferrous ions and sulfide ions

The reaction mixtures were analysed before and after treatment with cyanide ions in order to ascertain whether the phosphate species were adsorbed on the colloidal Fe-S surface during the reaction. When the untreated reaction mixtures were centrifuged and the supernatant solution was analysed by ^{31}P NMR spectroscopy, the resulting spectra exhibited no signals. This indicated that there was no appreciable amount of phosphate species in solution. When the ^{31}P NMR spectra were collected after treatment with cyanide ions, phosphate species were detected. Therefore it was concluded that the phosphate species are absorbed on the ferrous sulfide surface, prior to cyanide treatment. The results of these experiments were averaged to give yields of 90% of inorganic phosphate and 10% of pyrophosphate.

The pH (within the range 5.5 to 7) and amount of ferrous sulfide appeared to have no effect on the amount of pyrophosphate formed. This is consistent with the results observed previously for ferrous ions. The reproducibility of the reactions appeared to be somewhat better than that observed for the earlier ferrous ions experiments. All the results in the pH range (5.5 - 7) were within the range 10 – 13% yield of pyrophosphate, that is, within experimental error.

When an excess of ferrous ions over sulfide ions was used the average yield of pyrophosphate produced decreased to 8%.

2.5.4 Reaction of acetyl phosphate in the presence of ferrous sulfide and various nitrogen containing compounds

The synergy of metal ions and nitrogen nucleophiles to yield more pyrophosphate than either the metal ions or nitrogen nucleophiles alone has been shown in some cases. We have reproduced that result with magnesium ions and pyridine in section 2.3. Therefore we evaluated a number of nitrogen containing compounds in the presence of ferrous sulfide in order to ascertain whether a similar synergy between metal-sulfur and nitrogen nucleophile catalysis could be detected.

A variety of nitrogen containing compounds were screened for catalytic effect on the reaction in the presence of ferrous sulfide. The nitrogen containing compounds included amino acids, imidazole and pyridine derivatives and other compounds. The results are shown in *Table 2.16*.

Analysis of the results from these experiments indicated the yields of pyrophosphate were decreased by the addition of the nitrogen containing compounds. This may be due to increased competition for ligand binding sites on the ferrous sulfide surface. That is the carboxylic acid groups are anionic at the pH of the reaction mixture thus they may

compete with the phosphate species for ligand binding sites. These ligand-binding sites are proposed sites of catalysis of the reaction of pyrophosphate formation. These reactions were not investigated further due to the low yields of pyrophosphate that were observed.

Reaction	pH	% Pi	% PPi
Glycine	7	96	4
Histidine	7	97	3
Imidazole dicarboxylic acid	7	97	3
Pyridine dicarboxylic acid	7	99	1
Picolinic acid	7	98	2
L- Aspartic acid	7	100	0

Table 2.16 Effect of nitrogen-containing compounds on pyrophosphate formation

2.6 Summary

In this chapter we have described the use of a range of metal salts to promote pyrophosphate formation from reaction of inorganic phosphate and acetyl phosphate. Pyrophosphate was not formed in the reaction mixtures containing acetyl phosphate, inorganic phosphate and high concentrations of sodium or magnesium ions. However, when magnesium ions were present in conjunction with pyridine a small amount (1–4%)

of pyrophosphate was detected. Under the same conditions imidazole and magnesium ions did not appear to catalyse the formation pyrophosphate. The yields of pyrophosphate were highest at the limit of the magnesium phosphate solubility.

Ferrous ions were much more efficient at promoting the formation of pyrophosphate (yields of pyrophosphate of approximately 15%). Addition of pyridine or a variety of other nitrogen containing compounds did not enhance the pyrophosphate yield further. Reactions that contained acetyl phosphate, inorganic phosphate and ferrous sulfide produced significant amounts of pyrophosphate (10%). No synergy of ferrous salts and nitrogen nucleophiles catalysis was observed.

The promotion of pyrophosphate formation at near neutral pH by ubiquitous metal salts is considered to be a feasible route for prebiotic production of pyrophosphate. The high yielding ferrous ions and ferrous sulfide reactions are of particular interest in this regard. These reactions may represent prebioticly feasible reactions leading to important biological molecules. The near neutral aqueous conditions under which they proceeded could be similar to those which may have existed at early times in the earth's history.

2.7 References

1 W. P. Jencks & J. Carriuolo, *J. Biol. Chem.*, **234**, 1272 (1959).

2 D. R. Phillips, *J. Org. Chem.*, **34**, 2710 (1969).

3 D. E. Koshland, *J. Am. Chem. Soc.*, **73**, 4103 (1951).

4 G. Di Sabato & W. P. Jencks, *J. Am. Chem. Soc.*, **83**, 4393 (1961).

5 D. Herschlag & W. P. Jencks, *J. Am. Chem. Soc.*, **108**, 7938 (1986).

6 D. Herschlag & W. P. Jencks, *J. Am. Chem. Soc.*, **109**, 2987 (1987).

7 T. H. Fife & M. P. Pujari, *J. Am. Chem. Soc.*, **112**, 5551 (1990).

8 D. E. Koshland, *J. Am. Chem. Soc.*, **74**, 2286 (1952).

9 F. Lipmann & L. C. Tuttle, *J. Biol. Chem.*, **153**, 571 (1944).

10 R. C. Weast, *CRC Handbook of Chemistry and Physics*, CRC Press (1983).

11 A. W. D. Avison, *J. Chem. Soc.*, 732 (1955).

12 F. Lipmann & L. C. Tuttle, *J. Biol. Chem.*, **159**, 21 (1945).

13 D. Herschlag & W. P. Jencks, *J. Am. Chem. Soc.*, **111**, 7579 (1989).

14 C. H. Fiske & Y. Subbarrow, *J. Biol. Chem.*, **66**, 375 (1925).

15 U. Weber & H. Thiele, *NMR Spectroscopy: Modern Spectral Analysis*, Wiley (1998).

16 W. E. Morgan & J. R. Van Wazer, *J. Am. Chem. Soc.*, **97**, 6347 (1975).

17 A. L. Weber, *BioSystems*, **15**, 183 (1982).

18 A. L. Weber, *J. Mol. Evol.*, **18**, 24 (1981) and references therein.

19 M. T. Skoog & W. P. Jencks, *J. Am. Chem. Soc.*, **106**, 7597 (1984).

20 F. Cramer, H. Schaller & H. A. Staab, *Chem. Ber.*, 1622 (1961).

21 J. R. Van Wazer, C. F. Callis, J. N. Schoolery & R. C. Jones, *J. Am. Chem. Soc.*, **78**, 5715 (1956).

22 M. M. Crutchfiled, C. F. Callis, R. R. Irani & G. C. Roth, *Inorg. Chem.*, **1**, 813 (1962).

23 A. Kornberg, *J. Biol. Chem.*, **182**, 779 (1950) and references therein.

24 E. Etaix & R. Buvet, *Origins of Life*, **6**, 175 (1975) and references therein.

Chapter 3

Wächtershäuser Chemistry

3.1 Introduction

A chemoautotrophic theory for the origin of life has been proposed by Wächtershäuser, as introduced in Chapter one[1]. In this theory the reductive fixation of carbon and other feedstock compounds are mediated by the oxidative formation of pyrite (FeS_2) from ferrous sulfide and hydrogen sulfide (*Figure 3.1*).

$$FeS + H_2S \longrightarrow FeS_2 + 2H^+ + 2e^- \quad E^0 = -620\ mV$$

Figure 3.1 Oxidation of FeS to form pyrite

The low solubility of iron sulfides is another factor in this chemoautotrophic theory that has been put forward. The surface of pyrite contains ferrous ions, hence anionic compounds may bond to the surface, increasing the local concentration of potential reactants relative to the bulk aqueous solution[1].

Wächtershäuser and coworkers have shown that the reductions of a number of simple compounds is greatly enhanced by iron sulfide both in the presence and absence of hydrogen sulfide[2]. They have produced ammonia from nitrate; ethene and ethane from ethyne and mercapto compounds; acetic acid from mercaptoacetic acid; and cinnamate and phenylpropionate from phenylpyruvate. Their results are summarised in *Table 3.1*. Generally, these reactions involve reduction of various compounds in hot water using FeS/H_2S as a reagent system. It is presumed that the ferrous sulfide surfaces play a role in promoting the reaction[7]. This reductive chemistry may have provided the building blocks for many prebiotic reactions.

Reactant	Reaction conditions	Product	Yield %
Nitrate	FeS/H_2S pH = 4 100°C 3 days	Ammonia	42.3
Ethyne	FeS/H_2S pH = 6 100°C 14 days	Ethene	15.2
Ethyne	FeS/H_2S pH = 6 100°C 14 days	Ethane	0.6
Mercaptoacetic acid	FeS/H_2S 100°C 28 days	Acetic acid	52.0
Phenylpyruvate	FeS/H_2S 100°C 12 days	Cinnamate	0.03
Phenylpyruvate	FeS/H_2S 100°C 12 days	Phenyl propionate	2.4

Table 3.1 Reduction of a range of organic compounds

Organosulfur chemistry is likely to be significant in the reaction systems. In addition to the simple desulfurization of thiols, such as mercaptoacetic acid, other types of sulfur-based chemistry have been implicated. Reduction of mercaptoacetic acid in the presence of aniline has been reported to produce *N*-phenyl acetamide[3]. To account for these observations Wächtershäuser postulates that thioacetic acid is an intermediate in the reduction of mercaptoacetic acid (*Figure 3.2*)[3]. In this way, Wächtershäuser envisages the coupling of this redox chemistry to the generation of amide bonds *via* the reaction of thiocarboxylic acid with amines (*Figure 3.3*).

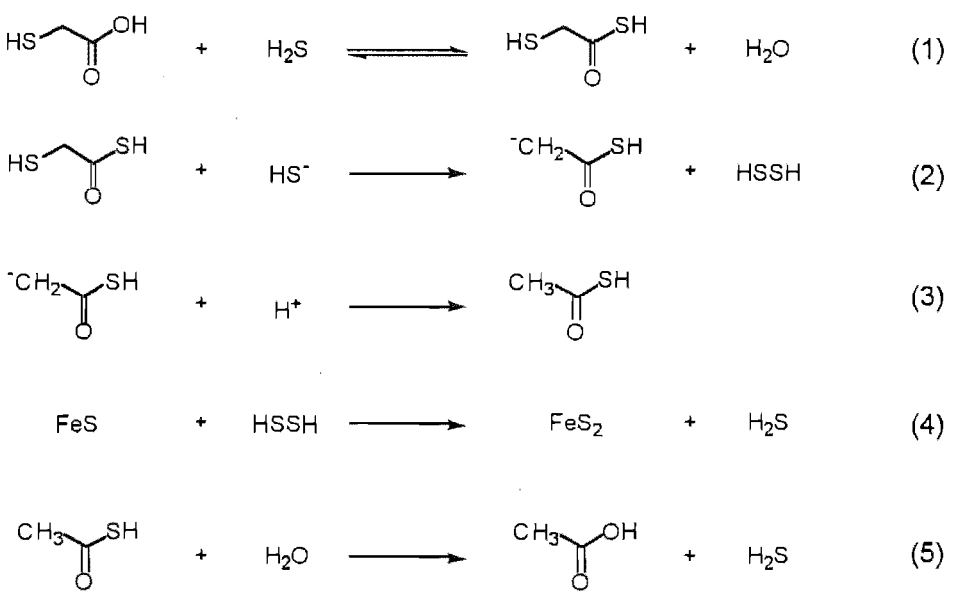

Figure 3.2 Wächtershäuser's proposed mechanism for reduction of mercaptoacetic acid

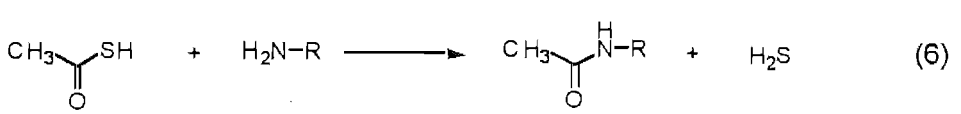

Figure 3.3 Amide bond formation

Each individual step of this proposed mechanism is chemically plausible, although this is by no means he only possible route to the reported products. The equilibrium for formation of mercaptothioacetic acid is unfavourable (equation 1, *Figure 3.2*). However, Wächtershäuser proposes that this equilibrium is made more favourable by the subsequent reduction of the mercaptothioacetic acid to form thioacetic acid (equation 2 & 3, *Figure 3.2*). Once the mercaptothioacetic acid is formed it may react with many different nucleophiles, in competition with the reduction reaction. Indeed, the reduction chemistry could be coupled with amide bond formation as shown in *Figure 3.4*. This chapter describes efforts to test aspects of this hypothesis.

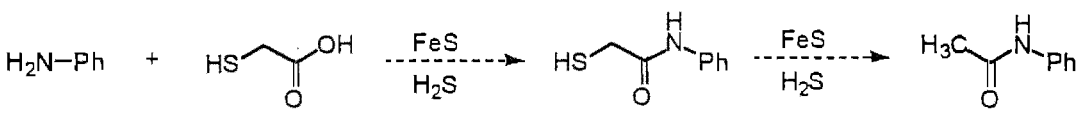

Figure 3.4 Coupling of reduction chemistry and amide bond formation

3.2 Reaction methodology for iron-sulfur mediated reduction

3.2.1 Introduction

The series of reduction reactions, mediated by ferrous sulfide and hydrogen sulfide studied by Wächtershäuser and coworkers *(Table 3.1)* includes the reduction of mercaptoacetic acid to form acetic acid, and the reduction of phenylpyruvate to form 3-

phenylpropionate[3]. We decided to use this chemistry as a starting point for our investigation. The reaction conditions and monitoring techniques they report were taken as a starting point for our reaction system. However, as our experimental equipment was not identical to that described by Wächtershäuser, we had to establish reaction methodology, within the constraints of our system, that could emulate their results.

3.2.2 Preparation of ferrous sulfide

The formation of ferrous sulfide required for our investigation by precipitation from ferrous sulfate and sodium sulfide under an atmosphere of nitrogen was investigated (*Figure 3.5*). When degassed aqueous solutions of ferrous sulfate and sodium sulfide were mixed a fine black precipitate formed immediately. We investigated the possible isolation of the ferrous sulfide. Isolation involved filtration of the black precipitate followed by washing with degassed water to remove any residual salts. The solid was dried under an atmosphere which is oxygen-free, in order to prevent the oxidation of ferrous ions to ferric ions.

$$FeSO_{4(aq)} + Na_2S_{(aq)} \xrightarrow{H_2O} FeS_{(s)} + Na_2SO_{4\,(aq)}$$

Figure 3.5 Formation of FeS

Unfortunately it was found that oxidation of the isolated ferrous sulfide occurred on standing. Therefore it was decided that the iron sulfide was best prepared *in situ* immediately before use.

3.2.3 Reaction vessel

These reactions require anaerobic conditions as oxygen can oxidise ferrous ions, sulfide ions and mercaptoacetic acid. A number of different reaction vessels and degassing procedures were investigated in an effort to establish experimental techniques that would enable us to limit these oxidation reactions. Glass ampoules provided the most convenient experimental vessel in which an anaerobic atmosphere could be maintained over the reaction mixtures during manipulations. These ampoules could be heated to 100°C safely.

Ampoules were chosen to have a diameter appropriate to fit a suba seal to maintain an airtight seal during manipulations (*Figure 3.6*). The glass ampoules were approximately 20 cm in length with a constriction half way up. The constriction was necessary to allow the glass ampoule to be easily sealed. After the reaction mixture was prepared it was frozen and the glass ampoule was sealed.

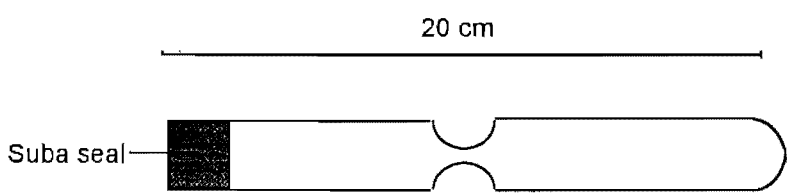

Figure 3.6 Diagram of glass ampoule

For the sealed tube reactions the ampoules were placed in an aluminium tubes. If the sealed ampoule exploded due to increased pressure during heating the aluminium tube could act as a safety barrier.

3.2.4 Analytical methodology for studying the formation of acetic acid

A preliminary goal of this work was to verify the reduction of organic compounds by the ferrous sulfide system of Wächtershäuser. Initially we focussed on the reductive generation of acetic acid from mercaptoacetic acid (*Figure 3.7*)[2]. It was necessary to establish a means of identifying and quantifying acetate at low levels in complex reaction mixtures in order to monitor this system.

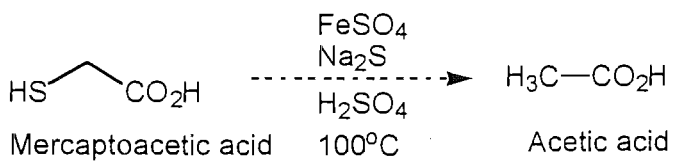

Figure 3.7 Reduction of mercaptoacetic acid to acetic acid

A number of different product detection methods were investigated for quantifying the anticipated levels of acetic acid. The reactions performed by Wächtershäuser and coworkers contained mercaptoacetic acid (5 mM) in water. Therefore the maximum concentration of acetic acid/acetate could be 5 mM. Wächtershäuser and coworkers monitored the formation of acetic acid by gas-liquid chromatography, glc. Therefore glc was investigated as an analytical tool. Although acetic acid was easily detected at 175 mM by glc, our glc system was found to be insufficiently sensitive to detect acetic acid at

17 mM. These concentrations of acetic acid/acetate were considerably higher than the maximum possible concentration of acetic acid that could be produced in the reactions.

Another possible technique for analysis of the proposed reaction mixtures was extraction into an organic solvent followed by analysis by ^{1}H NMR spectroscopy. A solution of 175 mM acetic acid was prepared and the pH was adjusted to pH=1. This solution was extracted with deuterated chloroform and ^{1}H NMR spectroscopy was performed. Analysis of the spectrum indicated the presence of acetate. A similar procedure employing 17 mM acetic acid gave no observable resonance at the appropriate chemical shift for acetic acid. Therefore, at the anticipated product concentration of less than 5 mM, the product acetic acid would not be detected.

Since, detection of acetic acid at concentrations less than 5 mM proved to be difficult, freeze-drying of the aqueous solution was investigated, as it could provide a means of concentrating the reaction mixtures. Solutions of dilute acetic acid with concentrations of 2.51 mM and 1.25 mM were prepared. These solutions were made strongly alkaline in order to generate acetate salts, in the hope of minimising loss of acetic acid through evaporation during freeze-drying. The residues remaining after freeze drying were dissolved in deuterium oxide and ^{1}H NMR spectroscopy was performed on these samples. Analysis of the ^{1}H NMR spectra showed the presence of resonances consistent with the presence of acetate ions. Therefore a combination of freeze-drying and ^{1}H NMR spectroscopy was a possible means of detecting acetic acid in the concentration range expected in the proposed reactions however there would be uncertainties in quantifying the precise levels of acetate produced. Since the quantification of low

concentrations of acetic acid proved to be more difficult than anticipated, our attention turned to a more easily monitored system.

3.2.5 Reaction of phenylpyruvate in the presence of ferrous sulfide and hydrogen sulfide

The reaction chosen for study was the formation of cinnamate and/or 3-phenylpropionate from phenylpyruvate (*Figure 3.8*)[2]. The product distribution is reported to be dependent on the reaction time. The reactant and products in this reaction have strong UV chromophores and thus can be easily quantified by UV detection.

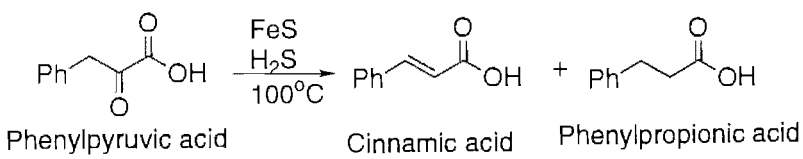

Figure 3.8 Reduction of phenylpyruvate

Phenylpyruvate was synthesised from *N*-acetyl glycine and benzaldehyde, followed by treatment with acid (*Figure 3.9*)[4]. The reported products of the reduction reactions, phenylpropionate and cinnamate, were available for use as standards for quantitative analysis.

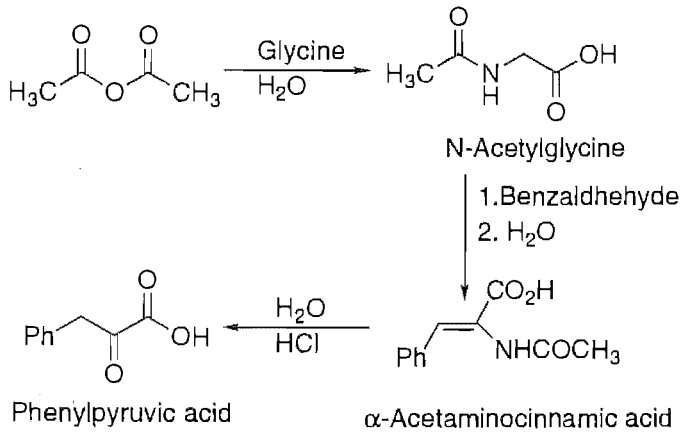

Figure 3.9 Synthesis of Phenylpyruvate

A study of HPLC conditions showed it was possible to separate phenylpyruvate, cinnamate and 3-phenylpropionate. A phosphate buffer has previously been used for this purpose[3]. This was investigated but abandoned due to problems caused by the insolubility of ferrous phosphate, generated *in situ* from residual ferrous ions in the reaction mixture. The optimised separation was achieved using a C_{18} column and eluted with a 0.05% TFA water/methanol solvent mixture.

A mixture containing phenylpyruvate, ferrous sulfide and hydrogen sulfide was heated for 21 days at 100°C. Both the ferrous sulfide and hydrogen sulfide were prepared *in situ*.. HPLC of the resulting supernatant revealed the presence of a significant amount of phenylpropionate had been produced. This result was confirmed by doping. The yield was estimated to be 12%, by comparison of peak areas with those of an authentic sample of known concentration.

Wächtershäuser and coworkers detected a 2.4% yield of 3-phenylpropionate after 12 days. Our reaction time was longer and thus the yield was larger. This result confirms that our reaction methodology is capable of emulating the reduction chemistry of Wächtershäuser and coworkers. Therefore the reaction methodology was deemed to be adequate to undertake the study of coupling the reduction reactions with amide bond formation. This involved studying the reaction of mercaptoacetic acid with aniline in the presence of ferrous sulfide and hydrogen sulfide to form *N*-phenyl acetamide.

3.3 Study of iron-sulfur mediated amide bond formation

3.3.1 Introduction

Wächtershäuser and coworkers have reported that mercaptoacetic acid and aniline in the presence of ferrous sulfide and hydrogen sulfide produces *N*-phenyl acetamide. They proposed a reaction mechanism for this reaction (*Figure 3.2 and Figure 3.3*), as discussed in section 3.1. Their failure to detect *N*-phenyl mercaptoacetamide in the reaction mixtures led them to postulate that thiol reduction was coupled to thiocarboxylic acid generation. However it is possible that *N*-phenyl mercaptoacetamide might be an intermediate in the reaction (*Figure 3.10*). A subsequent postulated nucleophilic attack by the amine of aniline at the carbonyl carbon of the thiocarboxylic acid could produce *N*-phenyl mercaptoacetamide (*reaction 2, Figure 3.10*). *N*-Phenyl mercaptoacetamide could then react with FeS to form *N*-phenyl acetamide.

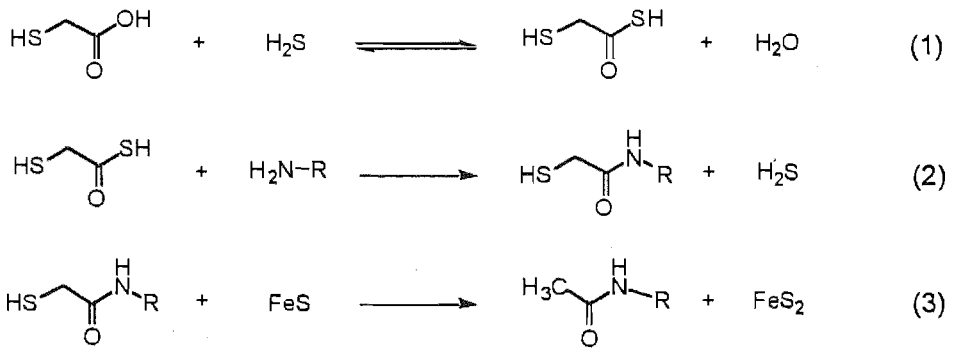

Figure 3.10 Alternative pathway to N*-phenyl acetamide*

We wanted to test the possible intermediacy of *N*-phenyl mercaptoacetamide on route to formation of *N*-phenyl acetamide. This provides a direct test of whether thiocarboxylic acid formation is dependent on the reduction chemistry.

3.3.2 Synthesis of *N*-phenyl mercaptoacetamide

Authentic samples of *N*-phenyl mercaptoacetamide and the corresponding disulfide were required to enable their identification in reaction mixtures. The disulfide was sought since it may arise from oxidation of the thiol during work up of the reaction mixtures. Both thiol and disulfide were synthesised from di(carboxymethyl)disulfide[5] Reaction of the diacid with aniline gave di(*N*-phenyl carbamoylmethyl)disulfide. Di(*N*-phenyl carbamoylmethyl)disulfide was reduced to form *N*-phenyl mercaptoacetamide (*Figure 3.11*)

The yield of reaction of di(carboxymethyl)disulfide and aniline was relatively low. Therefore alternative routes were pursued. The methyl ester of di(carboxymethyl)disulfide[6] was synthesised which in turn was reacted with aniline to form a small amount of crude di(*N*-phenyl carbamoylmethyl)disulfide (*Figure 3.12*).

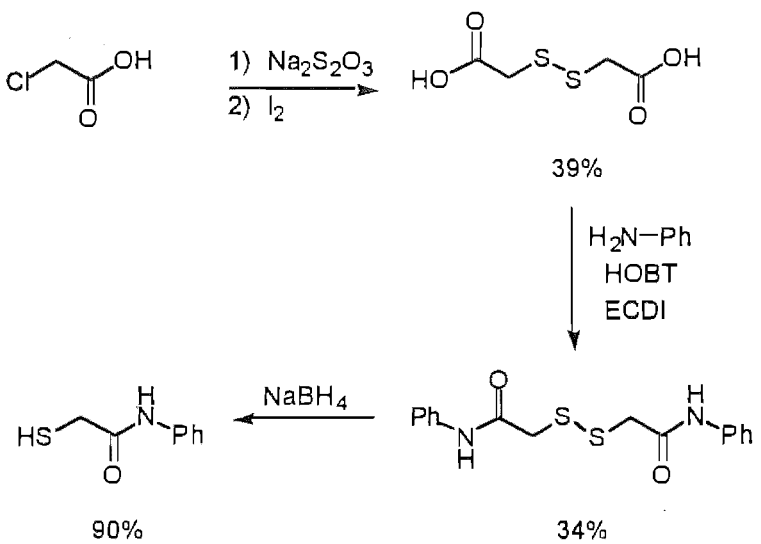

Figure 3.11 Synthesis of N-phenyl mercaptoacetamide

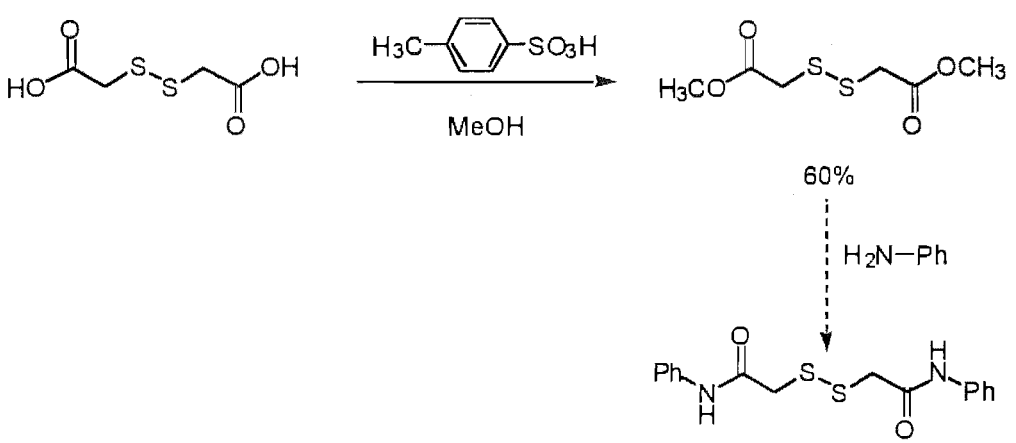

Figure 3.12 Attempted alternative synthesis of N-phenyl mercaptoacetamide

At the same time as the multi step synthesis of *N*-phenyl mercaptoacetamide *via* di(*N*-phenyl carbamoylmethyl)disulfide was being investigated, the viability of a one step synthesis of *N*-phenyl mercaptoacetamide was assessed. Attempts to form *N*-phenyl mercaptoacetamide by coupling mercaptoacetic acid and aniline with DCC were unsuccessful (*Figure 3.13*)[5], but refluxing the acid and amine with azeotropic removal of water gave the desired compound (*Figure 3.14*)[7].

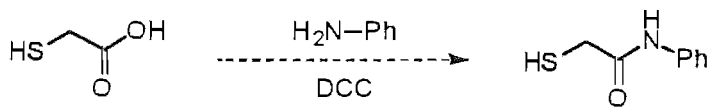

Figure 3.13 Attempted alternative synthesis of N-*phenyl mercaptoacetamide*

The latter method yielded the product *N*-phenyl mercaptoacetamide with a yield 68% upon crystallisation.

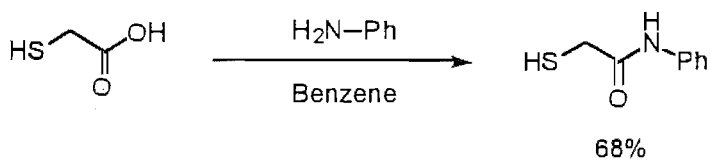

Figure 3.14 Synthesis of N-*phenyl mercaptoacetamide*

3.3.3 Formation of *N*-phenyl acetamide from *N*-phenyl mercaptoacetamide

With pure samples of *N*-phenyl mercaptoacetamide and the corresponding disulfide in hand we investigated HPLC conditions for analysing reaction mixtures. The solvent

gradient system used was that developed by Wächtershäuser and coworkers to detect *N*-phenyl acetamide in similar reaction mixtures. The water-methanol solvent system resolved all the UV-active constituents of interest: aniline, *N*-phenyl acetamide , *N*-phenyl mercaptoacetamide and di(*N*-phenyl carbamoylmethyl)disulfide. The retention times of the compounds of interest using this solvent system with a C_{18} column are listed in *Table 3.2*.

Compound	Retention time (Mins)
Aniline	5.25
N-Phenyl acetamide	32.37
N-Phenyl mercaptoacetamide	38.25
Di(*N*-phenyl carbamoylmethyl)disulfide	46.55

Table 3.2 HPLC retention times of possible reaction components

A reaction was performed using the postulated intermediate, *N*-phenyl mercaptoacetamide as the starting material. *N*-phenyl mercaptoacetamide, ferrous sulfide and hydrogen sulfide were mixed in degassed water, sealed and heated at 100°C for 7 days (*Figure 3.15*). The reaction mixture was worked up and analysed as before. Analysis of the HPLC data showed 4 % yield of *N*-phenyl acetamide. No starting material, *N*-phenyl mercaptoacetamide, was observed after the reaction time.

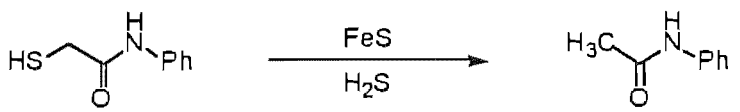

N-phenyl mercaptoacetamide 4 % *N*-phenyl acetamide

Figure 3.15 Formation of N-*phenyl acetamide from* N-*phenyl mercaptoacetic acid*

The reaction mixture was extracted with organic solvent in order to confirm the presence of *N*-phenyl acetamide. This residue was analysed by mass spectrometry. Mass spectrometry data from this residue confirmed the presence of *N*-phenyl acetamide. We have established that it is possible to convert *N*-phenyl mercaptoacetamide to *N*-phenyl acetamide under the same conditions as the reaction for which it is a proposed intermediate.

3.3.4 Attempts to detect of *N*-phenyl mercaptoacetamide in ferrous sulfide reaction mixtures

With a method for analysis of the reductive chemistry of mercaptoacetic acid and aniline in hand, we were able to examine the details of these reactions. Reaction mixtures were prepared using degassed milli-Q water which had undergone at least two freeze-pump-thaw cycles under an atmosphere of oxygen-free nitrogen.

The heterogeneous mixture of mercaptoacetic acid, aniline, ferrous sulfide and hydrogen sulfide were heated at 100°C for 7 days (*Figure 3.16*). The sealed tubes were opened at the end of the reaction time, the reaction mixture was centrifuged, and HPLC analysis

was performed. The analysis was repeated after treatment with cyanide ions to ensure that any ligands were desorbed from the surface. Analysis of the HPLC data showed 0.2 % *N*-phenyl acetamide was formed before and after cyanide treatment. No *N*-phenyl mercaptoacetamide or di(*N*-phenyl carbamoylmethyl)disulfide were detected.

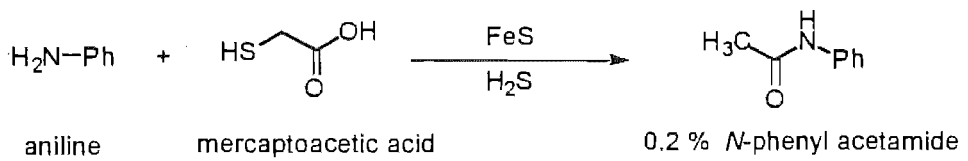

Figure 3.16 Formation of N-*phenyl acetamide from aniline and mercaptoacetic acid*

Although this yield of this reaction is somewhat smaller than that reported by Wächtershäuser (1.8% after 4 days), this is not unexpected due the different experimental methodology we were forced to adopt. For example, if the hydrogen sulfide concentration was less than optimal due to loses during sealing of the glass ampoules this could reduce the yield of product. Wächtershäuser reported a significantly reduced yield for these reactions in the absence of hydrogen sulfide[3]. Alternatively the pH may be less than optimal. The pH also has an effect on the stoichiometry and on the surface of the ferrous sulfide. If the solution is too acidic no ferrous sulfide precipitate forms.

Although no *N*-phenyl mercaptoacetamide was detected it may still be a reaction intermediate. The *N*-phenyl mercaptoacetamide may not have been detected for a number of reasons. The reaction is inefficient and the likely amount of the thiol is low. It is possible that any *N*-phenyl mercaptoacetamide accumulated in the reaction mixture

remained associated with the precipitated salts. Alternatively, *N*-phenyl mercaptoacetamide may not accumulate in the reaction mixture as the conversion of *N*-phenyl mercaptoacetamide to *N*-phenyl acetamide may be fast on the timescale of the reaction.

Another possible reason we were unable to detect the *N*-phenyl mercaptoacetamide as a reaction intermediate is its low solubility in water. Therefore if *N*-phenyl mercaptoacetamide was formed it may precipitate due to its low solubility. By replacing aniline with 4-aminobenzoic acid in the reaction mixture it was hoped water solubility of the proposed intermediate, *N*-(4-carboxyphenyl) mercaptoacetamide might be improved. Again HPLC could be used to analyse these reactions. Therefore authentic samples *N*-(4-carboxyphenyl) mercaptoacetamide and *N*-(4-carboxyphenyl) acetamide were required.

3.3.5 Synthesis of *N*-(4-Carboxyphenyl) acetamide

N-(4-Carboxyphenyl) acetamide was synthesised from 4-aminobenzoic acid and acetyl chloride (*Figure 3.17*).

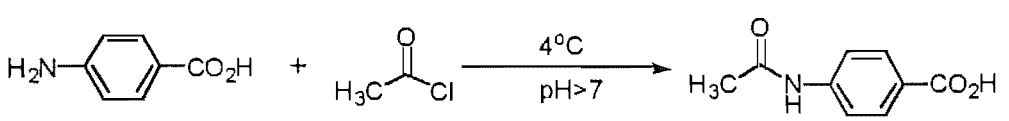

90.4 % *N*-(4-carboxyphenyl) acetamide

Figure 3.17 *Synthesis of* N-*(carboxyphenyl) acetamide*

Several different syntheses of *N*-(4-carboxyphenyl) mercaptoacetamide were attempted. 4-Aminobenzoic acid was reacted with chloroacetyl chloride to produce *N*-(4-carboxyphenyl) chloroacetamide[5]. The *N*-(4-carboxyphenyl) chloroacetamide was reacted with sodium thiosulfate but no *N*-(4-carboxyphenyl) mercaptoacetamide was detected in the reaction mixture (*Figure 3.18*).

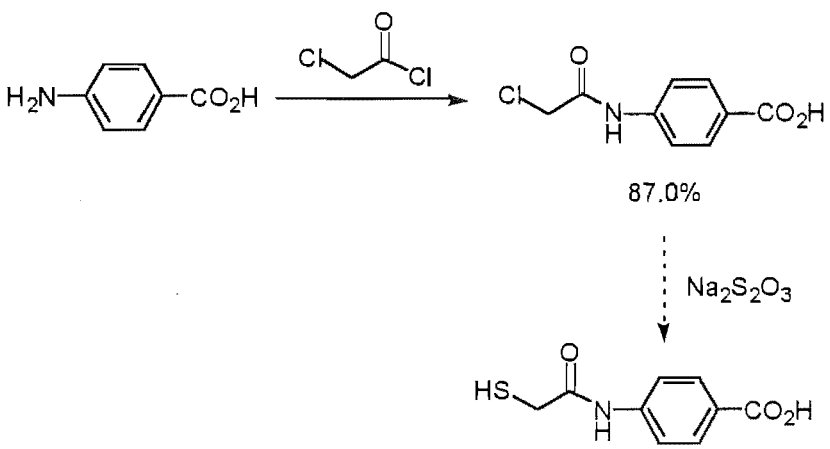

Figure 3.18 Attempted synthesis of N-*(4-carboxyphenyl) mercaptoacetamide*

4-Aminobenzoic acid was refluxed with mercaptoacetic acid under an atmosphere of oxygen free nitrogen with azeotropic removal of water (*Figure 3.19*). The product, *N*-(4-carboxyphenyl) mercaptoacetamide was precipitated by addition of water.

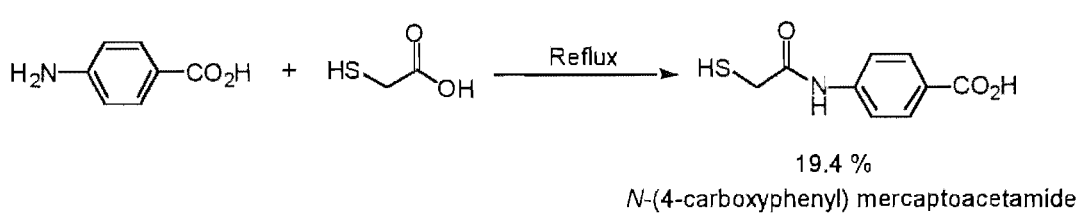

Figure 3.19 Synthesis of N-*(4-carboxyphenyl) mercaptacetamide*

Although the yield of this reaction was not high it provided enough *N*-(4-carboxyphenyl) mercaptoacetamide to perform the desired experiments. *N*-(4-Carboxyphenyl) mercaptoacetamide was oxidised to provide an authentic sample of the corresponding disulfide, di(*N*-(4-carboxyphenyl carbamoylmethyl)disulfide was synthesised by treating *N*-(4-carboxyphenyl) mercaptoacetamide with iodine (*Figure 3.20*).

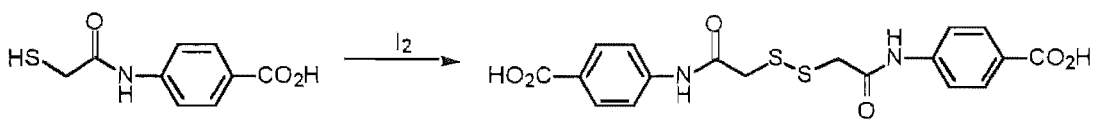

Figure 3.20 Synthesis of di-N-(4-carboxyphenyl carbamoylmethyl)disulfide

The optimised HPLC conditions utilised a solvent gradient of acetonitrile and water (0.05% TFA) on a C_{18} column. The retention times for the possible UV-active reaction constituents are shown in *Table 3.3*.

Compounds	Retention time (Mins)
4-Aminobenzoic acid	3.45
N-(4-Carboxyphenyl) mercaptoacetamide	8.43
N-(4-Carboxyphenyl) acetamide	4.49
Di-*N*-(4-carboxyphenyl carbamoylmethyl) disulfide	21.23

Table 3.3 HPLC retention times of possible reaction components

With the materials and analytical methodology in hand we proceeded to study the details of amide formation from 4-aminobenzoic acid.

3.3.6 Formation of *N*-(4-carboxyphenyl) acetamide from 4-aminobenzoic acid and mercaptoacetic acid

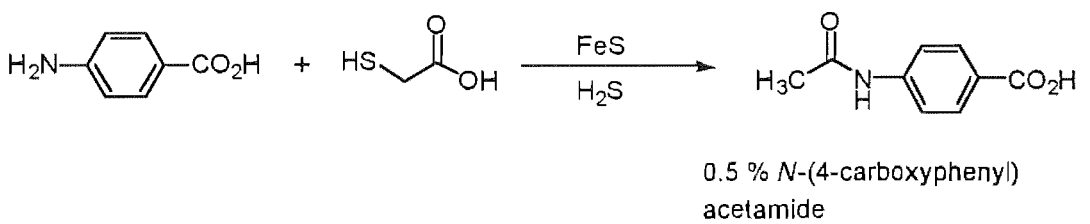

Figure 3.21 Formation of N-*(4-carboxyphenyl) acetamide from 4-aminobenzoic acid and mercaptoacetic acid*

4-Aminobenzoic acid, mercaptoacetic acid, ferrous sulfide and hydrogen sulfide were mixed in degassed water, sealed and heated at 100°C for 5 days (*Figure 3.21*). The sealed tube was opened and a sample of the centrifuged reaction mixture was analysed by HPLC. The presence of a small amount of the product, *N*-(4-carboxyphenyl) acetamide was confirmed by doping. The yield was estimated to be 0.5%, by comparison of peak areas with those of an authentic sample of known concentration. No *N*-(4-carboxyphenyl) mercaptoacetamide (or the corresponding disulfide) were detected in the reaction mixture.

When the possible intermediate, *N*-(4-carboxyphenyl) mercaptoacetamide was reacted under the same reaction conditions the yield of product, *N*-(4-carboxyphenyl) acetamide

was 6% (*Figure 3.22*). These results may indicate the desulfurization chemistry to yield *N*-(4-carboxyphenyl) acetamide is more efficient than the reaction of 4-amino benzoic acid and mercaptoacetic acid to form *N*-(4-carboxyphenyl) acetamide.

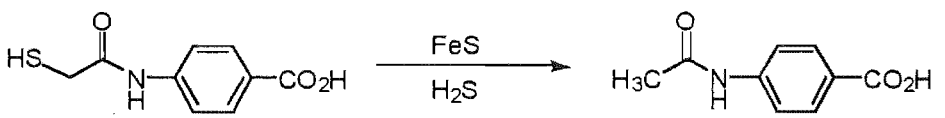

N-(4-carboxyphenyl) mercaptoacetamide

6 % *N*-(4-carboxyphenyl) acetamide

Figure 3.22 Formation of N-*(4-carboxyphenyl) acetamide from* N-*(4-carboxyphenyl) mercaptoacetamide*

Summary

Aniline and mercaptoacetic acid produce *N*-phenyl acetamide when heated in the presence of ferrous sulfide and hydrogen sulfide, but the yield (0.2%) was poor. No *N*-phenyl mercaptoacetamide was detected. When the postulated intermediate, *N*-phenyl mercaptoacetamide was heated with ferrous sulfide and hydrogen sulfide the product, *N*-phenyl acetamide was produced in 4% yield. No *N*-phenyl mercaptoacetamide was observed after the reaction time.

In an effort to improve the solubility of the possible product amides, aniline was replaced by 4-aminobenzoic acid in the reaction mixtures. When 4-aminobenzoic acid and mercaptoacetic acid were heated with ferrous sulfide and hydrogen sulfide the desulfurized product, *N*-(4-carboxyphenyl) acetamide, was formed with a yield of 0.5%. No *N*-(4-carboxyphenyl) mercaptoacetamide was detected in the reaction mixture. *N*-(4-

Carboxyphenyl) acetamide (6%) was also formed when *N*-(4-carboxyphenyl) mercaptoacetamide was heated with ferrous sulfide and hydrogen sulfide. Thus the carboxylic acid group did not lead to the detection of the corresponding thiol-containing intermediate, *N*-(4-carboxyphenyl) mercaptoacetamide.

These reactions give only low yields of amide products. The yield of desulfurized product from the mercapto-substituted acetamides was somewhat higher. Given the low yields of amides from the mercaptoacetic acid reactions, the absence of detectable mercaptoacetamide derivatives does not provide definitive information about the possible intermediacy of such species in the reaction. It is clear that mercaptoacetamide species can be desulfurized under the reaction conditions, so we decided to investigate the process further. If desulfurization of the mercaptoacetamide derivatives is facile then there is no reason to involve facile desulfurizaion of the mercaptothiol acids as a key feature in amide formation.

3.3.7 Formation of *N*-(4-carboxyphenyl) acetamide from *N*-(4-carboxyphenyl) mercaptoacetamide

N-(4-Carboxyphenyl) mercaptoacetamide was added to ferrous sulfide and heated at lower temperatures for shorter times to investigate the rate of desulfurization under these reaction conditions. Aqueous *N*-(4-carboxyphenyl) mercaptoacetamide was added to a mixture of ferrous ions and sulfide ions and heated 40°C for time ranging between 30 and 180 minutes. The reaction mixtures were analysed by HPLC. The yields of *N*-(4-carboxyphenyl) acetamide were determined, by comparison of peak areas with those of authentic samples of known concentrations and are shown in *Table 3.4* .

Time @ 40°C (mins)	% Yield *N*-(4-carboxyphenyl) acetamide
30	69
60	63
90	53
120	58
150	69
180	71

Table 3.4 Yields of N-*(4-carboxyphenyl) acetamide at 40°C*

The yield did not increase with time. The reaction had probably run to completion before the first sample was analysed, hence the reaction was studied at lower temperature.

3.3.8 Lower temperature desulfurization of *N*-(4-carboxyphenyl) mercaptoacetamide

Reactions of N-(4-carboxyphenyl) mercaptoacetamide with ferrous sulfide were carried out at 20°C for times ranging from 30 to 180 minutes. Analysis of these samples by HPLC chromatography indicated that *N*-(4-carboxyphenyl) acetamide was formed, and the yields at each time interval are shown in *Table 3.5*. The formation of *N*-(4-carboxyphenyl) acetamide appears to be complete after 30 minutes at 20°C.

Time @ 20°C (mins)	% Yield *N*-(4-carboxyphenyl) acetamide
30	81
60	99
90	79
120	80
150	84
180	78

Table 3.5 Yields of N-*(4-carboxyphenyl) acetamide at 20°C*

Summary

The formation of *N*-(4-carboxyphenyl) acetamide from mercaptoacetic acid and 4-aminobenzoic acid in the presence of ferrous sulfide and hydrogen sulfide is slow taking a number of days at 100°C to produce a detectable yield of product. Whereas the desulfurization of *N*-(4-carboxyphenyl) mercaptoacetamide induced by ferrous sulfide appeared to have reached completion after 30 minutes at 20°C.

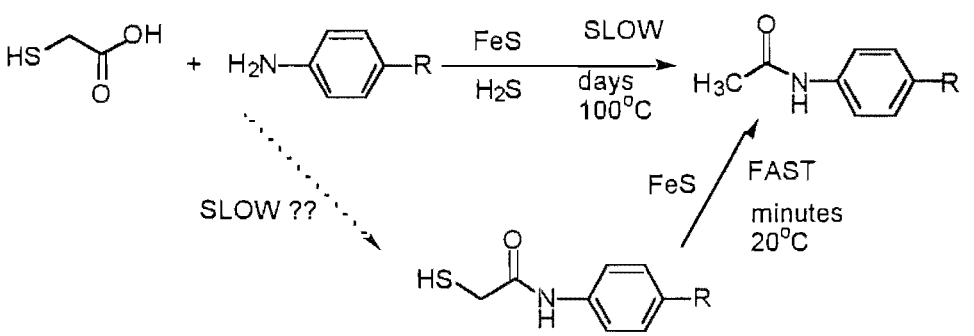

Figure 3.23 Proposed mechanism for the formation of N-*(4-carboxyphenyl) acetamide* via N-*(4-carboxyphenyl) mercaptoacetamide*

Therefore desulfurization chemistry appears to be rapid without requiring the intermediacy of thiocarboxylic acid functionality. There is, therefore no reason to involve the coupling of the thiocarboxylic acid formation and reductive desulfurization (*Figure 3.23*).

3.4 Conclusion

The mechanism of the reduction and amide formation reactions of aniline (or aniline derivatives) with mercaptoacetic acetic aid to from *N*-phenyl acetamide (or *N*-phenyl acetamide derivatives) has not been established unambiguously. We failed to detect a postulated intermediate *N*-phenyl mercaptoacetamide in the reaction mixtures. However we have established that *N*-phenyl mercaptoacetamide reacts rapidly and efficiently to give the product, *N*-phenyl acetamide, which is consistent with our not being able to detect this intermediate in the full reaction. Hence there is no need to propose, as Wächtershäuser does, that desulfurization must be coupled to thioacid formation. Having established the facility of desulfurization chemistry we were ready to turn our attention to amide formation for thiocarboxylic acids.

3.5 References

1 G. Wächtershäuser, *Pure & Appl. Chem.*, **65**, 1343 (1993).

2 E. Blöchl, M. Keller, G. Wächtershäuser & K. O. Stetter, *Proc. Natl. Acad. Sci. USA*, **89**, 8117 (1992).

3 M. Keller, E. Blöchl, G. Wächtershäuser & K. O. Stetter, *Nature*, **368**, 836 (1994).

4 A. H. Blatt, *Organic Synthesis Collective volumes 2*, Wiley, 519 (1943).

5 G. G. Stoner & G. Dougherty, *J. Am. Chem. Soc.*, **63**, 987 (1941).

6 T. C. Owen, J. M. Fayadh & J. S. Chen, *J. Org. Chem.*, **38**, 937 (1973).

7 J. A. Van Allen, *J. Am. Chem. Soc.*, **69**, 2914 (1947).

Chapter 4

Amide bond formation

4.1 Introduction

4.1.1 Thioesters and peptide formation

Amide bonds link amino acids together to form peptides and proteins. Thioesters are the activated acid intermediates that are used to produce the requisite amide links in non-ribosomal peptide biosynthesis (*Figure 4.1*).

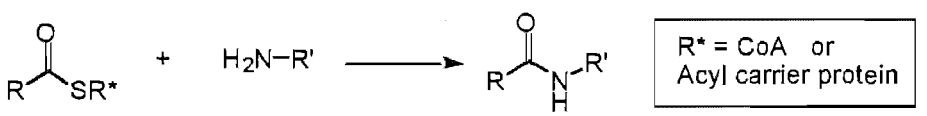

Figure 4.1 Non-ribosomal peptide biosynthesis

A number of bacterial peptides are formed from amino acid thioesters (*Figure 4.2*)[1,2]. This type of condensation reaction may give an insight into prebiotic peptide synthesis, as it provides a means of synthesising peptides from relatively simple starting materials without requiring the complex machinery of ribosomal peptide synthesis.

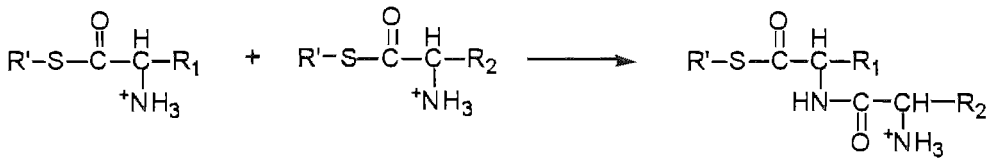

Figure 4.2 Bacterial peptide biosynthesis from amino acid thioesters

Wieland reports that peptides can from spontaneously from aminoacyl thioesters when incubated in alkaline aqueous solutions[3]. Peptides have also been detected when aqueous solutions of amino acids were heated with ferrous sulfide, nickel sulfide, carbon monoxide and thiol (or hydrogen sulfide) (*Figure 4.3*)[4].

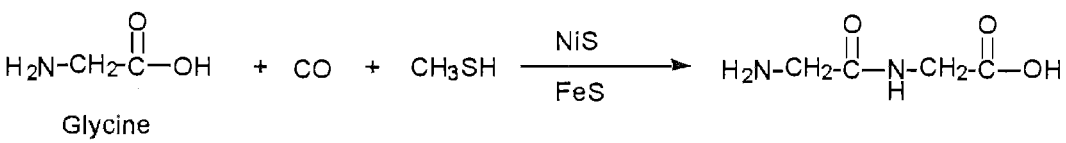

Figure 4.3 Formation of peptides from amino acid heated with carbon monoxide, thiol, nickel sulfide and ferrous sulfide

This research is based on the formation of amide bonds from thioesters as discussed in Chapter one (section 1.3). Carboxylic acids were produced from heating mixtures of thiols, carbon monoxide, nickel sulfide and ferrous sulfide[5]. Thioesters were also detected in these reaction mixtures (*Figure 4.4*).

Metal-bound thiocarboxylic acids are implicated in this reaction. A mechanism for this reaction has been put forward that includes a metal-bound thiocarboxylic acid as an intermediate (section 1.3).

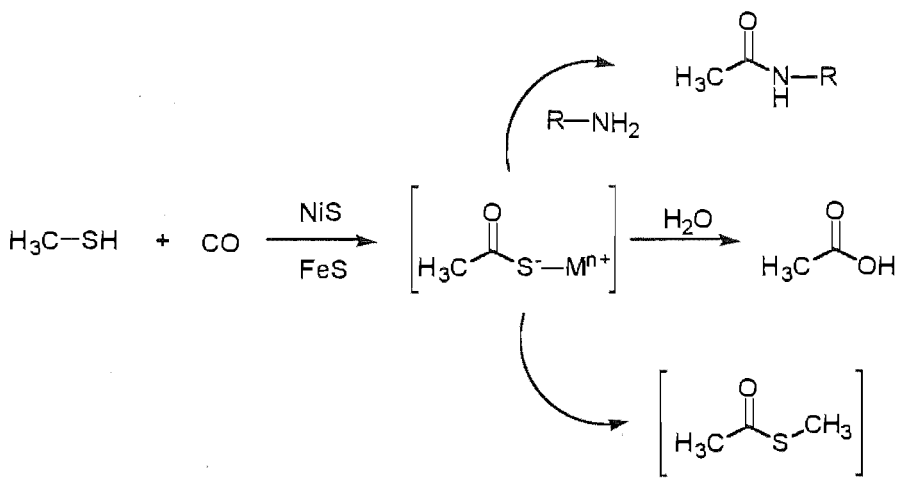

Figure 4.4 Proposed formation of thioesters, carboxylic acids and amide from thiols, carbon monoxide, nickel sulfide and ferrous sulfide

Could metal-bound thiocarboxylic acids have been the prebiotic precursors to thioesters? Metal-bound thiocarboxylic acids could be used to study acyl transfer to amines to form amides. Metal salt catalysis of the reaction of thiocarboxylic acids with amines to form amides was therefore investigated.

4.1.2 Formation of amide bonds from thiocarboxylic acids and amines

Thiocarboxylic acids have been reported to react slowly with amines[6] and amino acids[7] to give *N*-acyl derivatives. The mechanism of this reaction is not well understood. The reaction may proceed *via* the simple nucleophilic attack by the amine group at the

carbonyl centre of the thiocarboxylic acid. The slow nature of this class of reactions may be due to low electrophilicity of the carbonyl group of thiocarboxylic acids. *N*-Acylation can be facilitated by oxidation. The presumed intermediate is the corresponding disulfide. Liu and Orgel have proposed a mechanism in which the thiocarboxylic acid is oxidised to the dithiocarboxylic acid before reaction with the amine (*Figure 4.5*)[8].

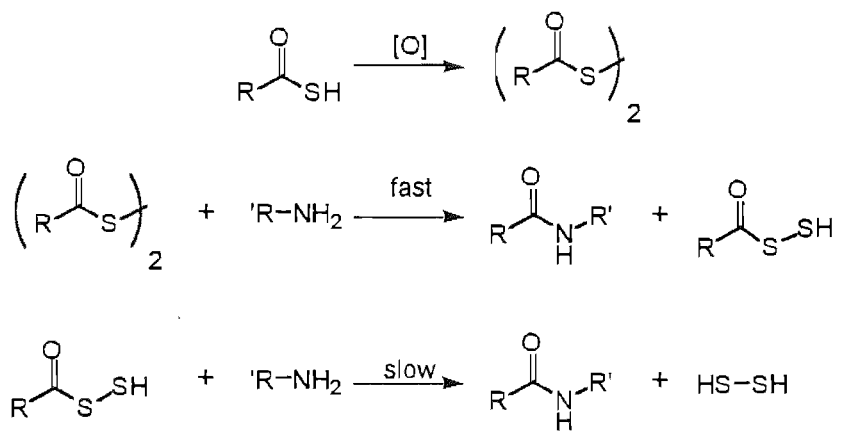

Figure 4.5 *Oxidative mechanism of* N-*acylation by thioacetic acid with amines*

We are interested in investigating catalysis of the reaction of thioacetic acid and simple amino acids. Initial studies assessed the affect of acidity, different amino acids, and metal salts on the reaction with a view to gaining insight into the nature of the reaction mechanism. In particular, the potential catalysis of this reaction by divalent metal ions was assessed.

4.2 Preliminary survey of the factors effecting the reaction of thioacetic acid and amino acids

4.2.1 Thioacetic acid

Aldrich supplies thioacetic acid with a stated purity of 97%. Thiocarboxylic acids are readily oxidised by oxygen in air to form the corresponding disulfide. In an effort to minimise the amount and formation of this disulfide impurity, small quantities of thioacetic acid were distilled when needed and stored under oxygen-free nitrogen at 4°C. These precautions ensured that thioacetic acid was the reactant rather than the disulfide.

4.2.2 Reaction of thioacetic acid with amino acids

The reaction of thioacetic acid with amino acids was investigated. In particular we are interested in the acylation reaction of glycine and alanine with thioacetic acid. For instance a thiocarboxylic acid (thiohippuric acid) is reported to *N*-acylate an amino acid (alanine) in DMF at 100°C with a yield of 70%[9]. *N*-acetyl glycine and *N*-acetyl alanine would be the expected products of the reaction of thioacetic acid with glycine or alanine respectively.

4.2.3 Reaction of thioacetic acid and glycine

A sample of commercially available *N*-acetyl glycine was analysed by ^{1}H NMR spectroscopy. The two observed resonances at 1.89 ppm and 3.82 ppm were assigned to the methyl protons and α-protons respectively. A ^{1}H NMR spectrum of thioacetic acid in deuterium oxide contains one signal at 2.37 ppm due to the methyl protons.

The proposed method for monitoring these reactions was ^{1}H NMR spectroscopy, through analysis of the integrations of the spectra. A ^{1}H NMR spectrum of a mixture of *N*-acetyl glycine, glycine and thioacetic acid showed that the resonances associated with the three compounds were sufficiently separated to allow accurate integration.

The relaxation times for the magnetisation which gives rise to the signals in ^{1}H NMR spectra, are generally fast, and therefore integration of the signals provides a reliable means of quantifying yields. The relative yields were determined using integrals measured for protons in similar chemical environments. For example, one methyl group compared with another methyl group.

Reaction mixtures containing thioacetic acid and glycine were prepared in deuterium oxide with a pH = 7. These solutions were reacted at 50°C for a range of times before analysis by ^{1}H NMR spectroscopy. The results of this reaction are shown in *Table 4.1*. The yields of *N*-acetyl glycine increase with time. After 72 hours the reaction was still not complete with a product yield of 50%.

Time (hours)	% Yield *N*-Acetyl glycine
24	17
48	35
72	50

Table 4.1. Yields of N-*acetyl glycine after 24, 48 and 72 hours at 50°C*

It should be noted that the remaining thioacetic acid might have been oxidised to dithiodiacetic acid during prolonged reaction times. The ^{1}H NMR chemical shifts of thioacetic acid and the corresponding disulfide in deuterium oxide are essentially identical. They can not therefore be distinguished under these conditions.

A larger scale reaction was carried out and the aqueous reaction mixture was extracted. Mass spectrometry was performed on this sample. The results were consistent with *N*-acetyl glycine formation and confirm the production of *N*-acetyl glycine in these reaction mixtures.

4.2.4 Reaction of thioacetic acid with *D,L*-alanine

The reaction of thioacetic acid and alanine to form *N*-acetyl-*D,L*-alanine was investigated. An authentic sample of *N*-acetyl-*D,L*-alanine was synthesised from *D,L*-alanine and acetic anhydride at 0°C (*Figure 4.6*). The ^{1}H NMR spectrum of this compound in deuterium oxide showed 3 resonances 1.40 ppm, 2.00 ppm and 4.32 ppm, due to the alanine methyl protons, the acetyl methyl protons and α-proton respectively.

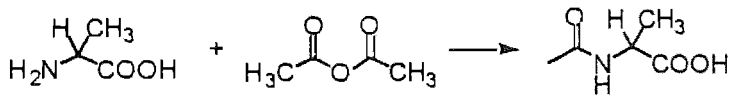

Figure 4.6 Synthesis of N-*acetyl*-D,L-*alanine*

Reaction mixtures containing thioacetic acid and alanine were prepared in deuterium oxide with a pH = 7.0. These solutions were reacted for various times before being analysed by ^{1}H NMR spectroscopy. The results of this reaction are shown in *Table 4.2*. No product *N*-acetyl-*D,L*-alanine was detected after 24 hours. However, after 48 and 72 hours, 11 and 30% of *N*-acetyl-*D,L*-alanine were detected respectively.

The experiment was repeated on a larger scale and extracted. The organic phase was analysed by mass spectrometry. The results were consistent with *N*-acetyl-*D,L*-alanine being present in the reaction mixture.

These *N*-acylation reactions show that thioacetic acid reacts more rapidly with glycine than with alanine. This may be due to steric effects.

Time (hours)	% Yield *N*-Acetyl-*D,L*-alanine
24	0.0
48	11
72	30

Table 4.2 Yields of N-*acetyl alanine after 24, 48 and 72 hours at 50°C*

4.2.5 Reaction of thioacetic acid and amino acids in the presence of ferrous ions

The effect of ferrous ions on the reaction of amino acids and thioacetic acid was investigated. At pH > 6, a mixture of thioacetic acid, an amino acid and ferrous ions is heterogeneous. The precipitate may adsorb organic compounds, thus it was necessary to find a method of removing possible products from the solid surface. This was achieved by adding 6 –10 molar equivalents of potassium cyanide (relative to ferrous ions) to the reaction mixture. The cyanide ions form a stable diamagnetic complex with the ferrous ions ($\log \beta_6 = 24$). Any insoluble ferrous compounds were removed by centrifugation. This enables us to detect, by ^{1}H NMR spectroscopy any organic compounds that were adsorbed on the solid surface.

Glycine and alanine were the amino acids investigated in these reactions. Thioacetic acid and glycine were dissolved in degassed deuterium oxide in the presence of ferrous ions. The pH was adjusted to 6-7 to give a blue/grey heterogenous mixture. These reaction mixtures were allowed to react for a range of times before addition of cyanide ions, centrifugation and analysis by ^{1}H NMR spectroscopy. The results of this reaction are shown in *Table 4.3*. *N*-Acetyl glycine was formed with yields of 86, 92, and 92% after 24, 48, and 72 hours respectively at 50°C.

Time (hours)	% Yield *N*-Acetyl glycine
24	86.
48	92
72	92

Table 4.3 Yields of N-*acetyl glycine in the presence of ferrous ions*

There is a significant increase in the rate of *N*-acetyl glycine formation in the presence of ferrous ions. In the absence of ferrous ions after 24 hours 17% of *N*-acetyl glycine had formed while in the presence of ferrous ions 86% had formed. After 48 hours of reaction time no thioacetic acid was detected and the yield of *N*-acetyl glycine did not change any further. The *N*-acylation reaction is presumably in competition with hydrolysis of thioacetic acid.

An analogous reaction was carried out with alanine. Thioacetic acid and *D,L*-alanine were dissolved in degassed deuterium oxide in the presence of ferrous ions. The pH was adjusted to 6 - 7 to give a blue/grey heterogenous mixture. These mixtures were allowed to react for various times before addition of cyanide ions, centrifugation and analysis by ^{1}H NMR spectroscopy. After 3, 24 and 48 hours in the presence of ferrous ions at 50°C produced 30, 43 and 45% for *N*-acetyl-*D,L*-alanine respectively. The results of this reaction are shown in *Table 4.4*.

Time (hours)	% Yield *N*-Acetyl-*D,L*-alanine
3	30
24	43
48	45

Table 4.4 Yields of N*-acetyl alanine in the presence of ferrous ions*

There is a significant increase in the rate of *N*-acetyl-*D,L*-alanine formation in the presence of ferrous ions. In the absence of ferrous ions no *N*-acetyl-*D,L*-alanine was detected after 24 hours at 50°C. In contrast the reactions containing ferrous ions had reacted significantly after 3 hours at 50°C.

Thus we conclude the rate of *N*-acylation by thioacetic acid is enhanced by the presence of ferrous ions. In the heterogeneous reaction containing ferrous ions, formation of N-acetyl products may be promoted by the surface of the precipitate. Alternatively complexation of the reactants may led to an increase in their reactivity.

4.2.6 Reaction of thioacetic acid with an amino acid with a thiol side chain.

The increased rate of acylation of alanine and glycine by thioacetic acid that was observed in the presence of ferrous ions led to the desire to investigate the effect of other structural changes in the amino acid component. Because of the potential prebiotic significance of thiols we undertook a study of the acylation of cysteine.

Thiols can stimulate acyl transfer to mercaptoamines *via* thio exchange (*Figure 4.7*)[10,11]. The thiol group acts as a nucleophile and attacks the carbonyl centre of the thiocarboxylic acid, to *S*-acylate the thioamine compound. The *S*-acylated thioamine compound can then undergo an intramolecular acyl transfer to the amine group to form the *N*-acylated compound which is observed. This process is efficient even in the absence of a catalyst. The thiol group is also capable of complexing with metal ions and therefore metal ions may affect the acylation reaction.

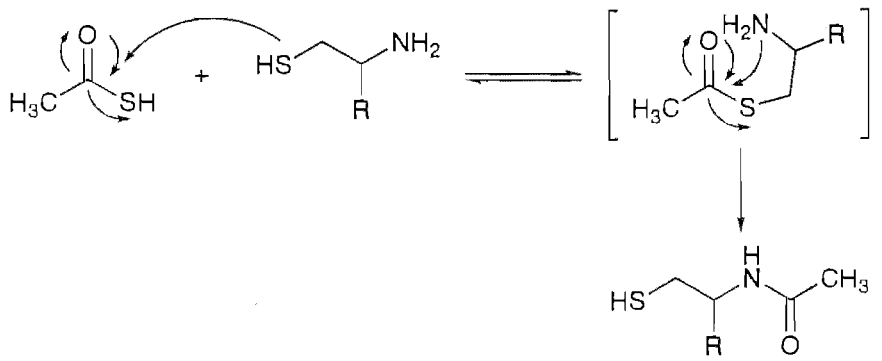

Figure 4.7 S-*Acylation followed by intramolecular acyl transfer*

Two types of acylation reaction are possible for this system, *S*-acylation and *N*-acylation. Cysteine was reacted with thioacetic acid in the presence and absence of ferrous ions. The results were then compared and contrasted with those seen for glycine and alanine. The possible products of reaction of cysteine with thioacetic acid are *N*-acetyl cysteine, *S*-acetyl cysteine and *N,S*-diacetyl cysteine (*Figure 4.8*). The initial *S*-acetylation product, *S*-acetyl cysteine, may undergo intramolecular acyl transfer and therefore is not likely be observed (see above)[10,11,12]. Once *N*-acetylation has occurred, however, an *S*-acetyl species may accumulate.

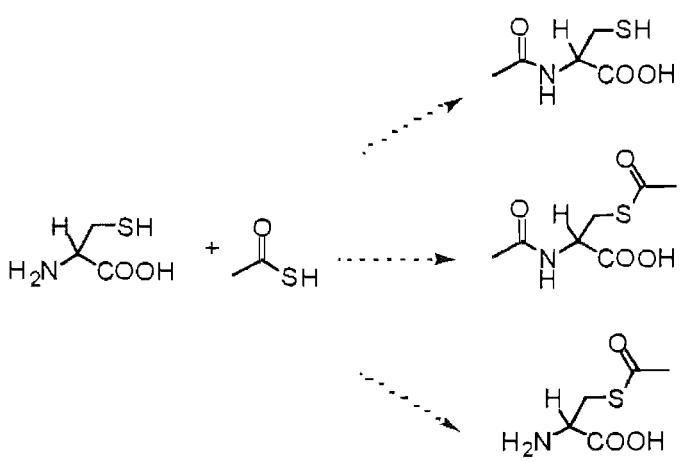

Figure 4.8 *Possible products of reaction of cysteine and thioacetic acid*

Authentic samples of the expected products were required to determine their spectral details, and for spiking reactions to identify reaction products. Therefore we required both *N*-acetylated products, *N,S*-diacetyl-*L*-cysteine and *N*-acetyl-*L*-cysteine. *N*-acetyl-*L*-cysteine is a commercial product whereas *N,S*-diacetyl-*L*-cysteine was synthesised by reaction of a basic solution of cysteine with acetic anhydride at 0°C (*Figure 4.9*)[13]. Both acetylated cysteine samples were appropriately characterised.

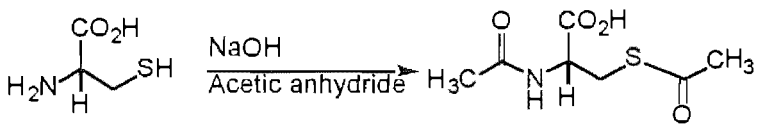

Figure 4.9 *Synthesis of* N,S-*diacetyl*-L-*cysteine*

The reaction of cysteine with thioacetic acid was investigated. *L*-Cysteine and thioacetic acid were dissolved in degassed deuterium oxide and the pH was adjusted to 6-7 by addition of sodium hydroxide. The reaction mixtures were heated at 50°C for time ranging from 24 to 72 hours. The yield of *N*-acetyl-*L*-cysteine and *N,S*-diacetyl-*L*-cysteine were calculated from the ratio of the β-proton multiplet of cysteine to the corresponding resonances of the acetylated products. The results of these reactions are shown in *Table 4.5*. The acetylation reaction was faster than for glycine or alanine. The yield of *N*-acetyl-*L*-cysteine increased from 63% to 100% between 24 to 72 hours. The yields of *N*-acetyl-*L*-cysteine are high relative to similar reaction with alanine. No *N,S*-diacetyl-*L*-cysteine was detected. Both these results are consistent with the acylation of the thiol group of cysteine followed by intramolecular acyl transfer.

Time (hours)	% Yield *N*-acetyl-*L*-cysteine	% Yield *N,S*-diacetyl-*L*-cysteine
24	63	0
48	83	0
72	100	0

Table 4.5 Yields of acetylated products from the reaction of thioacetic acid and cysteine

The reaction was repeated in the presence of ferrous ions. The reaction mixtures were heated at 50°C for times ranging from 24 to 72 hours. After the reaction time 10 molar equivalents of potassium cyanide was added to complex the ferrous ions before analysis by ^{1}H NMR spectroscopy. The results of these reactions are shown in *Table 4.6*. Both *N*-acetyl-*L*-cysteine and *N,S*-diacetyl-*L*-cysteine were detected in the presence of ferrous ions. The yields were relatively unchanged over the time period of these reactions. The yield of *N*-acetyl-*L*-cysteine was 25, 22 and 33% after 24, 48 and 72 hours respectively.

Time (hours)	% Yield *N*-acetyl-*L*-cysteine	% Yield *N,S*-diacetyl-*L*-cysteine
24	25	26
48	22	22
72	33	24

Table 4.6 Yields of acetylated products in the presence of ferrous ions

The results from reaction of *L*-cysteine and thioacetic acid in the presence and absence of ferrous ions differ markedly. *N*-acetyl-*L*-cysteine was the only product observed in

the reactions in the absence of added ferrous ions. While in the presence of ferrous ions both *N*-acetyl-*L*-cysteine and *N,S*-diacetyl-*L*-cysteine were detected. This may indicate the coordination of the ferrous metal centre is affecting the details of acyl transfer chemistry.

No *N,S*-diacetyl-*L*-cysteine was detected in the reaction mixtures containing *L*-cysteine and thioacetic acid in the absence of ferrous ions. Thioacetic acid was mixed with *N*-acetyl-*L*-cysteine in deuterium oxide in order to investigate whether *N*-acetyl-*L*-cysteine and thioacetic acid could react to form *N,S*-diacetyl-*L*-cysteine in the absence of ferrous ions. The reaction mixtures were heated at 50°C for times ranging from 24 to 72 hours. *N,S*-Diacetyl-*L*-cysteine was detected with yields of 15, 22 and 27% after 24, 48 and 72 hours respectively. The results of these experiments are shown in *Table 4.7.*

Time (hours)	% Yield *N,S*-diacetyl-*L*-cysteine
24	15
48	22
72	27

Table 4.7 *Yields of* N,S-*diacetyl*-L-*cysteine from* N-*acetyl*-L-*cysteine*

L-Cysteine and thioacetic acid forms *N*-acetyl-*L*-cysteine in high yield and *N*-acetyl-*L*-cysteine has been shown to react with thioacetic acid to form *N,S*-diacetyl-*L*-cysteine. This is consistent with slow *S*-acetylation of cysteine followed by a fast acyl transfer to form the *N*-acetylated product. Therefore with the approximately stoichiometric addition of thioacetic acid (allowing for some hydrolysis), *N*-acetyl-*L*-cysteine was

formed in almost quantitative yield. When more thioacetic aid was added to *N*-acetyl-*L*-cysteine the *N,S*-diacetyl-*L*-cysteine was formed as expected. This series of reaction is consistent with thermodynamic control as the *N*-acetyl product is more stable (*Figure 4.10*).

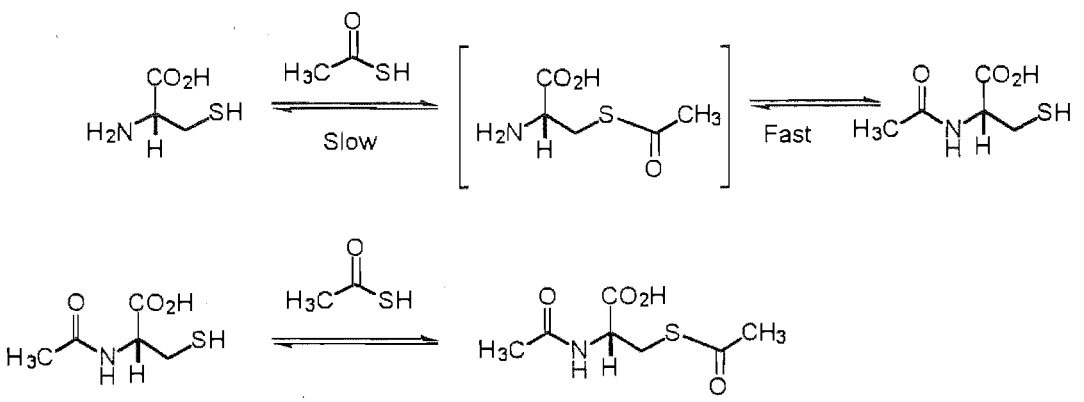

Figure 4.10 Formation of N-*acetyl cysteine and* N,S-*diacetyl cysteine*

In contrast, analysis of the reaction mixtures containing thioacetic acid, *L*-cysteine and ferrous ions indicated a mixture of *L*-cysteine, *N*-acetyl-*L*-cysteine and *N,S*-diacetyl-*L*-cysteine was produced. This result doesn't reflect "free" solution thermodynamics. The ferrous ions perturb the system and change the product distribution. This may be due to coordination chemistry. Cysteine is a good chelating ligand for ferrous ions. However, acetylation will reduce the ability of the acetylated product to complex with ferrous ions. The distribution of reactants and products that are ferrous bound and in solution complicates the interpretation of the results. Therefore the reaction of thioacetic aid with cysteine in the presence of ferrous ions was not studied further.

4.3 Probing the metal ion induced acyl transfer reaction

A detailed study of the reaction of thioacetic acid and alanine was carried out to delineate the factors associated with acyl transfer. Alanine was chosen as the amino acid to be used in the detailed study as the methyl protons in the ^{1}H NMR spectrum provided a suitable signal for quantification. Also alanine had been shown to react slower than glycine in the preliminary study, making the course of reaction easier to follow.

4.3.1 Effect of acidity and control of pH on the reactions of thioacetic acid with *D,L*-alanine

The pH was observed to drift downward from 7 to 3 during the reaction time in the preliminary reactions. Therefore we investigated the use of buffers to control the pH during the reaction. The pH range of interest is near neutral, a likely pH for the evolution of life. The buffers 4-(*N*-morpholine)ethane-sulphonic acid (MES), 1,4-piperazine-*N,N'*-bis(2-ethanesulphonic acid) (PIPES) and 4-(*N*-2-hydroxyethyl)-1-piperazine-*N*-2'-ethane-sulphonic acid (HEPES) have pK_as of 6.1, 6.8 and 7.5 respectively (*Figure 4.11*), thus spanning the pH range of interest.

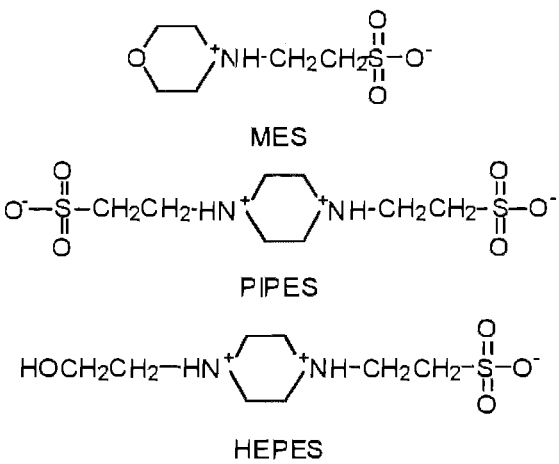

Figure 4.11 Structures of PIPES, MES and HEPES

Using the buffers described above, thioacetic acid was reacted with *D,L*-alanine in 1 M buffers at pH 6.1, 6.5 and 7.5. The results of these reactions are shown in *Figure 4.12*. The rate of reaction was higher at pH 6.5 than at either pH 6.1 or 7.5.

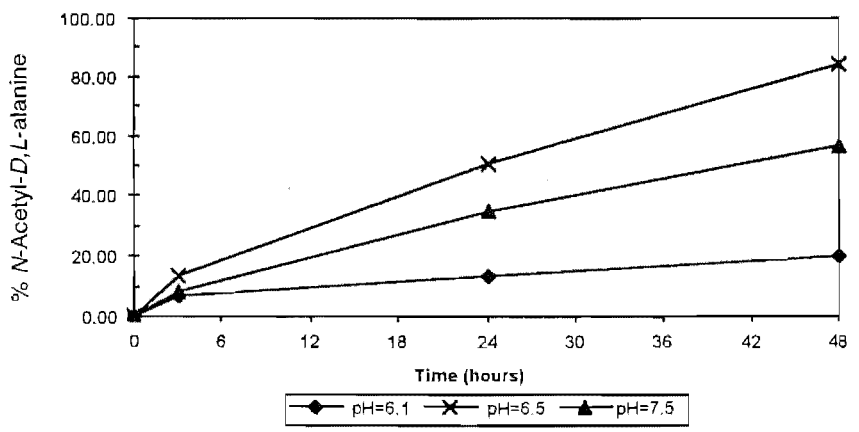

Figure 4.12 The relationship of % yield of N-*acetyl*-D,L-*alanine with pH*

The pH dependence of the reaction rate may be due to the intrinsic acid-base chemistry of the reactants. If the mechanism of reaction is nucleophilic attack by the amine group of alanine at the electrophilic carbonyl carbon of thioacetic acid, the preferred reaction pathway should occur when the thioacetic acid is protonated and the amine is

deprotonated. The former requires low pH while the latter requires high pH. The combination of these two should result in a bell shaped pH-reactivity profile with a maximum at a pH value, which is halfway between the pK_a values of the two functional groups. The pK_as of thioacetic acid and the amine group of alanine are 3.33 and 9.87 respectively[14]. Thus it is reasonable that the maximum may occur when the pH is 6.54, which is close to pH 6.5. It is less easy to understand why the alternative, oxidative, mechanism proposed by Orgel and Liu would display this kind of pH dependence. Impurities of oxidised thioacetic acid in the thioacetic acid may be responsible for the initial fast rate of reaction.

The effect of solution pH on the reaction of thioacetic acid with *D,L*-alanine in the presence of ferrous ions was investigated. Reaction mixtures containing *D,L*-alanine, thioacetic acid and ferrous ions were heated at 40°C and the pH was varied between 6–7.5. All solutions were degassed to minimise dissolved oxygen as previously described, and the heterogenous reaction mixtures were treated with potassium cyanide prior to analysis by ^{1}H NMR spectroscopy, in order to resolubilize any compounds coordinated to ferrous ions.

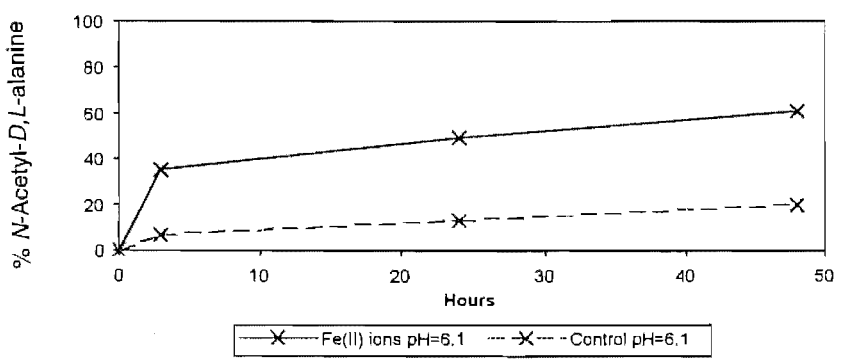

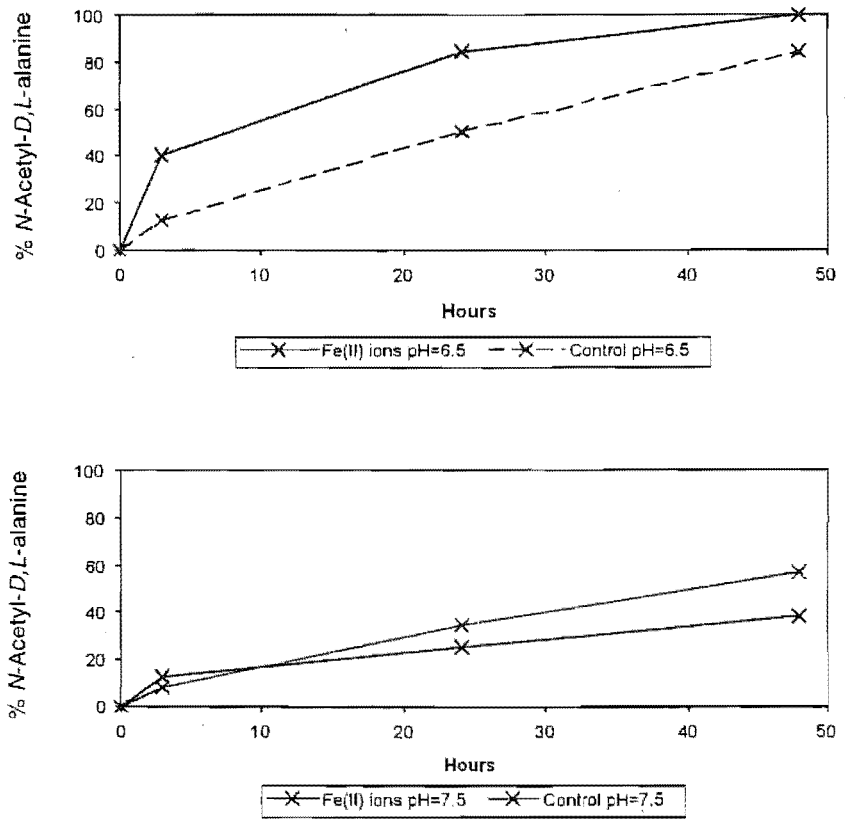

Figure 4.13 Comparison of % yield of N-*acetyl-* D,L-*alanine in the presence and absence of ferrous ions at pH = 6.1, 6.5 and 7.5*

The results of reaction at pH of 6.1, 6.5 and 7.5 are shown in *Figures 4.13*. The rate of ferrous mediated reaction relative to iron-free control was increased at pH = 6.1 and 6.5; whilst no equivalent change in rate was observed at pH = 7.5. Both the ferrous mediated reaction and control had a maximum rate of *N*-acetyl-*D,L*-alanine production at pH=6.5.

This reaction was studied after incubation for 18 hours at 40°C with pH between 6–7.5 (0.5 pH increment steps). The results are shown in *Figure 4.14*. The extent of reaction is greatest in the range pH 6.5 to 7, both in the presence and absence of ferrous ions.

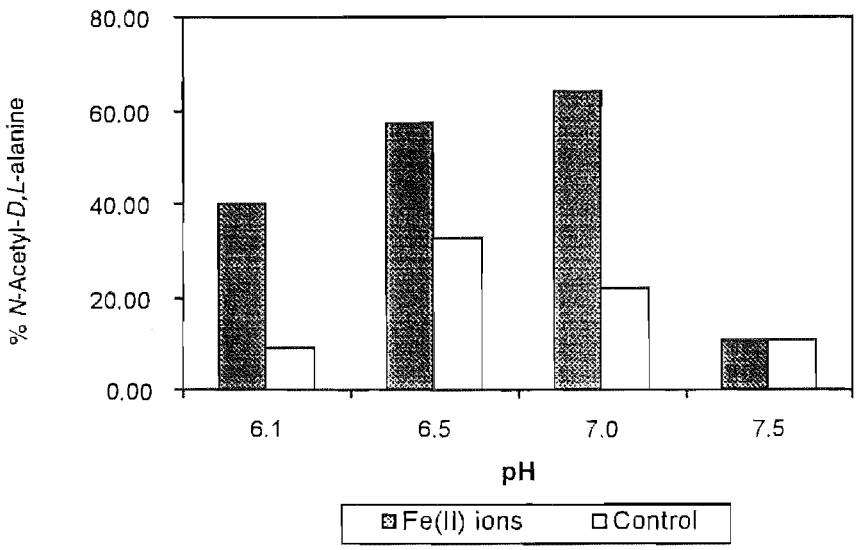

Figure 4.14 A measure of relative rates of % yield of N-*acetyl*-D,L-*alanine in the presence and absence of ferrous ions at pH = 6.1, 6.5, 7.0 and 7.5.*

The yields in the absence of ferrous ions are significantly lower than the parallel experiments in the presence of ferrous ions in the pH range 6.1 to 7.0. The yield of *N*-acetyl-*D,L*-alanine was the same in the presence and absence of ferrous ions at pH 7.5.

Work up procedure

There was the possibility that the increased reaction rates of reaction mixtures containing ferrous ions may be related to the associated work up procedure. Therefore we conducted experiments in order to determine whether the increase in rate was due to the work up procedure prior to analysis by ^{1}H NMR spectroscopy rather than to differences in the reaction conditions. Reactions containing thioacetic acid and *D,L*-alanine were heated for 3 hours at 40°C at pH 6.5. This reaction time was chosen to minimise any oxidation of thioacetic acid due to residual dissolved oxygen. After this reaction time ferrous ions and cyanide ions were added sequentially. Another series of reaction

containing *D,L*-alanine and thioacetic acid were prepared and heated at 40°C for 3 hours. Ferrocyanide ions were added prior to analysis by ^{1}H NMR spectroscopy. The control reaction contains only thioacetic acid and *D,L*-alanine. The results of these experiments are shown in *Figure 4.15*. There is no significant difference between the results. It appears that the work up is not responsible for the difference between reaction in the presence and absence of ferrous ions added.

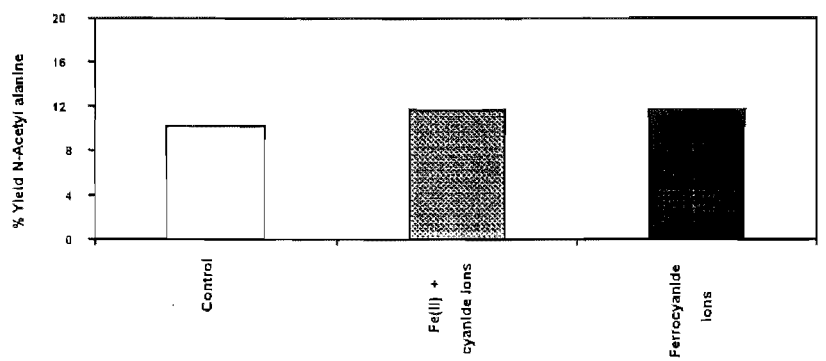

Figure 4.15 Workup procedure – comparison of control reactions with reaction mixtures that had been treated with ferrous ions and cyanide ions or ferrocyanide ions

4.3.2 Investigation of the mechanism of reaction.

The mechanism of reaction of thioacetic acid with amino acids is not well understood. The increased rate of reaction relative to samples with no ferrous ions (*Figure 4.14*) may be due to an oxidative reaction mechanism of acylation as proposed by Liu and Orgel[8] (as discussed earlier). Alternatively, the increase in rate may be due to the Lewis acid properties of ferrous ions. Coordination of one or both of the reactants to the ferrous ions may affect the rate of reaction. The thioacetic acid may coordinate with ferrous ions as shown in *Figure 4.16* and this may increase the electrophilicity of the carbonyl centre.

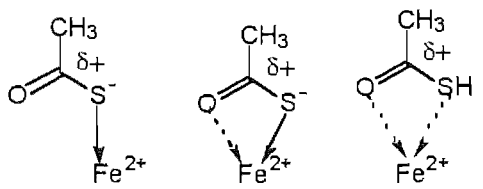

Figure 4.16 Possible coordination of thioacetic acid with ferrous ions

The alanine is also capable of coordinating to ferrous ions, thus the amine group of the alanine may be held in close proximity to the electrophilic carbonyl group of the thioacetic acid. One possible mode of coordination is shown in *Figure 4.17*.

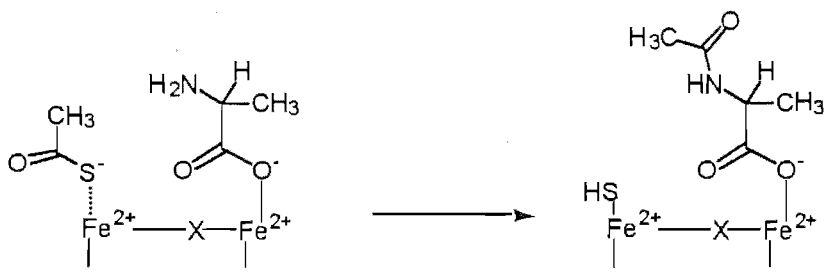

Figure 4.17 Possible mode of coordination of thioacetic acid and alanine

We compared reactions containing ferrous ions with ferrocyanide ions in order to investigate the increase rate of reaction and thus the mechanism of reaction in the presence of ferrous ions. This allows a distinction to be drawn between redox chemistry and coordination chemistry. All coordination sites are occupied in ferrocyanide ions therefore coordination of reactants or products is not possible. The redox potentials of ferrocyanide ions ($E^{\circ}_{red} = 0.358$) and ferrous ions ($E^{\circ}_{red} = 0.771$) are roughly similar[14], so that ferrocyanide ions should promote the reaction in a similar manner.

Reaction mixtures were prepared containing thioacetic acid and *D,L*-alanine with and without ferrous ions and ferrocyanide ions. These mixtures were heated for 18 hours at 40°C. The pH was buffered and varied between 6.5 and 7.5 using appropriate buffers. The results of these experiments are shown in *Figure 4.18*.

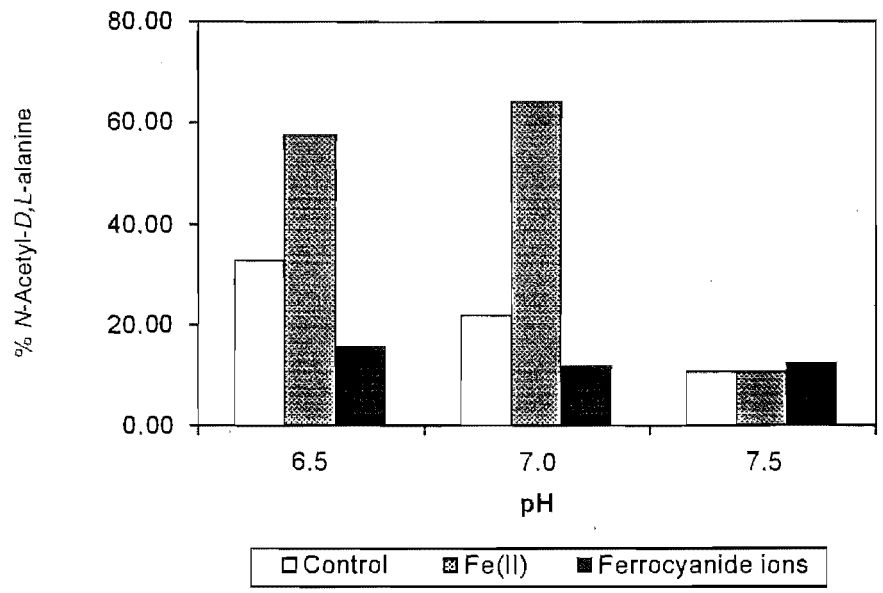

Figure 4.18 *Yield of* N-*acetyl*-D,L-*alanine in the presence of ferrous ions or ferrocyanide ions*

The presence of ferrocyanide ions does not appear to increase the rate of reaction of thioacetic acid with *D,L*-alanine, relative to the reactions containing ferrous ions or control reactions. At pH 7.5 the yields of *N*-acetyl-*D,L*-alanine were approximately the same for the reaction mixtures containing ferrous ions or ferrocyanide ions and for the control reaction mixtures. These yields were low relative to the yields at pH 6.5 or 7.0. This may be due the acid–base chemistry of the reactants as described previously. The yields of *N*-acetyl-*D,L*-alanine were much less for reaction mixtures containing ferrocyanide ions relative to reaction mixtures containing ferrous ions at pH 6.5 and 7. This may mean that coordination of thioacetic and/or *D,L*-alanine with ferrous ions is a

factor in the catalysis of the formation of *N*-acetyl-*D,L*-alanine. These results have been interpreted to mean coordination chemistry of ferrous ions is significant in the catalytic chemistry leading to formation of *N*-acetyl-*D,L*-alanine.

The possible importance of coordination was therefore investigated further by assessing other metal ions capable of promoting this chemistry. Non-redox active metal ions were chosen in order to eliminate the involvement of redox chemistry. The diamagnetic metal ions, zinc and cadmium ions were chosen. Zinc and cadmium ions may coordinate with the reactants and the reaction mixtures could be monitored directly by NMR spectroscopy.

The zinc and cadmium ions were added to buffered reaction mixtures containing thioacetic acid and *D,L*-alanine. The results were compared with reactions containing thioacetic acid and *D,L*-alanine in the presence and absence of ferrous ions. The results are shown in *Figure 4.19*.

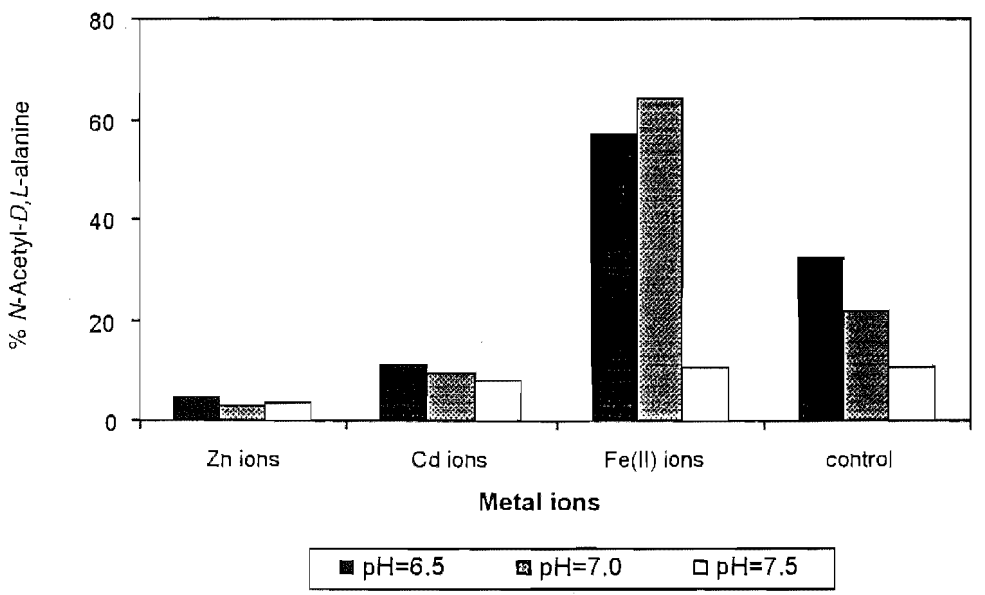

Figure 4.19 Yields of N-*acetyl*-D,L-*alanine in the presence of different metal ions*

Zinc ions and cadmium ions do not appear to catalyse the *N*-acylation of alanine when the reaction is attempted in the pH range 6.5-7.5. Rather, it was found that hydrolysis of thioacetic acid to acetic acid/acetate was enhanced by zinc and cadmium ions relative to the control (*Figure 4.20*). It was not possible to measure hydrolysis of thioacetic acid in the reactions containing ferrous ions as the thioacetic acid resonance overlapped with the buffer resonances in ^{1}H NMR spectrum. However, it was possible to observe that the amount of hydrolysis was greater in the presence of ferrous ions than in its absence.

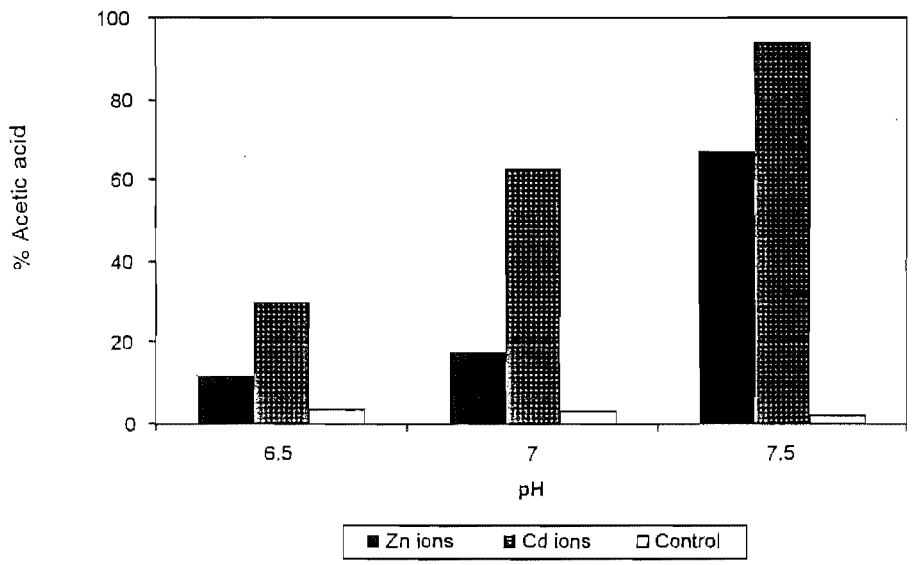

Figure 4.20 *Yield of acetic acid in the presence of zinc or cadmium ions*

The rates of hydrolysis of thioacetic acid in the presence of zinc or cadmium ions increase as the pH rises, presumably reflecting the increasing concentration of both free and coordinated hydroxide ions. The hydroxide ions may attack the electrophilic centre of thioacetic acid and lead to formation of acetic acid. The amount of hydrolysis of thioacetic acid in the absence of any metal ions appears to decrease slightly as the pH increases. However, the amount of hydrolysis in each of these cases is small which

means that the integrals are small and the experimental error is large. Therefore the change in amount of hydrolysis of thioacetic acid the absence of metal ions with changing pH is probably not significant over this pH range.

Either water or the amine group of the amino acid can act as nucleophiles and attack the electrophilic carbonyl centre of thioacetic acid. The hydrolysis of thioacetic acid reaction and the *N*-acylation reaction are in competition. The results observed are consistent with zinc and cadmium ions being better catalysts for the hydrolysis reactions than for the *N*-acylation reaction. Large amounts of acetic acid are observed in the reactions containing zinc or cadmium ions due to hydrolysis of thioacetic acid. Zinc ions are well known catalysts of hydrolysis reactions. This is due to the low pK_a of coordinated water and hence a proton can be removed to form a metal-bound hydroxide. The metal-bound hydroxide reacts to hydrolyse other species. Metal promoted hydrolysis reactions dominate in competition with other nucleophilic reactions for the zinc and cadmium systems. The amount of hydrolysis in the ferrous systems was unable to be determined but presumably hydrolysis can not be so great because high yields of *N*-acylation products were observed.

4.3.3 Reaction of thioacetic acid and HEPES buffer in the presence of cadmium ions or zinc ions

A large unidentified singlet was observed in the ^{1}H NMR spectrum at 1.80 ppm in reaction mixtures containing HEPES buffer, cadmium or zinc ions and thioacetic acid. The peak was not observed in reaction mixtures that were not buffered by HEPES, or in the absence of cadmium or zinc ions. A larger scale reaction containing thioacetic acid,

HEPES and zinc ions was performed in distilled water at pH=7.5. After the reaction time the solvent was removed at reduced pressure. The residue that remained was analysed by ^{1}H NMR spectroscopy, 2-D NMR spectroscopy and mass spectrometry. The singlet at 1.9 ppm was again present. It is possible that acylation of the alcohol group of HEPES may be occurring under the same conditions (*Figure 4.21*).

Therefore we tried to detect *O*-acetyl HEPES in order to support this hypothesis. The mass spectrum of the unknown contained a m/z peak consistent with the MH^+ ion of *O*-acetyl HEPES. High resolution mass spectrometry and 2-D NMR spectroscopic results were also consistent with the unidentified compound being *O*-acetyl HEPES. Therefore HEPES was not used as a buffer for any further reactions containing zinc and cadmium ions.

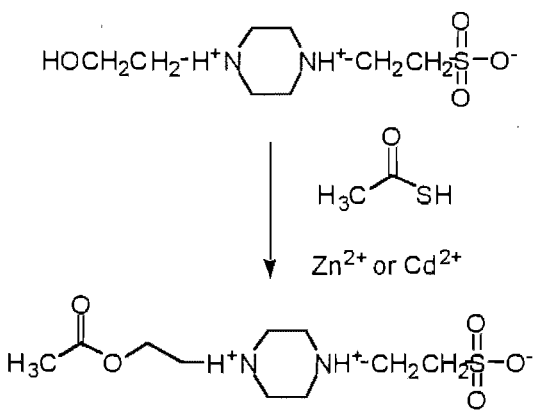

Figure 4.21 O-acetylation of HEPES by thioacetic acid

4.3.4 Reaction of thioacetic acid with *D,L*-alanine methyl ester in the presence of ferrous, ferrocyanide, zinc or cadmium ions

Little *N*-acetyl alanine was produced from thioacetic acid and alanine in the presence of zinc or cadmium ions compared with the similar reactions in the presence of ferrous ions. Instead, the presence of zinc or cadmium ions catalysed hydrolysis of thioacetic acid. It was decided to evaluate the *N*-acylation chemistry of alanine methyl ester to test the generality of these observations.

Alanine methyl ester was chosen as the amine group would be similar to alanine but the absence of the carboxylic acid group means the alanine methyl ester can only form weak bidentate complexes with metal ions. This is because the methyl ester is a much poorer ligand than the related carboxylate group. It was hoped that investigation of reaction of alanine methyl ester with thioacetic acid in the presence of ferrous, ferrrocyanide, zinc and cadmium ions would provide an insight into the reaction mechanism and, in particular, whether coordination is important.

The expected product of reaction of *D,L*-alanine methyl ester with thioacetic acid is *N*-acetyl-*D,L*-alanine methyl ester. *D,L*-Alanine methyl ester was synthesised from *D,L*-alanine and thionyl chloride in methanol (*Figure 4.22*). *N*-Acetyl-*D,L*-alanine methyl ester was synthesised from alanine methyl ester by reaction with acetic anhydride and pyridine (*Figure 4.22*). ^{1}H NMR spectroscopy was performed on samples of starting material and expected products dissolved in deuterium oxide.

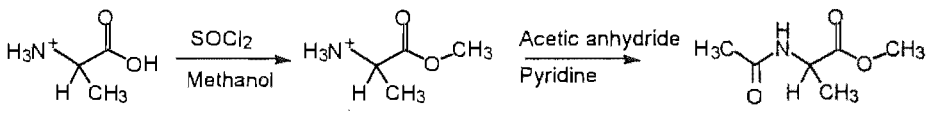

Figure 4.22 Synthesis of D,L-*alanine methyl ester and* N-*acetyl*-D,L-*alanine methyl ester*

Thioacetic acid was reacted with alanine methyl ester in the presence and absence of zinc ions, cadmium ions, ferrous ions and ferrocyanide ions at pH = 6.5. These reaction mixtures were heated at 40°C for 18 hours. The results of these experiments are shown in *Figure 4.23.*

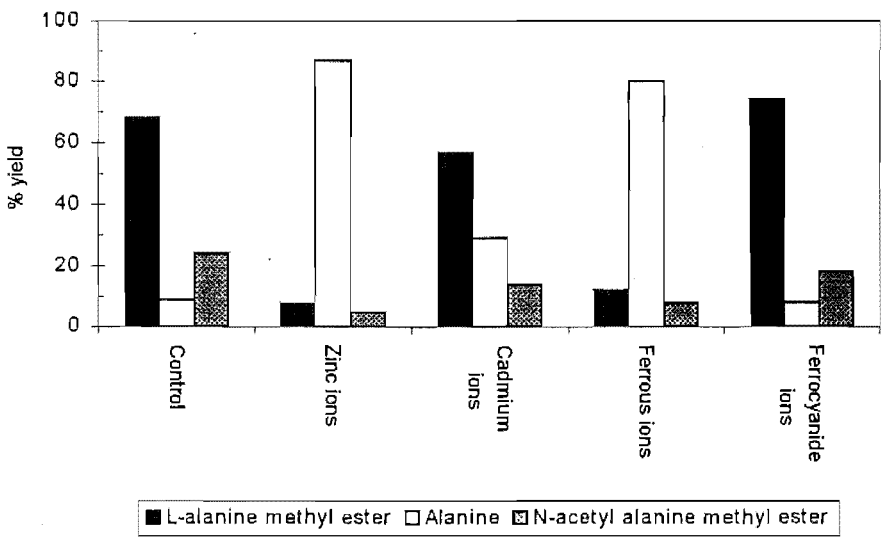

Figure 4.23 Reaction of thioacetic acid with D,L-*alanine methyl ester at pH=6.5*

The reaction of thioacetic acid and *D,L*-alanine methyl ester in the presence of zinc ions or ferrous ions produced a large amount of *D,L*-alanine. A significant amount of *D,L*-alanine was also detected in the reactions containing cadmium ions. While the control and ferrocyanide ions reactions produced significantly less *D,L*-alanine. The control reactions produced the most *N*-acetyl-*D,L*-alanine methyl ester. Only limited

conclusions can be drawn from these experiments as the results are complicated by the varied amount of hydrolysis of the *D,L*-alanine methyl ester in these reactions, however zinc, cadmium and ferrous ions are promoting hydrolysis of both methyl ester and thioacetic acid in preference to *N*-acylation.

4.3.5 Reaction of thioacetic acid and *D,L*-alanine in the presence of ferrous sulfide

Given the importance of iron-sulfur systems in biochemistry and geochemistry, as previously discussed in Chapter one, a combination of ferrous ions and sulfide ions was evaluated as possible catalysts for amide formation. Heterogeneous mixtures of iron sulfide, thioacetic acid and alanine were reacted at different pHs for a range of times before addition of cyanide ions, centrifugation and analysis by ^{1}H NMR spectroscopy. The results are shown in *Figure 4.24*.

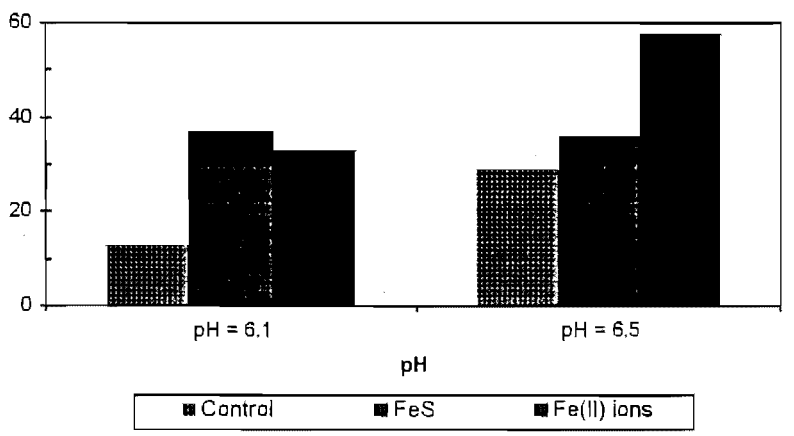

Figure 4.24 % yield of N-*acetyl*-D,L-*alanine in the presence and absence of ferrous ions and ferrous sulfide.*

Ferrous sulfide and ferrous ions both promote production of *N*-acetyl-*D,L*-alanine relative to the control at pH=6.1 and pH=6.5. Catalysis of *N*-acylation by ferrous sulfide is more marked at pH 6.1.

4.4 Di-peptide formation

4.4.1 Introduction

Thiocarboxylic acids acylate amino acids and this reaction has been shown to be promoted by metal ions (as has been shown above). A possible prebiotic biomimetic peptide forming reaction was evaluated in order to extend the analogy with non-ribosomal peptide biosynthesis. The ability of metal ions to facilitate the reaction of *N*-protected thioamino acids with amino acid esters, to produce dipeptide derivatives, was studied.

4.4.2 Synthesis of potassium *N*-(benzyloxycarbonyl)-*D,L*-thioalanine

The synthesis of potassium *N*-(benzyloxycarbonyl)-*D,L*-thioalanine is outlined in *Figure 4.25*[15]. Alanine was *N*-protected as its benzyloxycarbonyl (Z) derivative. The *N*-benzyloxycarbonyl-protected alanine was then reacted to form its *N*-hydroxysuccinimide ester. This ester was dissolved in DMF at 0°C and the resulting solution was treated with lithium sulfide to produce crystalline *N*-(benzyloxycarbonyl)-*D,L*-thioalanine in a 35% yield. *N*-(Benzyloxycarbonyl)thioamino acids are readily oxidised by atmospheric oxygen[15], whereas the potassium salts were reported to be stable at room temperature

for several months. Hence, the potassium salt of *N*-(benzyloxycarbonyl)-*D,L*-thioalanine (73% yield) was produced by treating the thiocarboxylic acid with potassium hydroxide. The crystalline salt was isolated by freeze drying and purified by recrystallisation.

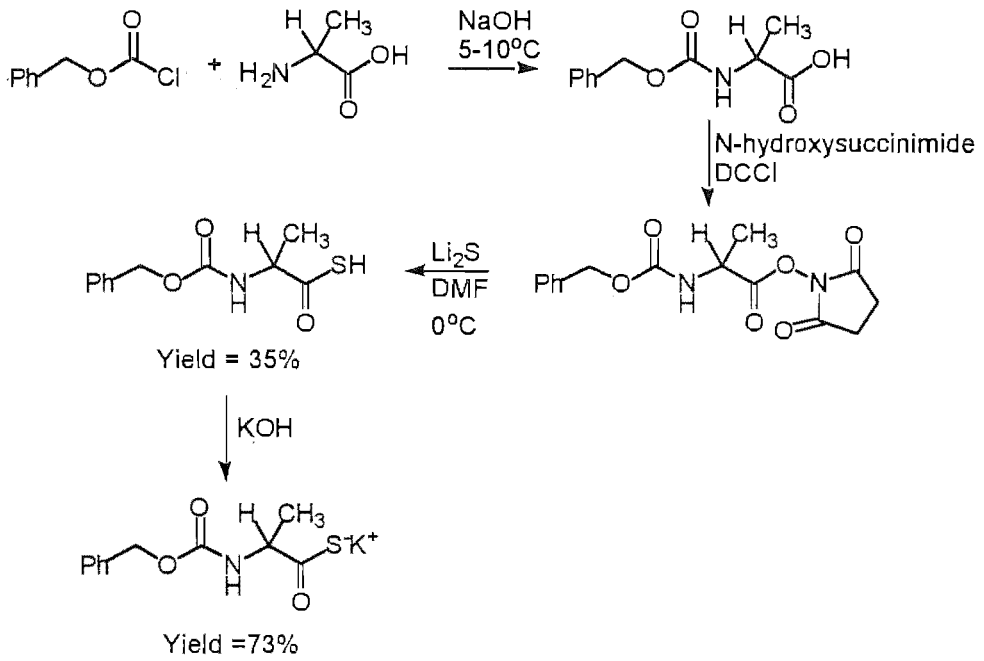

Figure 4.25 Synthesis of potassium N-*(benzyloxycarbonyl)*-D,L-*thioalanine*

4.4.3 Methods of analysis reaction of dipeptide formation

A method for analysing the proposed peptide coupling experiments was required. The expected product of the reaction of *N*-(benzyloxycarbonyl)thioamino acids with amino acid derivatives, would be an *N*-(benzyloxycarbonyl)dipeptide.

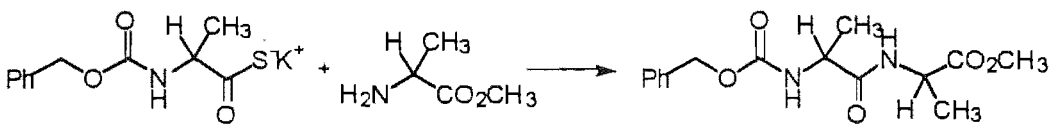

Figure 4.26 Reaction of N-*(benzyloxycarbonyl)*-D,L-*thioalanine with* L-*alanine methyl ester*

We chose *N*-(benzyloxycarbonyl)thioalanine and alanine as its *O*-protected methyl ester as the reactants. The expected product of reacting *N*-(benzyloxycarbonyl)-*D,L*-thioalanine with *L*-alanine methyl ester is *N*-(benzyloxycarbonyl)-*D,L*-alanyl-*L*-alanine methyl ester (*Figure 4.26*). A sample of *N*-(benzyloxycarbonyl)-*D,L*-alanyl-*L*-alanine methyl ester was provided by B. Hampton[16].

A number of different methods for analysing the reaction mixtures were investigated. Initially ^{1}H NMR spectroscopy was performed on solutions containing a mixture of *N*-(benzyloxycarbonyl)-*D,L*-alanyl-*L*-alanine methyl ester, *L*-alanine methyl ester and *N*-(benzyloxycarbonyl)-*D,L*-thioalanine. Unfortunately, in each case the alanine methyl peaks of the 3 components were not fully resolved in the spectrum. Therefore integration of a solution containing these three compounds would be difficult and potentially inaccurate.

It was possible to separate the different components of the mixture by exploiting the acid/base chemistry of the reactants and expected products. Aqueous solutions containing *N*-(benzyloxycarbonyl)-*D,L*-alanyl-*L*-alanine methyl ester, *L*-alanine methyl ester and *N*-(benzyloxycarbonyl)-*D,L*-thioalanine acid adjusted to pH=10 were extracted with chloroform. The *N*-(benzyloxycarbonyl)-*D,L*-alanyl-*L*-alanine methyl ester was extracted into the chloroform, while the *L*-alanine methyl ester and *N*-(benzyloxycarbonyl)–*D,L*-thioalanine acid remained in the aqueous layer. When the pH

was then adjusted to pH=1 by addition of hydrochloric acid a white precipitate formed. The heterogeneous mixture was re-extracted with chloroform. Most of the *N*-(benzyloxycarbonyl)-*D,L*-thioalanine was present in the chloroform phase, while the alanine methyl ester remained in the acidic aqueous layer. This aqueous solution also contained a small amount of *N*-(benzyloxycarbonyl)-*D,L*-thioalanine. This extraction technique provided a method for isolating *N*-(benzyloxycarbonyl)-*D,L*-alanyl-*L*-alanine methyl ester and thereby demonstrating its formation.

Reactions containing *L*-alanine methyl ester and *N*-(benzyloxycarbonyl)-*D,L*-thioalanine, with and without ferrous ions, were performed in degassed deuterium oxide. The reaction mixtures were heated at 50°C for 24 hours. After the reaction time the ferrous ions were removed by complexation with cyanide ions and the resulting solution had a pH=10. The reaction mixtures performed without ferrous ions were adjusted to pH=10. The reaction mixtures were extracted with an equal amount of chloroform and analysed by ^{1}H NMR spectroscopy. Analysis of the ^{1}H NMR spectra of the samples extracted with chloroform showed *N*-(benzyloxycarbonyl)-*D,L*-alanyl-*L*-alanine methyl ester was produced in the reaction mixtures. More *N*-(benzyloxycarbonyl)-*D,L*-alanyl-*L*-alanine methyl ester was produced in the reaction mixtures that contained ferrous ions relative to those that did not. No quantification of the relative yields was attempted because of the uncertainties introduced by the extraction methodology.

We turned to HPLC in order to provide quantitative analysis of the reaction mixtures. This separates the components and thus makes it easier to identify and quantify the compounds present. This is potentially important as the reactants and products may be hydrolysed under the reaction conditions (*Figure 4.27*).

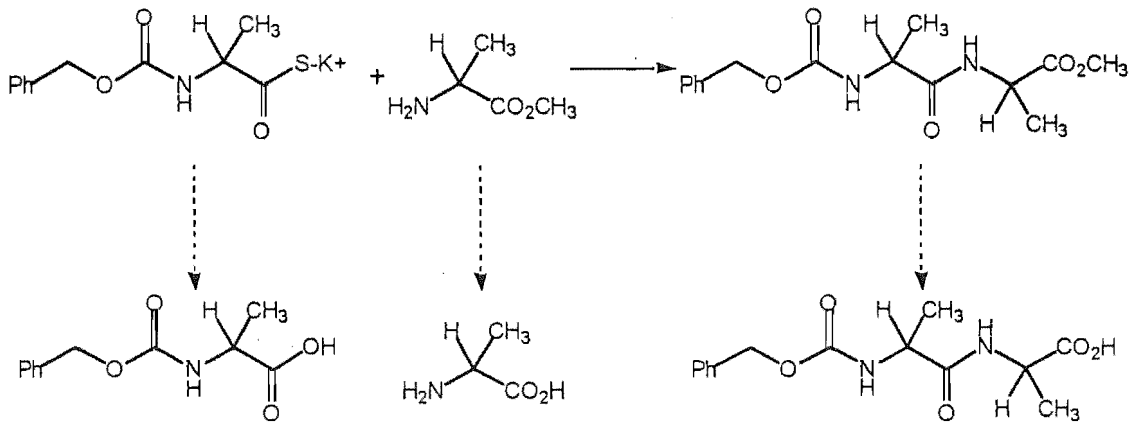

Figure 4.27 Hydrolysis products of the reaction reactants and product

The proposed hydrolysis products are *N*-(benzyloxycarbonyl)-*D,L*-Alanyl-*L*-alanine and *N*-(benzyloxycarbonyl)-*D,L*-alanine. Authentic samples of these compounds were synthesised. A sample of *N*-(benzyloxycarbonyl)-*D,L*-alanyl-*L*-alanine was provided by B. Hampton[16]. *N*-(benzyloxycarbonyl)-*D,L*-alanine was synthesised from *D,L*-alanine and benzyl chloroformate under basic conditions, as shown in *Figure 4.25*.

Conditions for the HPLC analysis were optimised using a C_{18} column eluted with an acetonitrile and water (0.05% v/v TFA) mixture. Resolution of all the reaction mixture components was achieved using a 25% acetonitrile and 75% water/TFA solvent mixture. The retention times of the compounds of interest were measured under these conditions and the results are shown in *table 4.8* .

Compound	Retention time (Min)
L-alanine methyl ester	2.65
L-alanine	2.06
N-Z-*D,L*-thioalanine	39.44
N-Z-*D,L*-alanine	13.55
N-Z-*D,L*-alanyl-*L*-alanine methyl ester	16.37
N-Z-*D,L*-alanyl-*L*-alanine	8.49

Table 4.8 HPLC retention time of reaction components

Known amounts of compounds of interest were used as standards to provide a calibration of the sensitivity of each compound at 203 nm. Given these calibrations, the integration of these peaks provides a means of determining the yields of the reactions.

4.4.4 Reaction of L-alanine methyl ester with the potassium salt of *N*-(benzyloxycarbonyl)-*D,L*-thioalanine in the presence and absence of ferrous species

L-Alanine methyl ester and the potassium salt of *N*-(benzyloxycarbonyl)-*D,L*-thioalanine were reacted in the presence of ferrous ions, ferrous sulfide or ferrocyanide ions in degassed PIPES buffer with a pH=6.5. Control reactions with no iron were also studied. The reaction mixtures were heated at 40°C for 18 hours. The reactions containing ferrous ions and ferrous sulfide were treated with cyanide before being analysed by HPLC. The averaged results are shown in *Table 4.9*.

	% Yield *N*-Z-*D,L*-thioalanine	% Yield *N*-Z-*D,L*-alanine	% Yield *N*-Z-*D,L*-alanyl-*L*-alanine methyl ester	% Yield *N*-Z-*D,L*-alanyl-*L*-alanine
Control	80	11	2	-
Fe^{2+}	12	28	26	1
$Fe(CN)_6^{4-}$	48	17	18	-
FeS	40	26	12	-

Table 4.9 % yields from the reaction of L-*alanine methyl ester with potassium salt of N-(benzyloxycarbonyl)-*D,L-*thioalanine*

In the absence of metal ions the yield of *N*-(benzyloxycarbonyl)-*D,L*-alanyl-*L*-alanine methyl ester was low. When ferrous ions or ferrocyanide ions are added the yield of *N*-(benzyloxycarbonyl)-*D,L*-alanyl-*L*-alanine methyl ester increased significantly. Although the solvent was degassed the solutions were not fastidiously anaerobic as some rust was formed during the reaction time. The yield of reaction with ferrous ions is larger than the yield for the reactions containing ferrous sulfide or ferrocyanide ions.

The dipeptide coupling, whilst enhanced by the presence of ion salts, is less facile than the analogous coupling chemistry between thioacetic acid and an amino acid. This could be due to the different coordination chemistry of the thiocarboxylic acid or amino acid components decreasing reactivity. The absence of a carboxylate in the *N*-donor may result in a change in reactivity of the adjacent amine. The increased steric bulk of the thiocarboxylic acid component may decrease its ability to coordinate with iron or decrease its intrinsic acyl transfer reactivity. In any event, the comparable effects of

ferrous ions, ferrous sulfide and ferrocyanide ions imply that coordination chemistry is not a key factor in this amide bond forming reaction.

Both reactions containing ferrous ions of ferrocyanide ions produced significantly more *N*-(benzyloxycarbonyl)-*D,L*-alanyl-*L*-alanine methyl ester than the control reaction. It is possible, in this case, that oxidation of thiocarboxylic acid may be an important factor in the increased yield of *N*-(benzyloxycarbonyl)-*D,L*-alanyl-*L*-alanine methyl ester. Ferrous ions and ferrocyanide ions can be oxidised to ferric and ferricyanide ions respectively by atmospheric oxygen. The ferric and ferricyanide ions are oxidants which could oxidise the *N*-(benzyloxycarbonyl)-*D,L*-thioalanine to form the more reactive disulfide.

These results contrast with the results of the similar reaction of thioacetic acid and alanine. The yields of *N*-acetyl alanine from thioacetic acid and alanine in the presence of ferrous ions were significantly higher than the yields in the presence of ferrocyanide ions. This was taken to imply that coordination was important in the promotion of the formation of *N*-acetyl alanine, whereas oxidation played little or no part in promoting formation of *N*-acetyl alanine. The different results are consistent with the reactants of *N*-(benzyloxycarbonyl)-*D,L*-thioalanine and/or alanine methyl ester being less able to form strong coordination complexes with ferrous ions. Thus the slower reaction pathway of oxidation of *N*-(benzyloxycarbonyl)-*D,L*-thioalanine may have become important.

4.5 Summary

We have described the evaluation of the ability of a range of metal salts to promote *N*-acylation of amino acid by thiocarboxylic acids in this chapter. Ferrous ions were observed to promote the formation of *N*-acetyl alanine from alanine and thioacetic acid. On the other hand, zinc and cadmium ions catalyse the hydrolysis of thioacetic acid to acetic acid in preference to the *N*-acylation reaction. When alanine methyl ester was reacted with thioacetic acid in the presence of zinc or cadmium ions, hydrolysis of both alanine methyl ester to alanine and thioacetic aid to acetic acid were facile.

Oxidation of thioacetic acid had been postulated to be a key step in the mechanism of this class of acyl transfer reaction (*Figure 4.5*). Ferrous ions were observed to promote the *N*-acylation. However, despite degassing the reaction mixtures were not fastidiously anaerobic and rust was observed at the solvent-atmosphere interface, denoting the generation of ferric ions *in situ*. Likewise, ferrocyanide ions can also be oxidised to ferricyanide ions by atmospheric oxygen. Reactions were performed to compare the yields of *N*-acetyl alanine in the presence of ferrous ions or ferrocyanide ions relative to the control reactions. The results described here indicate that ferrous ions were significantly better at promotion of the formation of *N*-acetyl alanine than ferrocyanide ions. These results may imply that oxidation is not essential for promotion of acyl transfer.

The latter part of this chapter describes the evaluation of a range of metal salts to promote peptide bond formation from an amino acid ester and *N*-protected thioalanine.

Ferrous ions and ferrocyanide ions were observed to promote the peptide formation to comparable extents. These results imply that coordination chemistry does not play a major role in this acyl transfer reaction. This result is consistent with an oxidative mechanism rather than a coordination mechanism. The difference in proposed reaction mechanism is not unreasonable due to the nature of the reactants, alanine methyl ester and *N*-(benzyloxycarbonyl)thioalanine. These protected amino acid derivatives may be less able to coordinate with metal ions, thus the coordination mechanism is blocked and the oxidative mechanism dominates.

We have shown that amide bond formation from thiocarboxylic acids and amino acids is promoted by mixtures containing ferrous ions. Thioesters are the activated acid intermediates in non-ribosomal peptide biosynthesis (*Figure 4.1*). Could metal-bound thiocarboxylic acids have been the prebiotic precursors to thioesters? The results described in this chapter may indicate metal-bound thiocarboxylic acids were possible prebiotic precursors to thioesters.

4.6 References

1 H. Kleinkauf & H. von Dohren, *Annu. Rev. Microbiol.*, **41**, 259 (1987).

2 F. Lipmann, *Science*, **173**, 875 (1971).

3 T. Weiland, in *The roots of modern biochemistry: Fritz Lipmann's squiggle and its consequences*, H. Kleinkauf, H. von Dohren & L. Jaenicke (eds), Walter de Grayter 212-221 (1988).

4 C. Huber & G. Wächtershäuser, *Science*, **281**, 670 (1998).

5 C. Huber & G. Wächtershäuser, *Science*, **276**, 245 (1997).

6 J. C. Sheehan & D. A. Johnson, *J. Am. Chem. Soc.*, **74**, 4726 (1952) and references therein.

7 G. C. Barrett & A. R Khokhar, *Chem. Com.*, 818 (1969) and references therein.

8 R. Liu & L. E. Orgel, *Nature*, **389**, 52 (1997).

9 M. W. Cronyn & J. Jiu, *J. Am. Chem. Soc.*, **74**, 4726 (1952).

10 P. E. Dawson, T. W. Muir, I. Clark-Lewis & S. B. H. Kent, *Science*, **266**, 776 (1994).

11 W. Lu, M. A. Qusim & S. B. H. Kent, *J. Am. Chem. Soc.*, **118**, 8518 (1996).

12 J. P. Tam, Y. Lu & Q Lu., *J. Am. Chem. Soc.*, **121**, 4316 (1999).

13 H. A. Smith & G. Gorin, *J. Chem. Soc.*, **26**, 820 (1961)

14 R. C. Weast, *CRC Handbook of Chemistry &Physics*, CRC Press (1983).

15 Y. V. Mitin & N. P. Zapevalova, *Int. J. Peptide Protein Res.*, **35**, 352 (1990).

16 B. Hampton, *Masters Thesis*, University of Canterbury (1999).

Chapter 5

Experimental

5.1 General Methods

Unless otherwise stated, all materials were obtained from Sigma Chemical Company Ltd., Aldrich Chemicals or BDH laboratory supplies were generally of analytical grade.

Thin layer chromatography (TLC) was performed on Merck DC-Plastikfolien Kieselgel 60 F_{254} 20 cm x 20 cm plastic-backed plates. Visualisation was afforded by ultra-violet light, ninhydrin spray or 2,4-DNP spray.

High speed centrifugation was performed on an Eppendorf Centrifuge 5403, on a small scale (<1.5 mL) at up to 15000 r.p.m., and on a large scale (<50 mL) at up to 5000 r.p.m.

Nuclear magnetic resonance (NMR) spectroscopy was performed either on a Varian Unity 300 instrument, or on a Varian XL 300 instrument. These spectrometers operate

at 300 MHz for ^{1}H nuclei, at 75 MHz for ^{13}C nuclei, or at 120 MHz for ^{31}P nuclei. The probe temperature of these instruments was 23°C, unless otherwise specified. Peak positions are quoted in ppm relative to the reference peaks, which were the residual proton signals for the solvents used (d_1-chloroform, d_4-methanol, d_6-DMSO, d_6-acetone, and d_3-acetonitrile). In the case of deuterium oxide a small amount of methanol was added as a reference compound. A sample of 85% phosphoric acid in deuterium oxide was used calibrate the spectrometer for ^{31}P NMR spectra. Multiplicities are denoted as singlet (s), doublet (d), triplet (t), quartet (q), doublet of doublets (dd) or multiplet (m).

All pH measurements on volumes less than 5 mL were performed using universal indicator paper (pH 0-14) to obtain the approx value and then pH paper with smaller increments (eg. pH 1-3). Alternatively, pH measurements for volumes larger than 5 mL were performed using a Jenway 3020 pH meter fitted with a Schott Gerate N37BNC electrode, calibrated against standard buffers at pH 4, 7 and 9. Measurement of pH/D of deuterium oxide solutions are reported as pH (with no correction).

Melting points (mp.) less than 200°C were recorded on a Reichert Hot-stage microscope and are uncorrected. Melting points greater then 200°C were measured using an Electrothermal melting point apparatus and are uncorrected.

Electron ionisation (EI) and fast atom bombardment (FAB) mass spectra, were recorded on a Kratos MS80RFA magnetic sector double focussing mass spectrometer operating a 4 KV accelerating voltage.

Heating blocks were made and supplied by the mechanical workshop of the Canterbury University Chemistry Department.

High performance liquid chromatographic (HPLC) analyses were achieved using a Phillips PU4100 Liquid Chromatograph System equipped with a Phillips PU4120 Diode Array Detector interfaced to a personal computer running Phillips PU6003 Diode Array Detector System Software (V3.0) and a colour plotter.

Water for high performance liquid chromatography (HPLC) was produced with a Milli-Q Water Purification System (Millipore).

5.2 Chapter Two – Experimental

5.2.1 Experimental from 2.2.2

Commercial lithium potassium acetyl phosphate

Acetyl phosphate, lithium potassium salt - Aldrich (before purification)

δ_H (D_2O, 300 MHz) 1.87 (s, Ac), 2.06 (s, AcPi).

δ_C (D_2O, 300 MHz) 24.13 (Ac), 24.18 (CH_3).

δ_P (D_2O, 300 MHz) 1.85 (s, Pi), -0.91 (s, AcPi), -6.52 (d, J = 20.8Hz, PPPi), -7.07 (s, PPi), -19.77 (t, J= 19.6Hz, PPPi).

Purification of commercial acetyl phosphate

A solution of acetyl phosphate (7.5 mg, 40.7 μmol) dissolved in deuterium oxide (150 μL) was prepared. Solutions of silver nitrate (1.73 mg, 10.2 μmol; 3.46 mg, 20.4 μmol; 6.92 mg, 40.7 μmol) dissolved in deuterium oxide (150 μL) were prepared. The acetyl phosphate and silver nitrate solutions were mixed and a precipitate of silver phosphates formed. The resulting mixtures were centrifuged, and the supernatants removed for analysis, by ^{31}P NMR spectroscopy.

Ag^+ (μmol)	% AcPi	% Pi	% PPi	% PPPi
-	34	27	11	28
10.2	44	22	9	25
20.4	48	22	8	22
40.7	64	14	4	18

Silver acetyl phosphate

(Silver acetyl phosphate was prepared according to the method of Lipmann and Tuttle[1]).

Di-sodium hydrogen phosphate (12.5 g, 47 mmol) was dissolved in water (300 mL) and heated to 80°C. A solution of silver nitrate (23.1 g, 136 mmol) in water (150 mL) was prepared and added slowly to the hot phosphate solution. The resulting reaction mixture was heated at 100°C for 30 minutes before the yellow precipitate of silver phosphate (18.1 g, 92.6%) was isolated by filtration.

Silver phosphate (18.1 g, 43.5 mmol) was mixed with 85 % v/v phosphoric acid (11 mL) and stirred at 0°C. Ether was added to the stirred reaction mixture. A solution of acetyl chloride (8 mL, 141.6 mmol) and ether (17 mL) was prepared and added dropwise to the silver phosphate reaction mixture. The resulting mixture was stirred at room temperature for a further 10 minutes after the addition was complete. The pH of the mixture was adjusted to 3 -3.5 with the addition of sodium bicarbonate (1 M). The

purplish solid including silver chloride was removed by filtration through cellite. The supernatant was extracted twice with ether to remove acetic acid. Sodium hydroxide (33% w/v) was added to the aqueous layer until the solution became cloudy. The solution was frozen in liquid nitrogen and filtered though cellite at < 5°C.

An aliquot of this solution was purified by addition of silver nitrate (25% w/v) at pH =7 to establish how much silver nitrate was necessary for a 10% excess of silver nitrate. The bulk reaction mixture was treated with silver nitrate and the disilver acetyl phosphate precipitate was isolated by filtration and washed with alcohol and ether. Sodium chloride was used to redissolve the silver acetyl phosphate for NMR purposes.

δ_P (D_2O, 300 MHz) 4.57 (Pi), -1.03 (AcPi), -4.61 (?), -42.49 (?).

Aqueous solution of acetyl phosphate

(Acetyl phosphate was formed using the method of Herschlag and Jencks[2]).

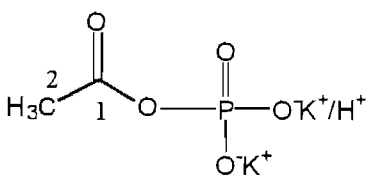

Potassium dihydrogen phosphate (2.16 g, 16 mmol) and potassium monohydrogen phosphate (2.78 g, 16 mmol) were dissolved in a mixture of pyridine (0.4 mL, 5 mmol) and water (16 mL). The reaction mixture was cooled in an ice bath to 0°C, and freshly distilled acetic anhydride (3.3 mL, 35 mmol) was added dropwise. The pH was maintained above 6.1 by addition of 4 M potassium hydroxide. The reaction mixture

was stirred for a further 10 mins at 0°C and extracted with ether (2 x 50 mL). The colourless aqueous solution of acetyl phosphate was stored at -20°C. The concentrations of the acetyl phosphate and total phosphate were determined colorimetrically and by ^{31}P NMR spectroscopy. This solution was spiked with authentic acetyl phosphate and a corresponding increase in the size of the peak assigned to acetyl phosphate was observed.

δ_H (D_2O, 300 MHz) 2.06 (s, AcPi) 1.84(s, Ac).

δ_P (D_2O, 300 MHz) 1.37 (s, Pi), -1.45 (s, AcPi)

Colorimetric determination of acetyl phosphate concentrations

Acetohydroxamic acid standard curve

(Acetohydroxamic acid standard curve was determined using the method of Herschlag and Jencks[3]).

A 0.20 M solution of acetohydroxamic acid in distilled water was prepared, in a 10 mL volumetric flask. A solution containing 10% ferric chloride and 0.7 M hydrochloric acid was prepared, in a 100 mL volumetric flask. The acetohydroxamic acid solution (1 mL) and ferric chloride solution (2 mL) were mixed and allowed to stand for 5 minutes at room temperature. A blank containing 1 mL of water and 2 mL of the ferric chloride solution was used to zero the UV machine. The absorbance of the resulting yellow solution was measured at 540 nm. The solution was diluted until it gave an absorbance

of between 0 and 1 in order to determine the appropriate concentration range for the assay. A 0.01 M solution of acetohydroxamic acid was then prepared and systematically diluted, assayed and graphed to produce a linear standard curve. The equation that represents this line is $y = -6.3878 \times 10^{-3} + 308.99x$ where y = absorbance measured at 540 nm and x = concentration of acetohydroxamic acid.

Acetyl phosphate concentration

A solution of 2 M hydroxylamine hydrochloride and 1.75 M sodium hydroxide was prepared and used within 12 hours. A solution of 10% ferric chloride and 0.7 M hydrochloric acid was prepared. A sample of the acetyl phosphate solution (1 mL) was mixed with hydroxylamine solution (1 mL) and allowed to stand at room temperature for 15 minutes. The ferric chloride solution (4 mL) was added and the absorbance measured at 540 nm. A blank containing water (2 mL) and ferric chloride solution (4 mL) was used to zero the UV machine. The acetyl phosphate solution was diluted until the absorbance measured was within the range 0-2. The concentration was calculated from an average of three absorbance measurements, using the equation $y = -6.4 \times 10^{-3} + 309x$ where y = absorbance measured at 540 nm and x = concentration of acetohydroxamic acid. The acetyl phosphate concentration of the original solution was generally in the range of 0.3-0.7 M.

Colorimetric determination of inorganic phosphate concentration

Total phosphate standard curve

(The total phosphate standard curve was determined using the method of Fiske and Subbarrow[4]).

A stock solution of 1 mM potassium dihydrogen phosphate was prepared. Copper sulfate (0.2 g, 0.8 mmol) and sodium acetate (4.6 g, 54 mmol) were dissolved in 2 M acetic acid (100 mL). A molybdate solution was prepared from ammonium molybdate ($(NH_4)_6Mo_7O_{24}.4H_2O$) (2.5g, 12.8 mmol), concentrated sulfuric acid (13.89 mL) and made up to 100 mL with distilled water. A 100 mL solution of reducing agent was prepared from 4-(methylamino)phenol sulfate (2 g, 5.8 mmol) in 10% sodium sulfite. A sample of the stock phosphate solution (1 mL) was mixed with the copper acetate solution (3 mL), the molybdate solution (0.5 mL) and the 4-(methylamino)phenol solution (0.5 mL). The resulting solution was allowed to stand at room temperature for 5 minutes, before measuring the absorbance of the blue solution, at 660 nm. A blank containing water (1 mL) and copper acetate (3 mL), molybdate solution (0.5 mL) and 4-(methylamino)phenol (0.5 mL) was used to zero the UV machine. The phosphate solution was systemically diluted, assayed and graphed to produce a linear standard curve. The equation that represents this line is $y = -3.5093 \times 10^{-3} + 733.37x$ where y = absorbance measured at 660 nm and x = concentration of phosphate.

The accuracy of the standard curve equation was checked using solutions of known concentration of sodium dihydrogen phosphate and tri-sodium phosphate.

Phosphate Compound	Concn mM	Measured Abs 660 nm	Calculated Abs 660 nm
NaH_2PO_4	0.51	0.358	0.368
NaH_2PO_4	1.27	0.848	0.928
Na_3PO_4	0.50	0.360	0.365
Na_3PO_4	1.26	0.875	0.921

Total phosphate concentration[4]

A sample of the acetyl phosphate solution (1 mL) was diluted 1000 fold. The diluted acetyl phosphate solution (1 mL) was mixed with the copper acetate solution (3 mL), the molybdate solution (0.5 mL) and the 4-(methylamino)phenol solution (0.5 mL) and allowed to stand at room temperature, for 5 minutes. The absorbance of this solution was measured, at 660 nm. The concentration was calculated from an average of three absorbance measurements using the standard curve equation $y = -3.5 \times 10^{-3} + 733x$ where y = absorbance measured at 660 nm and x = concentration of phosphate. The total phosphate concentration was generally in the range of 0.8 - 1.2 M.

T_1 NMR measurement for acetyl phosphate and inorganic phosphate

A solution (200 μL) containing acetyl phosphate (0.025M) and potassium dihydrogen phosphate (0.025M) was prepared and a T_1 measurement was carried out. This showed the T_1 of acetyl phosphate to be 2.441 seconds and the T_1 of inorganic phosphate to be

0.54 seconds. Therefore all phosphate NMR were run with a D_1 = 10 seconds and an acquisition time = 0.5 seconds and data was collected for 40 transients.

5.2.2 Experimental from 2.2.3

_N_-Phosphoryl pyridine

(*N*-Phosphoryl pyridine attempted to be prepared by minor modification of the method of Skoog and Jencks[5]).

An aqueous solution containing pyridine (15 mM) and potassium hydroxide (2.25 M) was prepared and cooled at 4°C. This solution (0.5 mL) was added to phosphorus oxychloride (30 μL) at 4°C. The resulting solution was mixed and added immediately to 3 mL of phosphate buffer (50 mM, pH=7) and potassium chloride (1 M). Attempts were made to monitor the decay of *N*-phosphoryl pyridine concentration at 265 nm. The absorbance of this solution was measured, but no decay was observed at this wavelength.

_N_-Phosphoryl Imidazole

(*N*-Phosphoryl imidazole was made was synthesised by the method described by Cramer *et al*[6]).

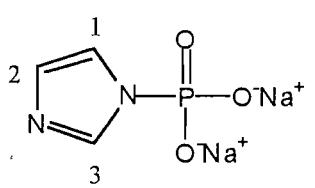

Phosphoric acid (200 mg, 2.04 mmol) was dissolved in acetonitrile (8 mL). Triethylamine (0.85 mL, 6.10 mmol) was added and the reaction was stirred at room temperature. *N,N'*-Carbonyldiimidazole (346 mg, 2.13 mmol) was added and the resulting reaction mixture was stirred for 3 hours under nitrogen. Sodium iodide (670 mg, 4.47 mmol) was dissolved in acetone (10 mL). A white precipitate formed immediately after addition of sodium iodide. The reaction mixture was cooled overnight at 4°C. The white imidazole phosphate precipitate (280.2 mg, 71.5%) was isolated by filtration and washed with a little cold acetone and ether. The white sodium salt decomposed at 210°C. It was stored in a vacuum desiccator.

δ_H(D_2O, 300 MHz) 7.25 (2H, s, CH_1 & CH_2), 7.79 (1H, s, CH_3)

δ_P (D_2O, 300 MHz) 3.50 (s, Pi), -3.70 (s, ImPi), -4.46 (d, J=18.30, PPPi), -5.24 (s, PPi), -19.27 (t, J=19.00, PPPi).

Attempted reaction of acetyl phosphate, inorganic phosphate and sodium ions in the presence and absence of pyridine and imidazole

A solution (300 μL) containing acetyl phosphate (10–25 mM), potassium di-hydrogen phosphate (10–25 mM), sodium ions (6-7 M) and deuterium oxide was prepared. Varied amounts of imidazole (13–20 mM) or pyridine (13–20 mM) were added to the reaction mixtures. These reaction mixtures were heated at the indicated temperature (30-54°C) for the times (4-20 hours) shown in tables. ^{31}P NMR spectroscopy was performed on the samples to analyse for pyrophosphate formation.

Time = 0 hr δ_P (D_2O, 300 MHz, 30°C) 1.18 (s, Pi), -1.89 (s, AcPi).

Pi & AcPi mM	[NaCl] M	Temp °C	Time hrs	Pyr mM	% PPi
16	7	30	4	-	0
16	7	30	4	20	0

Pi & AcPi mM	[$NaClO_4$] M	Temp °C	Time hrs	Pyr mM	% PPi
10	6	45	19	20	0
25	7	54	45	13	0

Pi & AcPi mM	[$NaClO_4$] M	Temp °C	Time hrs	Im mM	% PPi
10	6	30	21	20	0
16	7	30	20	20	0
25	7	54	45	13	0

Acetyl phosphate, inorganic phosphate with magnesium ions or imidazole.

Solutions (140 μL) containing acetyl phosphate (20 mM) and potassium di-hydrogen phosphate (20 mM) and deuterium oxide (40 μL) were prepared. Magnesium chloride (12 mg, 59.0 μmol) was added to samples requiring magnesium ions. Imidazole (20 mM) was added to the samples requiring imidazole. These mixtures were transferred to a 3 mm NMR tube and heated at 30°C in the NMR probe. ^{31}P NMR spectroscopy was

performed using an acquisition time of 0.5 sec and a delay time of 10 sec. This was repeated at hourly intervals for 14 hours.

Time = 0 hr δ_P (D_2O, 300 MHz, 30°C) 0.96 (s, Pi), -2.43 (s, AcPi).

Reactants	Time	% Pi	% AcPi	% PPi
AcPi	0 hrs	50	50	0
Pi	1	56	44	0
	2	62	38	0
	3	66	34	0
	4	71	29	0
	5	74	26	0
	6	77	23	0
	7	79	21	0
	8	81	19	0
	9	83	17	0
	10	84	16	0
	11	85	15	0
	12	86	14	0
	13	87	13	0

Reactants	Time	% Pi	% AcPi	% PPi
AcPi	0 hrs	38	62	0
Pi	1	48	52	0
Mg^{2+}	2	56	44	0
	3	62	38	0
	4	69	31	0
	5	73	27	0
	6	76	24	0
	7	80	20	0
	8	80	20	0
	9	84	16	0

	10	87	13	0
	11	88	12	0
	12	88	12	0
	13	90	10	0

Reactants	Time	% Pi	% AcPi	% PPi
AcPi	0 hrs	49	51	0
Pi	1	55	45	0
Im	2	60	40	0
	3	65	35	0
	4	69	31	0
	5	72	28	0
	6	75	25	0
	7	79	21	0
	8	81	19	0
	9	83	17	0
	10	87	13	0
	11	88	12	0
	12	90	10	0

Acetyl phosphate, inorganic phosphate, imidazole and magnesium ions

A solution (300 μL) containing acetyl phosphate (25 mM), potassium di-hydrogen phosphate (25 mM), imidazole (25 mM) and magnesium chloride (0.33 M) in deuterium oxide was prepared. This solution was heated at 23°C for 3 hours. ^{31}P NMR spectroscopy was performed using an acquisition time of 0.5 sec and a delay time of 10 sec.

A solution (300 μL) containing acetyl phosphate (90 mM), potassium di-hydrogen phosphate (90 mM), imidazole (90 mM) and magnesium chloride (0.85 M) in deuterium oxide was prepared. This solution was heated at 30°C for 3 hours. A white precipitate formed during the heating. ^{31}P NMR spectroscopy was performed using an acquisition time of 0.5 sec and a delay time of 10 sec.

Reaction	Temp °C	Time Hrs	% AcPi	% Pi	% PPi
2.1	23	48	14	84	2
2.2	30	3	21	77	2

Acetyl phosphate, inorganic phosphate in the presence of magnesium ions and imidazole buffers

Acetyl phosphate (25 mM), inorganic phosphate (25 mM) and magnesium chloride (0, 150 & 500 mM) were mixed with imidazole buffers with pH's of 6 and 7 (0.3 & 1.0 M). The pH of the solutions was 6-7. The resulting mixture was heated at 30°C for 2 hours. The solution was analysed by ^{31}P NMR spectroscopy. Integration of the peaks indicated that there was no soluble pyrophosphate present in any of the solutions.

$[Mg^{2+}]$ mM	[Im] mM	pH	% AcPi	% Pi	% PPi
0	300	6	41	59	0
150	300	6	32	68	0
150	300	7	30	70	0
500	1000	6	24	76	0
500	1000	7	22	78	0

Acetyl phosphate and imidazole in the presence of magnesium ions and inorganic phosphate buffers

Acetyl phosphate (25 mM), imidazole (50 mM) and magnesium chloride (300 mM) were mixed with phosphate buffer (300 mM) in deuterium oxide. The pH of the solutions was 6.8. The resulting mixture was heated at 30°C for 3.5 hours. The solution was analysed by ^{31}P NMR spectroscopy. Integration of the peaks indicated that there was no soluble pyrophosphate present in any of the solutions.

$[Mg^{2+}]$ mM	[Im] mM	% AcPi	% Pi	% PPi
125	100	18.	82	0
250	100	20	80	0
500	25	5	95	0
500	50	17	83	0

Acetyl phosphate, inorganic phosphate and pyridine

Solutions (300 μL) containing acetyl phosphate (25 mM), potassium di-hydrogen phosphate (25 mM), pyridine (25 mM) and deuterium oxide were prepared. This solution was transferred to a 3 mm NMR tube and heated at 30°C in the NMR machine. ^{31}P NMR spectroscopy was performed using an acquisition time of 0.5 sec and a delay time of 10 sec. This was repeated at hourly intervals for 14 hours. Integration of the peaks indicated that there was no soluble pyrophosphate present in any of the solutions.

Time	% Pi	% AcPi	% PPi
0 hrs	50	50	0
1	56	44	0
2	62	38	0
3	66	34	0
4	70	30	0
5	73	27	0
6	76	24	0
7	81	19	0
8	83	17	0
9	84	16	0
10	84	16	0
11	85	15	0
12	86	14	0
13	87	13	0

Acetyl phosphate, inorganic phosphate and magnesium ions in the presence of varied pyridine concentrations

Solutions (300 μL) containing acetyl phosphate (25 mM), potassium di-hydrogen phosphate (25 mM), pyridine (25, 50, 75 & 100 mM), magnesium chloride (0.33 M) and deuterium oxide were prepared. These solutions were heated at 30 or 37°C for 17 hours. ^{31}P NMR spectroscopy was performed using an acquisition time of 0.5 sec and a delay time of 10 sec. Integration of the peaks indicated that there was soluble pyrophosphate present in most of the solutions.

[Pyr] mM	Temp °C	% AcPi	% Pi	% PPi
25	30	0	97	3
25	37	0	97	3
50	30	0	97	3
50	37	0	96	4
75	30	0	98	2
75	37	0	98	2
100	30	0	100	0
100	37	0	100	0

Acetyl phosphate, inorganic phosphate and pyridine in the presence of varied magnesium ions concentrations

Solutions (300 μL) containing acetyl phosphate (25 mM), potassium di-hydrogen phosphate (25 mM), pyridine (50 mM), magnesium chloride (0, 100, 200, 300, 400 & 500 mM) and deuterium oxide were prepared. These solutions were heated at 20, 30, 40

or 50°C for 6 hours. ^{31}P NMR spectroscopy was performed using an acquisition time of 0.5 sec and a delay time of 10 sec.

20°C

$[Mg^{2+}]$ mM	% Pi	% AcPi	% PPi
0	66	34	0
100	74	26	0
200	78	22	0
300	75	25	0
400	78	22	0
500	79	21	0

30°C

$[Mg^{2+}]$ mM	% Pi	% AcPi	% PPi
0	87	13	0
100	92	8	0
200	92	8	0
300	91	7	2
400	92	7	1
500	89	8	3

40°C

$[Mg^{2+}]$ mM	% Pi	% AcPi	% PPi
0	100	0	0
100	100	0	0
200	100	0	0
300	100	0	0
400	99	0	1
500	98	0	2

50°C

$[Mg^{2+}]$ mM	% Pi	% AcPi	% PPi
0	100	0	0
100	100	0	0
200	100	0	0
300	100	0	0
400	100	0	0
500	100	0	0

Acetyl phosphate, inorganic phosphate and pyridine in the presence of magnesium ions and phosphate buffers

Acetyl phosphate (25 mM), inorganic phosphate (25 mM), pyridine (50 mM) and magnesium chloride (300 mM) were mixed with phosphate buffer (0.33 M) in deuterium oxide. The pH of the solutions was 6.8. The resulting mixture was heated at 30°C for 3 hours. The solution was analysed by ^{31}P NMR spectroscopy. Integration of the peaks indicated that there was no soluble pyrophosphate in any of the solutions.

Acetyl phosphate, inorganic phosphate and pyridine in the presence of magnesium ions and phthalate buffers

Acetyl phosphate (25 mM), inorganic phosphate (25 mM), pyridine (50 mM) and magnesium chloride (300 mM) were mixed with phthalate buffer (0.1 M) in deuterium oxide. The pH of the solutions was 5.8. The resulting mixture was heated at 30°C for 3

hours. The solution was analysed by ^{31}P NMR spectroscopy. Integration of the peaks indicated that there was no soluble pyrophosphate in any of the solutions.

Acetyl phosphate, inorganic phosphate and adenine or adenosine in the presence of magnesium ions

Acetyl phosphate (25 mM), inorganic phosphate (25 mM), adenine or adenosine (50 mM) and magnesium chloride (300 mM) were mixed in deuterium oxide. The resulting mixture was heated at 30°C for 6 hours. The solution was analysed by ^{31}P NMR spectroscopy. Integration of the peaks indicates 2% soluble pyrophosphate was formed in the reactions containing adenine. However no signal consistent with pyrophosphate formation was observed in the reactions containing adenosine.

5.2.3 Experimental from 2.2.4

Resolubilizing ferrous phosphate and ferrous acetyl phosphate

A solution containing acetyl phosphate and inorganic phosphate in deuterium oxide was prepared. This solution was analysed by ^{31}P NMR spectroscopy in order to determine the ratio of acetyl phosphate to inorganic phosphate. Ferrous sulfate was added to the solution and a precipitate formed. Potassium cyanide was added to the reaction mixture. The resulting reaction mixtures were mixed and then centrifuged to facilitate removal of the precipitate. ^{31}P NMR spectroscopy was performed on these samples and the amount

of cyanide was increased until the ratio of inorganic phosphate to acetyl phosphate was returned to the original ratio. This occurred when cyanide concentrations were greater than 6 times the ferrous ion concentration.

Acetyl phosphate, inorganic phosphate and ferrous ions (0.33 M)

Acetyl phosphate (25 mM) and inorganic phosphate (25 mM) were added to deuterium oxide. Ferrous chloride (0.33 M) was added and the resulting heterogeneous reaction mixture was heated at 30°C for 18 hours. After which time potassium cyanide (45 mg, 2.3 M) was added and the reaction mixture was centrifuged. Analysis of the solution by ^{31}P NMR spectroscopy and integration of the signals indicated a yield of 15% pyrophosphate and 75% inorganic phosphate.

Acetyl phosphate, inorganic phosphate and ferrous ions (0.125 M) with varied degassing procedures

Heterogeneous mixtures of acetyl phosphate, inorganic phosphate and ferrous chloride were prepared using deuterium oxide. The first series of reaction mixtures employed deuterium oxide straight from the bottle. The heterogeneous reaction mixtures of the second series had oxygen-free nitrogen (OFN) bubbled through the reaction mixture for approximately 20 seconds before the reaction vessel was capped. Reaction mixtures of the third series under went two freeze-pump-thaw cycles under an atmosphere of oxygen-free nitrogen before use. All reactions were heated at 54°C for 2 hours. The samples were treated with potassium cyanide and centrifuged. Analysis of the

supernatant by ^{31}P NMR spectroscopy and integration of the signals allowed determination of the yield of phosphate species.

Method of degassing	% Pi	% AcPi	% PPi
-	88	0	12
Bubbling OFN	83	0	17
Freeze-pump-thaw	81	0	19

General method for reactions containing acetyl phosphate, inorganic phosphate, ferrous ions and nitrogen-containing compounds if required.

A heterogeneous mixture of acetyl phosphate, inorganic phosphate, ferrous ions and nitrogen-containing compounds is required was prepared. Oxygen-free nitrogen was bubbled through the samples for approximately 20 seconds before the vessel was capped and heated at the appropriate temperature. After the reaction time had been reached the samples were treated with potassium cyanide (8 molar equivalents relative to ferrous ions). The heterogeneous mixtures were centrifuged and the supernatant was analysed by ^{31}P NMR spectroscopy.

5.2.4 Experimental from 2.2.5

Effect of the order of mixing acetyl phosphate, inorganic phosphate, ferrous ions and sulfide ions

The first series of reaction mixtures was prepared by adding sodium sulfide (0.1 M) to ferrous chloride (0.1 M) and mixing. Acetyl phosphate (25 mM) and inorganic phosphate (25 mM) solution when then added. The second series of reaction mixtures was prepared by the addition of acetyl phosphate (25 mM) and inorganic phosphate (25 mM) solution to ferrous chloride (0.1 M). The resulting reaction mixture was added to sodium sulfide (0.1 M). While in the third series a solution of acetyl phosphate (25 mM), inorganic phosphate (25 mM) and sodium sulfide (0.1 M) was added to ferrous chloride (0.1 M). All the heterogeneous mixtures had oxygen-free nitrogen bubbled through them for approximately 20 seconds before the reaction vessels were capped. The reaction mixtures were heated at 54°C for 2 hours. The samples were treated with potassium cyanide and centrifuged. Analysis by ^{31}P NMR spectroscopy and integration of the signals was used to determine the yields of phosphate species.

Order of Addition	pH	%Pi	%PPi
1.Fe^{2+}-2.S^{2-}-3.AcPi/Pi	7	87	13
1.Fe^{2+}-2.AcPi/Pi-3.S^{2-}	7	90	10
1.Fe^{2+}-2.S^{2-}/AcPi/Pi	7	90	10

General method for reactions containing acetyl phosphate, inorganic phosphate, ferrous sulfide and nitrogen-containing compounds if required

A heterogeneous mixture of acetyl phosphate, inorganic phosphate, sodium sulfide, ferrous chloride and nitrogen-containing compounds was prepared and oxygen-free nitrogen was bubbled through the samples for approximately 20 seconds before the vessel was capped and heated for the appropriate temperature and time. After the reaction time has been reached the samples were treated with potassium cyanide (8 molar equivalents relative to ferrous ions). The heterogeneous mixtures were centrifuged and the supernatant was analysed by ^{31}P NMR spectroscopy.

5.2.5 Experimental references for chapter two

1 F. Lipmann & L. C. Tuttle, *J. Biol. Chem.*, **153**, 571 (1944).

2 D. Herschlag & W. P. Jencks, *J. Am. Chem. Soc.*, **108**, 7938 (1986).

3 D. Herschlag & W. P. Jencks, *J. Am. Chem. Soc.*, **111**, 7579 (1989).

4 C. H. Fiske & Y. Subbarrow, *J. Biol. Chem.*, **116**, 375 (1925).

5 M. T. Skoog & W. P. Jencks, *J. Am. Chem. Soc.*, **106**, 7597 (1984).

6 F. Cramer, H. Schaller & H. A. Staab, *Chem. Ber.*, 1612 (1961).

5.3 Chapter Three – Experimental

5.3.1 Experimental from 3.2

Ferrous sulfide

Milli-Q water, through which oxygen-free nitrogen had bubbled for two hours, was transferred by cannula to a suba sealed round bottomed flask, which had been flushed with oxygen-free nitrogen. Two freeze-pump-thaw cycles were performed on this solution under an atmosphere of oxygen-free nitrogen.

Ferrous sulfate (9.45 g, 34 mmol) and sodium sulfide (8.17 g, 34 mmol) were weighed into a reaction vessel. The reaction vessel was sealed with a suba seal and evacuated. The degassed water was transferred by cannula into the flask and a black precipitate formed immediately. The black precipitate was isolated by filtration and washed with degassed water while under an atmosphere of oxygen-free nitrogen. The ferrous sulfide (2 g, 67%) was then transferred to a vacuum desiccator to dry. Rust was observed to have formed after 24 hours.

Trial extraction of acetic acid into chloroform

Aqueous solutions of acetic acid (1% or 0.1% v/v, 4 mL) were prepared. The pH was adjusted to 1 by addition of sulfuric acid. The resulting solution was extracted with deuterated chloroform (0.5 mL). The organic solution was dried with magnesium sulfate and analysed by ^{1}H NMR spectroscopy. A signal was observed in the ^{1}H NMR spectrum consistent with acetic acid for the 1% v/v acetic acid solution. Only the solvent signal was detected in the extraction of the 0.1% v/v acetic acid solution.

***N*-Acetyl glycine**

(*N*-Acetyl glycine was prepared according to the method reported in Organic Synthesis Collective Volumes[1]).

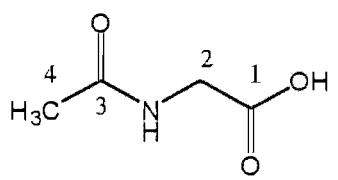

Glycine (75 g, 1 mol) was dissolved in water (300 mL) by vigorous stirring in a 1 L round bottom flask. Acetic anhydride (215 g, 2 mol) was added in one portion, and the resulting mixture was stirred for 20 minutes, during which time an exothermic reaction occurred, resulting in the formation of a white precipitate. The solution was stored at 4°C overnight. Filtration, followed by washing with ice cold water, gave *N*-acetyl

glycine as a white powder (84.61 g, 72%) with a melting point of 200-205°C (literature mp[1] = 207-208°C) after drying at 100°C.

δ_H (D_2O, 300 MHz) 1.89 (3 H, s, CH_3), 3.82 (2 H, s, CH_2).

2-Acetamidocinnamic acid

(2-Acetamidocinnamic acid was prepared according to the method reported in Organic Synthesis Collective Volumes[1]).

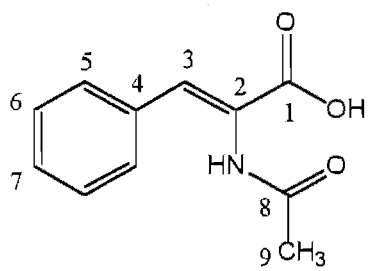

N-Acetyl glycine (84.54 g, 0.72 mol), anhydrous sodium acetate (43.4 g, 0.53 mol), benzaldehyde (114.17 g, 1.08 mol) and acetic anhydride (193.7 g, 1.90 mol) were added to a loosely stoppered 1 L round bottomed flask. The reaction mixture was stirred and heated at 100°C until the solid had dissolved, after which time it was heated at reflux for one hour. White crystals formed upon cooling at 4°C. Water (125 mL) was added, and the solid mass of crystals broken up with a stirring rod. Filtration was followed by washing with water and then with cold ether, gave white crystals (46.33 g), which were dried under reduced pressure.

These crystals (46.33 g) were dissolved in a solution of acetone (450 mL) and water (175 mL), and heated at reflux for four hours. Acetone was removed by distillation at atmospheric pressure. Water (400 mL) was added to the residual solution, and the resulting mixture was boiled for 5 minutes in order to ensure that all the 2-acetamidocinnamic acid was in solution. The solution was filtered and washed with boiling water (75 mL). Any crystals that formed in the filtrate were redissolved by gentle heating on a hot plate. Decolourising carbon (10 g) was added, and the mixture was gently heated for 5 mins. After filtration the reaction mixture was cooled at 4°C, to yield white crystals of 2-acetamidocinnamic acid. The crystals were collected by filtration, and washed with ice water. After drying at 100°C the 2-acetamidocinnamic acid (29.42 g, 20%) was stored at -20°C.

δ_H (Acetone - d_6, 300 MHz) 2.14 (3 H, s, CH_3), 7.43 (3H, m, Ph), 7.71 (2H, t, Ph), 8.78 (1 H, s, CH).

3-Phenylpyruvic acid

(3-Phenylpyruvic acid was prepared according to the method reported in Organic Synthesis Collective Volumes[1]).

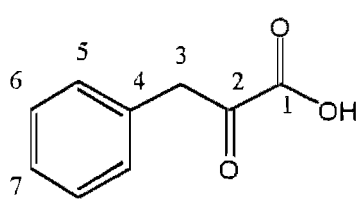

2-Acetamidocinnamic acid (10 g, 0.05 mol) was dissolved in 1 M hydrochloric acid (200 mL) and heated at reflux for 3 hours. The reaction mixture was cooled at 4°C, in order to enhance crystallisation. This mixture was stored at 4°C until needed. (The literature notes no decomposition was observed when the product was kept suspended in cold, dilute acid)[1]. When the 3-phenylpyruvic acid was required for the subsequent step, the crystals were collected by filtration, and washed with a small quantity of ice cold water, to yield 3-phenylpyruvic acid crystals (5.42 g, 66%) with a melting point of 149-154°C (literature mp[1] = 150-154°C).

δ_H ($CDCl_3$, 300 MHz) 6.42 (2H, s, CH_2), 7.21(1H, m, Ph), 7.31 (2H, m, Ph), 7.76 (2H, d, Ph).

δ_C ($CDCl_3$, 300 MHz) 109.56 (C3), 126.96 (Ph), 128.06 (Ph), 129.24 (Ph), 134.85 (Ph), 141.44 (CO), 166.58 (CO).

Formation of 3-phenylpropionic acid from 3-phenylpyruvic acid

(The reaction conditions for the formation of 3-phenylpropionic acid from 3-phenylpyruvic acid were those of Blochl *et al* with minor modification[2]).

Milli-Q water, through which oxygen-free nitrogen had bubbled for two hours, was transferred by cannular to a suba sealed round bottomed flask, which had been flushed with oxygen-free nitrogen. Two freeze-pump-thaw cycles were performed on this solution under an atmosphere of oxygen-free nitrogen.

3-Phenylpyruvic acid (68 mg, 0.4 mmol), sodium sulfide (1.05 g, 4.4 mmol), crushed commercial grade ferrous sulfide (0.26 g, 3.0 mmol), and a stirring bar were added to a glass ampoule. The glass ampoule was sealed with a suba seal, evacuated with a high vacuum pump, and flushed with oxygen-free nitrogen. The degassed water (20 mL) was syringed into the glass ampoule, and the pH adjusted, using concentrated sulfuric acid, until only a small amount of black solid remained. The tube was frozen in liquid nitrogen and sealed. The sealed tube was placed in an aluminium tube as a safety precaution, with glass wool covering the ends, and heated in an oil bath at 100°C for 21 days.

At the end of the reaction time, the tube was allowed to cool to room temperature before freezing in liquid nitrogen and opening. The resulting solution was centrifuged before being analysed by HPLC. A C_{18} column was employed and was eluted with a mixture of methanol and water (1:1) containing 0.05% v/v trifloroacetic acid. A peak was observed at the appropriate retention time for 3-phenylpropionic acid, and spiking with a solution of known concentration of phenylpropionic acid produced a corresponding increase in the size of the peak assigned to 3-phenylpropionic acid.

% Yield 3-phenylpropionic acid =12%

5.3.2 Experimental from 3.3

Di(carboxymethyl)disulfide

(Di(carboxymethyl)disulfide was synthesised by Stoner and Dougherty's method[3]).

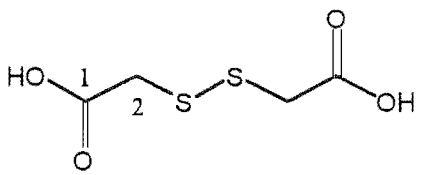

Chloroacetic acid (19 g, 201 mmol) was dissolved in water (90 mL) and neutralised with saturated sodium carbonate. A solution of sodium thiosulfate (50 g, 316 mmol) in water (60 mL) was added, and the reaction mixture was heated at reflux for 1 hour. Iodine (25.2 g, 99 mmol) was added to the hot solution in small portions. The solution was acidified with concentrated sulfuric acid (6 mL) and extracted with ether (300 mL). The organic layer was dried with magnesium sulfate, and the solvent was removed at reduced pressure. The residue was dissolved in acetone (20 mL) and filtered into toluene (200 mL). The solvent was removed at reduced pressure until the solution became turbid. White di(carboxymethyl)disulfide crystals (7.14 g, 39.0%) formed upon standing overnight and these were collected by filtration, and washed with a small quantity of ice-cold toluene. These crystals had a melting point of 99-102°C (literature mp.[3] = 106°C)

δ_H (Acetone, 300 MHz) 3.83 (2H, s, CH_2).

δ_H (D_2O, 300 MHz) 3.40 (2H, s, CH_2).

δ_C (D_2O, 300 MHz) 41.61 (C2), 174.08 (C1).

m/z (FAB) $^{12}C_4{}^{1}H_7{}^{16}O_4{}^{32}S_2$ requires 182.9758 measured 182.97910

Di(*N*-phenyl carbamoylmethyl)disulfide[4]

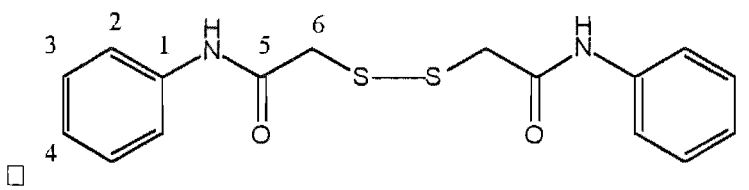

Di(carboxymethyl)disulfide (500 mg, 3 mmol), aniline (0.55 mL, 6 mmol), 1-hydroxybenzotriazole hydrate (810 mg, 6 mmol) were dissolved in dry THF (20 mL), and cooled to 0°C. 1-(3-dimethylaminopropyl)-3-ethyl-carbodiimide (EDCI) (1.15 g, 6 mmol) was added, and the reaction mixture stirred at 0°C for 1 hour and at room temperature for another hour. The THF was removed under reduced pressure, to yield a yellow oil. The oil was dissolved in ethyl acetate (100 mL), and sequentially extracted with saturated sodium bicarbonate (100 mL), 10% citric acid (100 mL), saturated sodium bicarbonate (50 mL) and water (100 mL). The organic layer was dried with magnesium sulfate, and the solvent removed at reduced pressure, to yield a yellow residue, which was recrystallised from ethyl acetate. The resulting white crystals of di(*N*-phenyl carbamoylmethyl)disulfide (310 mg, 34%) had a melting point of 156-161°C.

δ_H (CD_3OD, 300 MHz) 3.67 (2H, s, CH_2), 7.10 (1H, m, Ph), 7.30 (2H, m, Ph), 7.57 (2H, d, Ph).

δ_H (DMSO, 300 MHz) 3.66 (2H, s, CH_2), 7.06 (1H, m, Ph), 7.29 (2H, m, Ph), 7.51 (2H, d, Ph), 10.21 (2H, s, NH).

δ_C (DMSO, 300 MHz) 43.35 (C6), 120.18 (Ph), 124.66 (Ph), 129.56 (Ph), 139.02 (Ph), 167.73 (C5).

m/z (FAB) $^{12}C_{16}{}^{1}H_{17}{}^{16}O_2{}^{14}N_2{}^{32}S_2$ requires 333.07315 measured 333.07353

_N_-Phenyl mercaptoacetamide

(The reduction procedure was attempted from the method described in Experimental Organic Chemistry[5]).

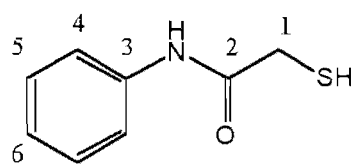

Di(N-phenyl carbamoylmethyl)disulfide (20 mg, 60 μmol) was dissolved in ethanol (5 mL). Sodium borohydride (2.3 mg) was dissolved in water (1 mL) and added dropwise to the ethanol solution. The resulting mixture was stirred for 30 minutes at room temperature before being poured into ice water (5 mL). The pH was adjusted to 1 by addition of hydrochloric acid (1 M) and the resulting mixture was stirred for 10 minutes. The aqueous solution was extracted with ether. The organic phase was dried with magnesium sulfate and the solvent was removed at reduced pressure to yield *N*-phenyl acetamide, as a colourless oil (18 mg, 90%).

δ_H (methanol -d_4, 300 MHz) 3.69 (2H, s, CH_2), 7.11 (1H, m, Ph), 7.30 (2H, m, Ph), 7.54 (2H, d, Ph).

δ_C (methanol-d_4, 300 MHz) 29.59 (C1), 121.59 (Ph), 125.81 (Ph), 130.12 (Ph), 171.62 (C2).

Methyl ester of di(carboxymethyl) disulfide

(Methyl ester of di(carboxymethyl) disulfide was produced by the method of Owen *et al*[6]).

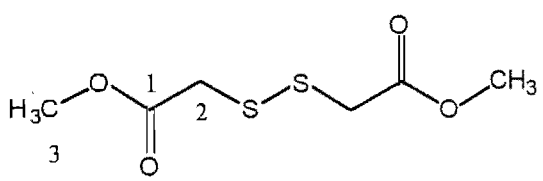

Di(carboxymethyl)disulfide (0.5 g, 2.7 mmol) and *p*-toluenesulfonic acid (16 mg, 84 μmol) were dissolved in dry methanol (2 mL, 49.4 mmol). The resulting solution was heated at reflux for 4 hours. The solvent was removed at reduced pressure. The oily residue was dissolved in chloroform and extracted with 5% w/v sodium bicarbonate. The organic layer was dried with magnesium sulfate and the solvent was removed at reduced pressure to yield a colourless oil of the methyl ester of di(carboxymethyl)disulfide (343 mg, 60%).

δ_H ($CDCl_3$, 300 MHz) 3.57 (2H, s, CH_2), 3.74 (3H, s, CH_3).

δ_C ($CDCl_3$, 300 MHz) 40.73(C3), 52.16 (C2), 169.34 (C1).

Di(*N*-phenyl carbamoylmethyl)disulfide

(Synthesis of di(*N*-phenyl carbamoylmethyl)disulfide was adapted from Owen *et al*[6]).

Methyl ester of di(carboxymethyl)disulfide (0.3 g, 1.4 mmol), aniline (3.5 mL, 38 mmol) and *p*-toluenesulfonic acid (8 mg, 42 μmol) mixed. The resulting solution was heated at reflux for 4 hours. 10% v/v Hydrochloric acid (50 mL) was added to the reaction mixture and extracted with chloroform. The organic solvent was dried with magnesium sulfate and removed at reduced pressure to yield colourless oil that was a mixture of starting material and di(*N*-phenyl carbamoylmethyl)disulfide (56 mg).

***N*-Phenyl mercaptoacetamide**

(*N*-Phenyl mercaptoacetamide was prepared by the method of Van Allen[7]).

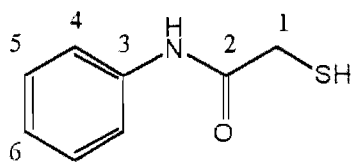

Freshly distilled mercaptoacetic acid (25.2 g, 0.274 mol), aniline (25.5 g, 0.274 mol) and benzene (140 mL) were added to a round bottom flask equipped with a Dean-Stark condenser. The reaction mixture was heated at reflux, under a nitrogen atmosphere, for 6 hours. An equal volume of pet ether was added to the reaction mixture, and upon cooling at 4°C, a white precipitate formed. The *N*-phenyl mercaptoacetamide precipitate was collected by filtration, and recrystallised from ethanol and water. The white crystals

of *N*-phenyl mercaptoacetamide (8.5034 g, 68.39%) had a melting point of 104-107 °C (Literature mp.[7] = 100°C).

δ_H (methanol-d_4, 300 MHz) 3.67 (2H, s, CH_2), 7.10 (1H, m, Ph), 7.31 (2H, m, Ph), 7.54 (2H, d, Ph).

δ_C (methanol-d_4, 300 MHz) 29.54 (C1), 121.59 (Ph), 125.81(Ph), 130.12(Ph), 171.85 (C2).

m/z (FAB) 168 (MH^+), 154, 136.

Formation of *N*-phenyl acetamide from aniline and mercaptoacetic acid

(*N*-Phenyl acetamide was formed using the reaction conditions developed by Keller[8]).

Oxygen-free nitrogen was bubbled through Milli-Q water for two hours. Three freeze-pump-thaw cycles were performed on this solution under an atmosphere of oxygen-free nitrogen. Mercaptoacetic acid was distilled under reduced pressure. A stock solution of mercaptoacetic acid (50 mM) was prepared using the degassed Milli-Q water, and frozen immediately by immersion of the flask in liquid nitrogen.

Sodium sulfide (480 mg, 2.0 mmol), ferrous sulfate (556 mg, 2.0 mmol) and a stirring bar were placed in a glass ampoule. The glass ampoule was sealed with a suba seal, evacuated with a high vacuum pump, and flushed with oxygen-free nitrogen. Mercaptoacetic acid (0.5 mg, 50 μmol) and aniline (9.11 μL) were added to the ampoule using a syringe. Degassed water (10 mL) was syringed into the glass ampoule, and the

pH adjusted using concentrated sulfuric acid, until only a small amount of black solid remained. The tube was frozen in liquid nitrogen and sealed. The sealed tube was placed in an aluminium tube as a safety precaution, with glass wool covering the ends, and heated in an oil bath at 100°C for 7 days.

The tube was removed from the heating bath, allowed to cool to room temperature before being frozen in liquid nitrogen, and opened. A portion of the reaction mixture was centrifuged and filtered. A sample of the supernatant (20 μL) was removed and loaded onto a C_{18} HPLC column. The methanol and 0.05% TFA/water gradient solvent system used to separate the products. The solvent system was as follows: 5% methanol (6 min); 5-10% methanol (6-8 min); 10-15% methanol (8-12 min); 15% methanol (12-20 min); 15-40% methanol (20-40 min) and 40% methanol (40-60 min). The flow rate was 1 mL/min. Compounds were detected by monitoring the absorbance of the effluent at 254 nm.

A peak was observed in the HPLC trace at an appropriate retention time for *N*-phenyl acetamide, and spiking with a solution of *N*-phenyl acetamide showed a corresponding increase in the size of the peak assigned to *N*-phenyl acetamide. Integration and analysis of this peak estimated the yield of *N*-phenyl acetamide to be 0.2%.

Formation of *N*-phenyl acetamide from *N*-phenyl mercaptoacetamide

Oxygen-free nitrogen was bubbled through Milli-Q water for two hours. Three freeze-pump-thaw cycles were performed on this solution under an atmosphere of oxygen-free nitrogen.

Sodium sulfide (480 mg, 2 mmol), ferrous sulfate (556 mg, 2 mmol), *N*-phenyl mercaptoacetamide (16.7 mg, 100 μmol) and a stirring bar were placed in a glass ampoule. The glass ampoule was sealed with a suba seal, evacuated with a high vacuum pump, and flushed with oxygen-free nitrogen. Degassed water (10 mL) was syringed into the glass ampoule and the pH adjusted using concentrated sulfuric acid, until only a small amount of black solid remained. The tube was frozen in liquid nitrogen and sealed. The sealed tube was placed in an aluminium tube as a safety precaution, with glass wool covering the ends and heated in an oil bath at 100°C for 7 days.

The tube was removed from the heating bath, and allowed to cool to room temperature before being frozen in liquid nitrogen, and opened. A portion of the reaction mixture was centrifuged and filtered. A sample of the supernatant (20 μL) was removed and loaded onto a C_{18} HPLC column. A methanol and 0.05% TFA/water gradient solvent system was used to separate the products. The solvent system was as follows: 5% methanol (6 min); 5-10% methanol (6-8 min); 10-15% methanol (8-12 min); 15 % methanol (12-20 min); 15-40% methanol (20-40 min) and 40% methanol (40-60min). The flow rate was 1 mL/min. Compounds were detected by monitoring the absorbance of the effluent at 254 nm.

A peak was observed in the HPLC trace at an appropriate retention time for *N*-phenyl acetamide, and spiking with a solution of *N*-phenyl acetamide showed a corresponding increase in the size of the peak assigned to *N*-phenyl acetamide. Integration of this peak and analysis indicated a yield of 4% of *N*-phenyl acetamide.

The reaction mixture was extracted into chloroform, dried and the solvent removed at reduced pressure and mass spectrometry was performed on the resulting residue.

m/z (EI) 135 (M^+), 119, 106, 93, 77 & 66.

_N_-(4-Carboxyphenyl) acetamide

(*N*-(4-Carboxyphenyl) acetamide was prepared by the general method outlined in Textbook of practical organic chemistry [4]).

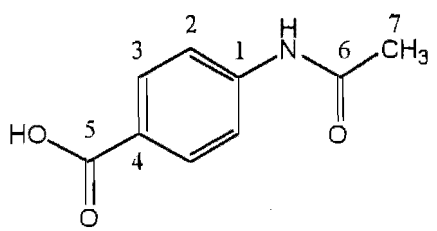

4-Aminobenzoic acid (5 g, 36 mmol) and sodium hydroxide (2.9 g, 73 mmol) were dissolved in water (50 mL) and cooled to 0°C. Acetic anhydride (4.1 mL, 43 mmol) was added dropwise, while maintaining the pH > 7 by the addition of 4 M sodium hydroxide. The reaction was allowed to warm to room temperature and then stirred overnight. A

cream precipitate formed during this time. The reaction mixture was acidified with 2 M hydrochloric acid and filtered to collect the cream precipitate of *N*-(4-carboxyphenyl) acetamide. Recrystallisation from ethanol and water yielded cream plates (458 mg, 7.1%) that decomposed when heated to 255-258°C (literature mp.[9] = 259-262°C dec).

δ_H (DMSO, 300 MHz) 2.17 (3H, s, CH_3), 7.76 (2H, d, J = 8.30 Hz, Ph), 7.96 (2H, d, J = 6.8 Hz, Ph), 10.36 (1H, s, NH).

δ_C (DMSO, 300 MHz) 24.28 (C6), 118.34 (Ph), 125.71 (Ph), 130.48 (Ph), 143.27 (Ph), 167.29 (CO), 169.08 (CO).

m/z (EI) 179 (M^+), 137, 120, 92, 65.

_N_-(4-Carboxyphenyl) chloroacetamide

(*N*-(4-Carboxyphenyl) chloroacetamide was prepared by the general method outlined in Textbook of practical organic chemistry[4]).

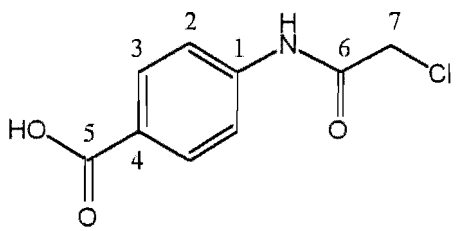

4-Aminobenzoic acid (5 g, 36 mmol) triethylamine (5.5 mL, 40 mmol) and 4-dimethylaminopyridine, DMAP (220 mg, 1.8 mmol) were dissolved in dichloromethane (100 mL). The resulting mixture was cooled at 0°C. Chloroacetyl chloride (3.2 mL, 40 mmol) was added dropwise. The reaction mixture was allowed to warm to room

temperate and stirred for 24 hours. A 10 % v/v hydrochloric acid solution was added and the mixture was extracted into ethyl acetate. The organic phase was dried and the solvent was removed at reduced pressure to yield a cream precipitate of *N*-(4-carboxyphenyl) chloroacetamide (7 g, 87%) with a melting point of 210 –215°C.

δ_H (Acetone, 300 MHz) 2.82 (2H, s, CH_2), 6.35 (2H, d, Ph), 6.50 (2H, d, Ph).

m/z (EI) $^{12}C_9{}^{1}H_8{}^{16}O_3{}^{14}N_1{}^{37}Cl_1$ requires 215.01632 measured 215.01467

_N_-(4-Carboxyphenyl) mercaptoacetamide

(*N*-(4-Carboxyphenyl) mercaptoacetamide was prepared by the adaptation of method Van Allen[7]).

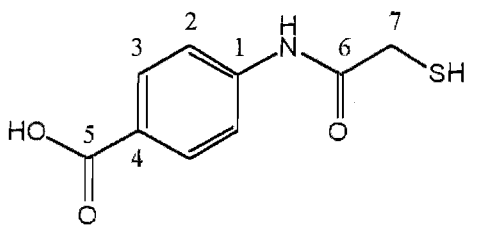

4-Aminobenzoic acid (5 g, 36 mmol) and mercaptoacetic acid (2.5 mL, 36 mmol) were mixed to form a slurry. The slurry was refluxed under an atmosphere of oxygen-free nitrogen for 2 hours. The reaction mixture was allowed to cool before being poured into water (100 mL). The white precipitate that formed was collected by filtration, and washed with 2 M hydrochloric acid and water. The precipitate was recrystallised from ethanol and water, to yield white needles of *N*-(4-carboxyphenyl) mercaptoacetamide (1.49 g, 19.4%), with a melting point of 215 -218°C.

δ_H (Acetonitrile, 300 MHz) 2.38 (1H, t, J = 8.30 Hz, SH), 3.38 (2H, d, J = 8.30 Hz, CH_2), 7.74 (2H, d, J = 8.79 Hz, Ph), 8.02 (2H, d, J = 8.79 Hz, Ph), 8.84 (1H, s, NH).

δ_C (Acetonitrile, 300 MHz) 35.47 (CH_2), 118.29 (Ph), 119.62 (Ph), 126.04 (Ph), 167.01 (CO), 167.27(CO).

δ_H (DMSO, 300 MHz) 3.00 (2H, s, CH_2), 7.69 (2H, d, J = 8.79 Hz, Ph), 7.89 (2H, d, J = 8.79 Hz, Ph), 10.39 (1H, s, NH).

m/z (EI) 211(M^+), 137, 120, 92, 65.

Di(*N*-(4-carboxyphenyl carbamoylmethyl)disulfide

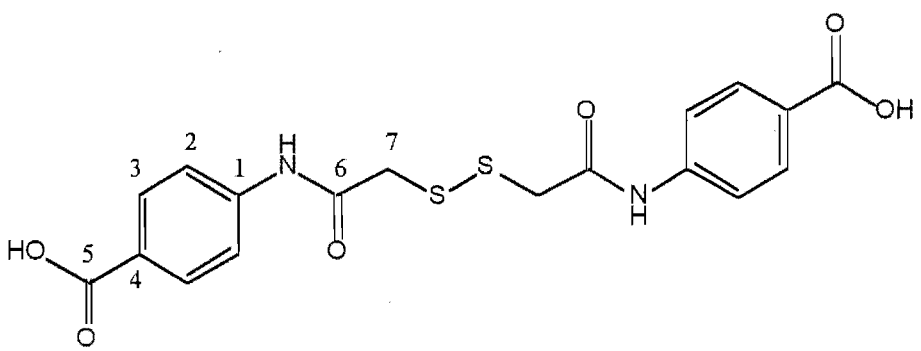

N-(4-Carboxyphenyl) mercaptoacetamide (300 mg, 1.42 mmol) was dissolved in hot ethanol (15 mL). Iodine (360 mg, 1.42 mmol) was added in small portions to the hot solution. The precipitate which formed was collected by filtration and washed with water. The white di(*N*-(4-carboxyphenyl carbamoylmethyl)disulfide precipitate (212 mg, 35.2%) decomposed at 255-260°C.

δ_H (DMSO, 300 MHz) 3.87 (2H, s, CH_2), 7.79 (2H, d, J = 8.30 Hz, Ph), 7.89 (2H, d, J = 8.30 Hz, Ph), 10.58 (1H, s, NH).

δ_C (DMSO, 300 MHz) 43.28 (C7), 118.68 (Ph), 125.60 (Ph), 130.56 (Ph), 142.87 (Ph), 167.00 (CO), 167.39 (CO).

HPLC solvent system used to separate 4-aminobenzoic acid, *N*-(4-carboxyphenyl) acetamide, *N*-(4-carboxyphenyl) mercaptoacetamide and di(*N*-(4-carboxyphenyl carbamoylmethyl)disulfide

A C_{18} column was used for HPLC separation of 4-aminobenzoic acid, *N*-(4-carboxyphenyl) acetamide, *N*-(4-carboxyphenyl) mercaptoacetamide and di-(*N*-(4-carboxyphenyl carbamoylmethyl)disulfide. The solvent gradient of water (TFA 0.05%) and acetonitrile (20-40% acetonitrile from 0–30 minutes) was used to elute the column.

Formation of *N*-(4-carboxyphenyl) acetamide from mercaptoacetic acid and 4-aminobenzoic acid

Oxygen-free nitrogen was bubbled through Milli-Q water for two hours. Three freeze-pump-thaw cycles were performed on this solution under an atmosphere of oxygen-free nitrogen. Mercaptoacetic acid was distilled under reduced pressure.

Sodium sulfide (480 mg, 2.0 mmol), ferrous sulfate (556 mg, 2.0 mmol) and a stirring bar were placed in a glass ampoule. The glass ampoule was sealed with a suba seal, evacuated with a high vacuum pump, and flushed with oxygen-free nitrogen. Mercaptoacetic acid (7 μl, 100 μmol) and 4-aminobenzoic acid (14 mg, 100 μmol) were added to the ampoule using a syringe. Degassed water (10 mL) was syringed into the

glass ampoule, and the pH adjusted using concentrated sulfuric acid, until only a small amount of black solid remained. The tube was frozen in liquid nitrogen and sealed. The sealed tube was placed in an aluminium tube as a safety precaution, with glass wool covering the ends and heated in an oil bath at 100°C for 5 days.

The tube was removed from the heating bath, and allowed to cool to room temperature before being frozen in liquid nitrogen, and opened. A portion of the reaction mixture was centrifuged and filtered. A sample of the supernatant (20 μL) was removed and loaded onto a C_{18} HPLC column. An acetonitrile and 0.05% TFA/water gradient solvent system was used to separate the products. The solvent system was 80% water (0.05% TFA) and 20% acetonitrile initially. Over 30 minutes the solvent system changed to 70% water (0.05% TFA) and 30% acetonitrile. The flow rate was 1 mL/min. Compounds were detected by monitoring the absorbance of the effluent at 254, 203 and 266 nm.

A peak was observed in the HPLC trace at an appropriate retention time for *N*-(4-carboxyphenyl) acetamide, and spiking with a solution of *N*-(4-carboxyphenyl) acetamide showed a corresponding increase in the size of the peak assigned to *N*-(4-carboxyphenyl) acetamide. Integration of this peak and analysis indicated that a yield of 0.5% of *N*-(4-carboxyphenyl) acetamide was achieved in this reaction.

Formation of *N*-(4-carboxyphenyl) acetamide from *N*-(4-carboxyphenyl) mercaptoacetamide

Oxygen-free nitrogen was bubbled through Milli-Q water for two hours. Three freeze-pump-thaw cycles were performed on this solution under an atmosphere of oxygen-free nitrogen.

Sodium sulfide (480 mg, 2 mmol), ferrous sulfate (556 mg, 2 mmol), *N*-(4-carboxyphenyl) mercaptoacetamide (21 mg, 100 μmol) and a stirring bar were placed in a glass ampoule. The glass ampoule was sealed with a suba seal, evacuated with a high vacuum pump and flushed with oxygen-free nitrogen. Degassed water (10 mL) was syringed into the glass ampoule and the pH adjusted using concentrated sulfuric acid, until only a small amount of black solid remained. The tube was frozen in liquid nitrogen and sealed. The seal tube was placed in an aluminium tube as a safety precaution, with glass wool covering the ends and heated in an oil bath at 100°C for 5 days.

The tube was removed from the heating bath, and allowed to cool to room temperature before being frozen in liquid nitrogen, and opened. A portion of the reaction mixture was centrifuged and filtered. A sample of the supernatant (20 μL) was removed and loaded onto a C_{18} HPLC column. An acetonitrile and water (0.05% TFA) gradient solvent system used to separate the products. The solvent system was 80% water (0.05% TFA) and 20% acetonitrile initially. Over 30 minutes the solvent system changed to 70% water (0.05% TFA) and 30% acetonitrile. The flow rate was 1

mL/min. Compounds were detected by monitoring the absorbance of the effluent at 254, 203 and 266 nm.

A peak was observed in the HPLC trace at an appropriate retention time for *N*-(4-carboxyphenyl) acetamide, and spiking with a solution of *N*-(4-carboxyphenyl) acetamide showed a corresponding increase in the size of the peak assigned to *N*-(4-carboxyphenyl) acetamide. Integration of this peak and analysis indicated that a yield of 6% of *N*-(4-carboxyphenyl) acetamide was achieved in this reaction.

Formation of *N*-(4-carboxyphenyl) acetamide from *N*-(4-carboxyphenyl) mercaptoacetamide (20°C or 40°C)

Two freeze-pump-thaw cycles were performed on Milli-Q water under an atmosphere of oxygen-free nitrogen.

Sodium sulfide (1.44 g, 6.0 mmol) and ferrous sulfate (1.65 g, 5.9 mmol) weighed into a flask equipped with a suba seal. A solution of degassed Milli-Q water and *N*-(4-carboxyphenyl) mercaptoacetamide (30 mg, 142 μmol) was added to the sealed flask. The pH of the resulting mixture was 6-6.5. The black slurry was stirred at 20 or 40°C with 1 mL samples withdrawn at 30, 60, 90, 120, 150, 180, 210 and 240 minutes. Each sample was centrifuged and filtered before 20 μL was loaded onto the C_{18} HPLC column. An acetonitrile and 0.05% TFA/water gradient solvent system used to separate the products. The solvent system was 80% water (0.05% TFA) and 20% acetonitrile initially. Over 30 minutes the solvent system changed to 70% water (0.05% TFA) and

30% acetonitrile. The flow rate was 1 mL/min. Compounds were detected by monitoring the absorbance of the effluent at 254, 203 and 266 nm.

A peak was observed in the HPLC trace at an appropriate retention time for *N*-(4-carboxyphenyl) acetamide, and spiking with a solution of *N*-(4-carboxyphenyl) acetamide showed a corresponding increase in the size of the peak assigned to *N*-(4-carboxyphenyl) acetamide.

Time @ 20°C (mins)	% Yield *N*-(4-carboxyphenyl) mercaptoacetamide	% Yield *N*-(4-carboxyphenyl) acetamide
30	0	81
60	0	99
90	0	79
120	0	80
150	0	84
180	0	78

Time @ 40°C (mins)	% Yield *N*-(4-carboxyphenyl) mercaptoacetamide	% Yield *N*-(4-carboxyphenyl) acetamide
30	0	69
60	0	63
90	0	53
120	0	58
150	0	69
180	0	71

Two control reactions were performed, one contained ferrous ions and the other contained sulfide ions these samples were heated at 20 or 40°C for 180 minutes. No peak was observed in the HPLC trace at a retention time consistent with *N*-(4-carboxyphenyl) acetamide.

5.3.3 Experimental references for chapter three

1 A. H. Blatt, *Organic Synthesis Collective Volume Two*, Wiley (1943).

2 E. Blochl, M. Keller, G. Wächtershäuser & K. O. Stetter, *Pro. Natl. Acad. Sci.* USA, **89**, 8117 (1992).

3 G. G. Stoner & G. Dougherty, *J. Am. Chem. Soc.*, **63**, 987 (1941).

4 A. I. Vogel & B. S. Furniss, *Textbook of practical organic chemistry*, Wiley (1989).

5 L. M. Harwood & C. J. Moody, *Experimental Organic Chemistry: principles and practise*, Blackwell Scientific Publications, 486 (1989).

6 T. C. Owen, J. M. Fayadh & J. S. Chen, *J. Org. Chem.*, **38**, 937 (1973).

7 J. A. Van Allen, *J. Am. Chem.Soc.*, **69**, 2914 (1947).

8 M. Keller, E. Blochl, G. Wächtershäuser & K. O. Stetter, *Nature*, **368**, 836 (1994).

9 *Aldrich Catalogue Handbook of Fine Chemicals* (1996).

5.4 Chapter Four - Experimental

5.4.1 Experimental from 4.2

Formation of *N*-acetyl glycine from thioacetic acid and glycine

A solution containing thioacetic acid (0.05 M) and glycine (0.025 M) in deuterium oxide (300 μL) was prepared. The pH was adjusted to 6-7 using 2 M sodium hydroxide. The solution was heated at 50°C in a thermostated water bath. Solvent suppressed ^{1}H NMR spectra were run at 24, 48 and 72 hours and signals integrated at each time. ^{1}H NMR samples were spiked with *N*-acetyl glycine to check assignment of peaks.

δ_H (D_2O, 300mHz) 1.89 (CH_3), 3.82 (CH).

Time hrs	% Yield glycine	% Yield *N*-acetyl glycine
24	83	17
48	65	35
72	50	50

Large scale reaction of thioacetic acid and glycine

A solution containing thioacetic acid (0.05 M) and glycine (0.025 M) in water (600 μL) was prepared. The pH was adjusted to 6-7 using 2 M sodium hydroxide. The solution was heated in a thermostated water bath at 50°C for 12 days. The pH of the solution after reaction was 4.5-5. The reaction mixture was acidified using 2 M hydrochloric acid and extracted with 2 x 2 mL ethyl acetate. The organic phase was dried with magnesium sulfate and the solvent removed under reduced pressure. The white precipitate (1.8 mg) was submitted for mass spectrometry.

m/z (EI)117 (M^+), 99 & 72.

Formation of *N*-acetyl glycine from thioacetic acid, glycine and ferrous ions

A solution containing thioacetic acid (0.05 M), glycine (0.025 M) and ferrous chloride (0.125 M) in deuterium oxide (300 μL) was prepared. Oxygen free nitrogen was bubbled through the solution for 30 seconds and the pH was adjusted to 6-7 using 2 M sodium hydroxide. The solution was heated at 50°C in a thermostated water bath. Rust was observed in all samples. The pH after incubation was 3. After heating for the appropriate time interval, 20-30 mg potassium cyanide was added to the reaction mixture. The solution was thoroughly mixed using a vortex mixer. After centrifuging the mixture to remove the ferrocyanide, a solvent suppressed ^{1}H NMR spectrum was run

on the orange solution and the signals integrated. ^{1}H NMR samples were spiked with *N*-acetyl glycine to check assignment of peaks.

Time hrs	% Yield glycine	% Yield *N*-acetyl glycine
24	14	86
48	8	92
72	8	92

_N_-acetyl-_D,L_-alanine

(*N*-acetyl-*L*-alanine was prepared adapting the general acetylation method described in Organic Synthesis Collective Volumes Two[1]).

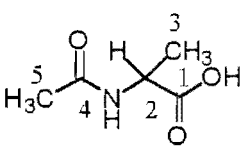

D,L-Alanine (8.9 g, 100 mmol) was dissolved in 60 mL hot water and allowed to cool to room temperature. Freshly distilled acetic anhydride (18.2 mL, 193 mmol) was added dropwise to the solution and the resulting reaction mixture was stirred for 15 minutes. The solution was acidified with 2 M hydrochloric acid and extracted with ethyl acetate (2 x 100 mL). The ethyl acetate was dried using magnesium sulfate before the solvent was removed under reduced pressure to yield an oil. After standing overnight the oil crystallised and any remaining solvent or acetic acid was removed under reduced pressure to yield white crystalline *N*-acetyl-*D,L*-alanine (7.91g, 60.37%).

δ_H (D_2O/methanol, 300 MHz) 1.40 (3H, d, CH_3), 2.00 (3H, s, $COCH_3$), 4.32 (1 H, q, CH).

δ_C (D_2O/methanol, 300 MHz) 17.35 (CH_3), 22.17 (CH_3), 39.58 (C2), 174.43 (CO), 177.26 (CO).

m/z (EI) 131(M^+), 86, 74 & 44.

Formation of *N*-acetyl-D,*L*-alanine from thioacetic acid and *D,L*-alanine

A solution containing thioacetic acid (0.05 M) and *D,L*-alanine (0.025 M) in deuterium oxide (300 μL) was prepared. The pH was adjusted to 7 using 2 M sodium hydroxide. The solution was heated at 50°C in a thermostatted water bath. Solvent suppressed ^1H NMR spectra were run at 24, 48 and 72 hours and signals integrated at each time. ^1H NMR samples were spiked with *N*-acetyl-*D,L*-alanine to check assignment of peaks.

Time hrs	% Yield *D,L*-alanine	% Yield *N*-acetyl-*D,L*-alanine
24	100	0
48	89	11
72	70	30

Large scale reaction of thioacetic acid and *D,L*-alanine

A solution containing 0.05 M thioacetic acid and 0.025 M *D,L*-alanine in water (600 μL) was prepared. The pH was adjusted to 6-7 using 2 M sodium hydroxide. The solution

was heated in a thermostated water bath at 50°C for 12 days. The pH of the solution after reaction was 6. The reaction mixture was acidified using 2 M hydrochloric acid and extracted with 2 x 2 mL ethyl acetate. The organic phase was dried with magnesium sulfate and the solvent removed under reduced pressure. The white precipitate was submitted for mass spectrometry.

m/z (EI) 131(M^+), 86 & 74.

Formation of *N*-acetyl-*D,L*-alanine from thioacetic acid, *D,L*-alanine and ferrous ions

A solution containing thioacetic acid (0.05 M), *D,L*-alanine (0.025 M) and ferrous chloride (0.125 M) in deuterium oxide (300 μL) was prepared. Oxygen free nitrogen was bubbled through the solution for 30 seconds and the pH was adjusted to 6-7 using 2 M sodium hydroxide. The solution was heated at 50°C in a thermostated water bath. After heating for the appropriate time interval 20-30 mg potassium cyanide was added to the reaction mixture. The solution was thoroughly mixed using a vortex mixer. After centrifuging the mixture to separate any precipitate, a solvent suppressed ^{1}H NMR spectrum was run on the orange supernatant solution and the signals integrated. ^{1}H NMR samples were spiked with *N*-acetyl-*D,L*-alanine to check assignment of peaks.

Time hrs	% Yield *D,L*-alanine	% Yield *N*-acetyl-*D,L*-alanine
3	70	30
24	57	43
48	55	45

_N,S_-Diacetyl-_L_-cysteine

(*N,S*-Diacetyl-*L*-cysteine was prepared according to the method of Smith & Gorin[2,3]).

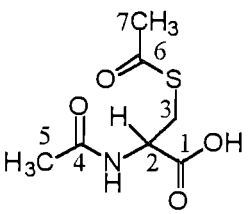

L-Cysteine hydrochloride (1g, 6 mmol) and sodium hydroxide (0.71g, 8 mmol) were dissolved in water (4 mL) at 0°C. Acetic anhydride (1.07 mL, 11 mmol) was added dropwise and the solution was allowed to warm to room temperature. The reaction mixture was acidified with 2 M hydrochloric acid and extracted with ethyl acetate (3 x 50 mL). The organic layer was dried with magnesium sulfate before the solvent was removed at reduced pressure to yield a colourless oil. The oil was dissolved in hot ethyl acetate (5 mL) yielded white crystals of *N,S*-diacetyl-*L*-cysteine (710 mg, 60.87%) upon standing.

δ_H (D_2O, 300 MHz) 1.83 (3H, s, CH_3CON), 2.20 (3H, s, CH_3COS), 3.06 (1H, m, CHH'), 3.28 (1H, m, CHH'), 4.45 (1H, t, J=4.9 Hz, CH).

δ_C (D_2O, 300 MHz) 23.72 (C2), 31.93 (C3), 54.39 (C5), 175.58 (C1/4), 176.32 (C1/4), 202.05 (C6).

m/z (FAB) 206 (MH^+), 164, 137.

m/z $^{12}C_7{}^1H_{12}{}^{16}O_4{}^{14}N_1$ requires 206.04871 measured 206.04876.

Reaction of *L*-cysteine and thioacetic acid

A solution containing thioacetic acid (0.05 M) and *L*-cysteine (0.025 M) in deuterium oxide (300 μL) was prepared. Oxygen free nitrogen was bubbled through the solution for 30 seconds and the pH was adjusted to 6-7 using 2 M sodium hydroxide. The solution was heated at 50°C in a thermostated water bath. After heating for the appropriate time interval a solvent suppressed ^1H NMR spectrum was obtained from the solution and the signals integrated. The yield of *N*-acetyl-*L*-cysteine and *N,S*-diacetyl-*L*-cysteine were calculated from the ratio of the α-proton multiplet of cysteine to the corresponding resonances for the acetylated compounds.

Time (hrs)	% Yield *L*-cysteine	% Yield *N*-acetyl-*L*-cysteine	% Yield *N,S*-diacetyl-*L*-cysteine
24	37	63	0
48	17	83	0
72	0	100	0

Reaction of *L*-cysteine, thioacetic acid and ferrous ions

A solution containing thioacetic acid (0.05 M), *L*-cysteine (0.025 M) and ferrous chloride (0.125 M) in deuterium oxide (300 μL) was prepared. Oxygen free nitrogen was bubbled through the solution for 30 seconds and the pH was adjusted to 6-7 using 2 M sodium hydroxide. The solution was heated at 50°C in a thermostated water bath. Potassium cyanide (20-30 mg) was added to the reaction mixture after heating for the appropriate time interval. The solution was thoroughly mixed using a vortex mixer. After centrifuging the mixture to remove any precipitate, a solvent suppressed ^{1}H NMR spectrum was obtained from the orange solution and the signals were integrated. The yield of *N*-acetyl-*L*-cysteine and *N,S*-diacetyl-*L*-cysteine were calculated from the ratio of the α-proton multiplet of cysteine to the corresponding resonances in the acetylated derivatives.

Time (hrs)	% Yield *L*-cysteine	% Yield *N*-acetyl-*L*-cysteine	% Yield *N,S*-diacetyl-*L*-cysteine
24	49	25	26
48	56	22	22
72	43	33	24

Formation of *N,S*-diacetyl-*L*-cysteine from *N*-acetyl-*L*-cysteine and thioacetic acid

A solution containing thioacetic acid (0.05 M) and *N*-acetyl-*L*-cysteine (0.025 M) in deuterium oxide (300 μL) was prepared. The pH was adjusted using 2M sodium

hydroxide to 6–7. The reaction mixtures were heated at 50°C for 24, 48 and 72 hours. After heating for the appropriate time interval a solvent suppressed ^{1}H NMR spectrum was run on the solution and the signals were integrated. The yield of *N*-acetyl-*L*-cysteine and *N,S*-diacetyl-*L*-cysteine were calculated from the ratio of the α-proton multiplet of cysteine to the corresponding resonances of the acetylated derivatives.

Time hrs	% Yield *N*-acetyl-*L*-cysteine	% Yield *N,S*-diacetyl-*L*-cysteine
3	85	15
24	78	22
48	73	27

5.4.2 Experimental from 4.3

Formation of *N*-acetyl-*D,L*-alanine from thioacetic acid & *D,L*-alanine at pH = 6.1, 6.5 and 7.5

Solutions of PIPES buffers (1 M) were prepared in deuterium oxide and the pH was adjusted to 6.1 and 6.5 respectively, using 2 M sodium hydroxide in deuterium oxide. A HEPES buffer (1 M) solution was prepared with a pH of 7.5. These buffer solutions underwent 2 freeze-pump-thaw cycles under an atmosphere of oxygen free nitrogen. Solutions of *L*-alanine and thioacetic acid in buffer were prepared and added to the vials. The resulting reaction mixture contained *D,L*-alanine (0.025 M) and thioacetic acid (0.05

M). The vials were flushed with oxygen free nitrogen and capped. The colourless reaction mixtures were heated at 40°C for 3, 24 and 48 hours. After 3, 24 and 48 hours the reaction mixtures were centrifuged and analysed by ^{1}H NMR spectroscopy. The spectra were referenced to 3-(trimethylsiyl)-1-propanesulfonic acid sodium salt hydrate.

pH	Time (hours)	% Yield *N*-acetyl-*D,L*-alanine
6.1	3	7
6.1	24	13
6.1	48	20
6.5	3	13
6.5	24	51
6.5	48	84
7.5	3	8
7.5	24	35
7.5	48	57

Formation of *N*-acetyl-*D,L*-alanine from mixtures of thioacetic acid, *D,L*-alanine and ferrous ions at pH = 6.1, 6.5 and 7.5

Solutions of PIPES buffers (1 M) were prepared in deuterium oxide and the pH was adjusted to 6.1 and 6.5 respectively, using 2 M sodium hydroxide in deuterium oxide. A HEPES buffer (1 M) solution was prepared with a pH of 7.5. These solutions underwent 2 freeze-pump-thaw cycles under an atmosphere of oxygen free nitrogen. Ferrous chloride (668 μg, 37.5 μmol) was weighed into 1 mL Wheaton vials. Solutions of *L*-alanine and thioacetic acid in the appropriate buffer were prepared and added to the

vials. The resulting reaction mixture contained ferrous chloride (0.125 M), *D,L*-alanine (0.025 M) and thioacetic acid (0.05 M). The vials were flushed with oxygen free nitrogen and capped. The reaction mixtures were heated at 40°C. After 3, 24 and 48 hours the reaction mixtures were grey and heterogenous with a small amount of rust. The pH was unchanged. Potassium cyanide (30 mg) was added to the reaction vials and after mixing they were centrifuged and analysed by ^{1}H NMR spectroscopy. The spectra were referenced to 3-(trimethylsiyl)-1-propanesulfonic acid sodium salt hydrate.

pH	Time (hours)	% Yield *N*-acetyl-*D,L*-alanine
6.1	3	35
6.1	24	50
6.1	48	61
6.5	3	41
6.5	24	85
6.5	48	100
7.5	3	12
7.5	24	26
7.5	48	39

Formation of *N*-acetyl-*D,L*-alanine from mixtures of thioacetic acid, *D,L*-alanine and ferrous ions at pH = 6.1, 6.5, 7.0 and 7.5

Solutions of PIPES buffers (1 M) were prepared in deuterium oxide and the pH was adjusted to 6.1 and 6.5 respectively, using 2 M sodium hydroxide in deuterium oxide. A HEPES buffer (1 M) solution was prepared with a pH of 7.5. These solutions

underwent two freeze-pump-thaw cycles under an atmosphere of oxygen free nitrogen. Ferrous chloride (668 μg, 37.5 μmol) was weighed into 1 mL Wheaton vials. The control reaction contained no ferrous ions. Solutions of *D,L*-alanine and thioacetic acid in the appropriate buffer were prepared and added to the vials. The resulting reaction mixture contained ferrous chloride (0.125 M), *D,L*-alanine (0.025 M) and thioacetic acid (0.05 M). The vials were flushed with oxygen free nitrogen and capped. The reaction mixtures were heated at 40°C for 18 hours. Potassium cyanide (30 mg) was added to the reaction vials that contained ferrous ions and after mixing they were centrifuged and analysed by ^{1}H NMR spectroscopy. The spectra were referenced to 3-(trimethylsiyl)-1-propanesulfonic acid sodium salt hydrate.

pH	Control % Yield *N*-acetyl-*D,L*-alanine	Ferrous ions % Yield *N*-acetyl-*D,L*-alanine
6.1	9	40
6.5	33	57
7.0	22	64
7.5	11	11

Investigation of the workup procedure of reactions containing thioacetic acid, *D,L*-alanine and ferrous ions.

Reactions containing thioacetic acid (0.05 M) and *D,L*-alanine (0.25 M) in deuterium oxide (300μL) were heated for 3 hours at 40°C at pH 6.5. After the reaction time ferrous ions (0.125 M) and then potassium cyanide (20-30 mg) were added to one series

of reaction mixtures. Another series of samples had potassium ferrocyanide (0.125 M) added after heating. The third series were controls to which no ferrous ions were added. The reaction mixtures were then analysed by ^{1}H NMR spectroscopy.

	% Yield *N*-acetyl-*D,L*-alanine
Control	10
Ferrous ions + cyanide ions	12
Ferrocyanide ions	12

Formation of *N*-acetyl-*D,L*-alanine from thioacetic acid and *D,L*-alanine in the presence of ferrous ions or ferrocyanide ions

A 1 M solution of buffers (PIPES or HEPES) were prepared in deuterium oxide and the pH was adjusted to the desired value, using 2 M sodium hydroxide in deuterium oxide (PIPES buffer for pH = 6.5 and HEPES buffer for pH = 7.0 and 7.5). These solutions underwent two freeze-pump-thaw cycles under an atmosphere of oxygen free nitrogen. Ferrous chloride (7.5 mg, 37.5 μmol) was weighed into 1 mL Wheaton vials. Potassium ferrocyanide (15.8 mg, 37.5 μmol) was weighed into another series of Wheaton vials. The control reaction contained no ferrous ions. Solutions of *D,L*-alanine and thioacetic acid in the appropriate buffer were prepared and added to the vials. The vials were flushed with oxygen free nitrogen and capped. The reaction mixtures were heated at 40°C for 18 hours. Potassium cyanide (30 mg) was added to the reaction vials that contained ferrous ions and after mixing they were centrifuged. All samples were

analysed by ^{1}H NMR spectroscopy. The spectra were referenced to 3-(trimethylsiyl)-1-propanesulfonic acid sodium salt hydrate.

	% Yield *N*-acetyl-*D,L*-alanine		
	pH = 6.5	pH = 7.0	pH = 7.5
Control	32	22	11
Ferrous ions	57	64	11
Ferrocyanide ions	16	12	12

Reaction of thioacetic acid and *D,L*-alanine in the presence of zinc or cadmium ions

1 M solutions of PIPES buffers were prepared in deuterium oxide and the pHs were adjusted to the desired values, using 2 M sodium hydroxide in deuterium oxide. These solutions underwent two freeze-pump-thaw cycles under an atmosphere of oxygen free nitrogen. Zinc chloride (0.125 M) or cadmium fluoride (0.125 M) were weighed into 1 mL Wheaton vials. The control reactions contained no metal ions. Solutions of *D,L*-alanine (0.025 M) and thioacetic acid (0.05 M) in the appropriate buffer were prepared and added to the vials (300 μl). The vials were flushed with oxygen free nitrogen and capped. The reaction mixtures were heated at 40°C for 18 hours. All samples were analysed by ^{1}H NMR spectroscopy.

	% Yield *N*-acetyl-*D,L*-alanine		
	pH = 6.5	pH = 7.0	pH = 7.5
Control	33	22	11
Zinc ions	4	3	3
Cadmium ions	11	10	8

Reaction of HEPES buffer in the presence of zinc chloride and thioacetic acid

A HEPES buffer (1 M) solution was prepared in distilled water with a pH=7.5. Thioacetic acid (0.05 M) and zinc chloride (0.1 M) were added to the HEPES buffer (50 mL). The resulting reaction mixture was heated at 40°C for 24 hours. The solvent was removed at reduced pressure. The white residue was analysed by ^{1}H NMR spectroscopy and mass spectrometry.

δ_H (D_2O, 300 MHz) 1.92 (s, CH_3CO-HEPES), 2.12 (s, CH_3COOH), 2.9-3.01(m), 3.14-3.26 (m), 3.33 (bs), 3.89 (dd).

m/z (EI) $C_{10}H_{21}O_5N_2S$ requires 281.1112 measured 281.11804

Reaction of thioacetic acid and *D,L*-alanine methyl ester in the presence of zinc, cadmium, ferrocyanide or ferrous ions

1 M solutions of PIPES buffers were prepared in deuterium oxide and the pH was adjusted to the desired values, using 2 M sodium hydroxide in deuterium oxide. These solutions underwent two freeze-pump-thaw cycles under an atmosphere of oxygen free

nitrogen. Zinc chloride (0.125 M) or cadmium fluoride (0.125 M) or potassium ferrocyanide (0.125 M) or ferrous chloride (0.125 M) were weighed into 1 mL Wheaton vials. The control reactions contained no metal ions. Solutions of *D,L*-alanine methyl ester (0.025 M) and thioacetic acid (0.05 M) in the appropriate buffer were prepared and added to the vials (300 μl). The vials were flushed with oxygen free nitrogen and capped. The reaction mixtures were heated at 40°C for 18 hours. Samples that contained ferrous ions were treated with potassium cyanide (20–30 mg) before analysis. All samples were analysed by ^{1}H NMR spectroscopy.

pH=6.5	*D,L*-alanine methyl ester	*D,L*-alanine	*N*-acetyl-*D,L*-alanine methyl ester	*N*-acetyl-*D,L*-alanine
Control	68	9	24	0
Zn^{2+}	8	87	5	0
Cd^{2+}	57	29	14	0
Fe^{2+}	12	80	8	0
$Fe(CN)_6^{4-}$	74	8	18	0

pH=6.5	Thioacetic acid	Acetic acid
Control	89	3
Zn^{2+}	85	13
Cd^{2+}	61	34
Fe^{2+}	trace	
$Fe(CN)_6^{4-}$	86	3

Reaction of thioacetic acid and *D,L*-alanine in the presence of ferrous sulfide

1 M solutions of PIPES buffers were prepared in deuterium oxide and the pH was adjusted to the desired values, using 2 M sodium hydroxide in deuterium oxide. These solutions underwent two freeze-pump-thaw cycles under an atmosphere of oxygen free nitrogen. Ferrous chloride (0.1 M) and sodium sulfide (0.1 M) were weighed into 1 mL Wheaton vials. The control reactions contained no ferrous sulfide. Solutions of *D, L*-alanine (0.025 M) and thioacetic acid (0.05 M) in the appropriate buffer were prepared and added to the vials (300 µl). The vials were flushed with oxygen free nitrogen and capped. The reaction mixtures were heated at 40°C for 18 hours. Samples that contained ferrous sulfide were treated with potassium cyanide (20–30 mg) and centrifuged before analysis. All samples were analysed by ^{1}H NMR spectroscopy.

	% Yield *N*-acetyl-*D,L*-alanine @ pH = 6.1	% Yield *N*-acetyl-*D,L*-alanine @ pH = 6.5
Control	13	29
FeS	37	36

5.4.3 Experimental from 4.4

_N_-(Benzyloxycarbonyl)-_D,L_-alanine

(_N_-(Benzyloxycarbonyl)-_D,L_-alanine was synthesised by the general method outlined by Bodanszky & Bodanszky[4]).

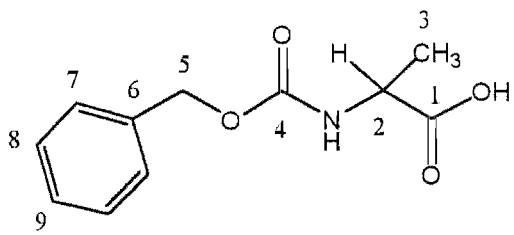

_D,L_ Alanine (6 g, 67 mmol) was dissolved in 2 M sodium hydroxide (40 mL). The solution was stirred and cooled in an ice bath. Benzyl chloroformate (10.58 mL, 74 mmol) and 2 M sodium hydroxide (40 mL) were added alternately, in small portions. The temperature was maintained between 5-10°C by limiting the rate of addition of the reactants and the pH was kept above 7 by addition of sodium hydroxide. The reaction mixture was stirred at room temperature for a further 1 hour after addition of the reactants was complete. The solution was extracted with ether (4 x 50 mL). The aqueous layer was acidified with 2 M hydrochloric acid until the pH was less than 3 and a white precipitate had formed. The reaction mixture was extracted with ether (4 x 100 mL). The organic layer was dried with magnesium sulfate and filtered. The solvent was removed at reduced pressure to yield a white precipitate. The white solid was recrystallised from ethyl acetate and pet ether to yield white plates (2.88 g, 19.2%) with a melting point of 110-115°C.

δ_H ($CDCl_3$, 300 MHz) 1.46 (3H, d, J = 7.33 Hz, CH_3), 4.41 (1H, m, CH), 5.12 (2H, s, CH_2), 5.34 (1H, d, J = 6.84 Hz, NH), 7.33 (5H, m, Ph).

δ_C ($CDCl_3$, 300 MHz) 18.36 (C3), 49.44 (C2), 67.14 (C5), 128.13 (Ph), 128.25 (Ph), 128.56 (Ph), 155.83 (C4), 177.68 (C1).

m/z (EI) 223(M^+), 108, 107, 91, 79, 65.

_N_-Hydroxysuccinimide

(_N_-Hydroxysuccinimide was prepared by the method of Anderson *et al*[5]).

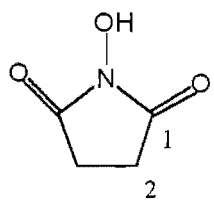

Succinic anhydride (40 g, 400 mmol) and hydroxylamine hydrochloride (28 g, 403 mmol) were mixed in a 500 mL round-bottomed flask. The flask was heated in an oil bath at 125°C while on a rotary evaporator. Fusion occurred with the evolution of gas. The resulting oil was heated to 160°C over the next hour. The reaction mixture was removed from the oil bath and allowed to cool, before ether (160 mL) was added. After vigorous stirring an amber solid was produced and the ether was decanted off. Dry 1-butanol (160 mL) was added and heated to boiling. The hot mixture was filtered and the filtrate was cooled in ice. The cream precipitate was recrystallised from ethyl acetate to yield white crystals (6.67g, 14.5%) with a melting point of 96-99°C. The _N_-hydroxysuccinimide was stored in a desiccator over phosphorous pentoxide.

δ_H (DMSO, 300 MHz) 2.6 (4H, s, CH_2), 10.56 (1H, s, OH).

_N_-hydroxysuccinimide ester of _N_-(benzyloxycarbonyl)-_D,L_-alanine

(_N_-hydroxysuccinimide ester of _N_-(benzyloxycarbonyl)-_D,L_-alanine was prepared by the method of Anderson *et al* [5]).

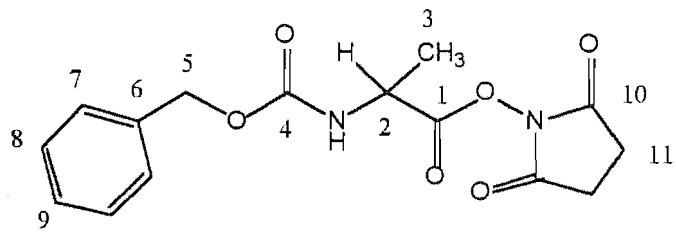

A solution of _N_-(benzyloxycarbonyl)-_D,L_-alanine (2 g, 9 mmol) and _N_-hydroxysuccinimide (1.03 g, 9 mmol) in 1,4-dioxane (20 mL) was prepared. This solution was vigorously stirred at 50°C. _N,N_-Dicyclohexylcarbodiimide (1.85 g, 9 mmol) was added and the resulting mixture was allowed to warm to room temperature and stirred overnight. The reaction mixture was filtered and the solid was washed with 1,4-dioxane. The solvent was removed at reduced pressure to yield a colourless oil. The oil was extracted with ether. Any residual ether was removed at reduced pressure. The oil was dissolved in the minimum amount of hot isopropyl alcohol and cooled in ice. The white precipitate (1.15 g, 40.0%) that formed was isolated by filtration.

δ_H ($CDCl_3$, 300 MHz) 1.58 (3H, d, J = 7.33 Hz, CH_3), 2.80 (4H, s, $2CH_2$), 4.76 (1H, m, CH), 5.12 (2H, s, CH_2), 5.53 (1H, d, J = 7.81 Hz), 7.34 (5H, m, Ph).

δ_C ($CDCl_3$, 300 MHz) 18.45 (C3), 33.81 (C5), 47.99 (C2), 67.15 (C11), 128.10-128.46 (Ph), 155.28 (C4), 168.65 (C1/C10), 168.69 (C1/C10).

_N_-(Benzyloxycarbonyl)-_D,L_-thioalanine

(_N_-(Benzyloxycarbonyl)-_D,L_-thioalanine was synthesised according to the method Mitin *et al*[6]).

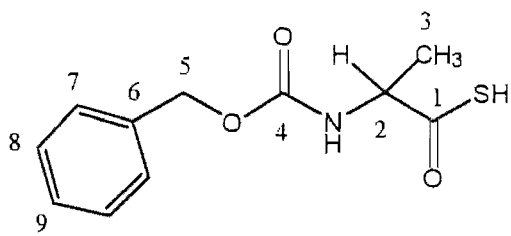

A solution of _N_-(benzyloxycarbonyl)-_D,L_-alanine _N_-hydroxysuccinimide ester (804 mg, 2.5 mmol) in DMF (5 mL) was cooled at 0°C. Lithium sulfide (230 mg, 5.0 mmol) was mixed with DMF (2.5 mL). The blue suspension was added to the _N_-hydroxysuccinimide ester solution and stirred for 1 hour. The yellow solution was acidified with hydrochloric acid (0.36 M) to yield a white precipitate. The heterogenous mixture was extracted with ethyl acetate (2 x 50 mL). The organic layer was washed with water (2 x 50 mL) and dried with magnesium sulfate. The magnesium sulfate was removed by filtration and the solvent was removed at reduced pressure to yield a pale yellow oil. The oil was repeatedly extracted with hot pet ether. The pet ether solution was cooled in ice and the resulting crystals were isolated by filtration. The white plates (208 mg, 34.8%) were dried at room temperature.

δ_H ($CDCl_3$, 300 MHz) 1.42 (3H, d, CH_3), 4.44 (1H, t, CH), 5.15 (2H, s, CH_2), 7.34–7.37 (5H, m, Ph).

δ_C ($CDCl_3$, 300 MHz) 18.18 (C3), 57.58 (C2), 67.35 (C5), 128.16 (Ph), 128.32 (Ph), 128.57 (Ph), 155.54 (C4), 200.00 (C1).

m/z (FAB) $^{12}C_{11}{}^{1}H_{14}{}^{14}N_1{}^{16}O_3{}^{32}S_1$ requires 240.06942 measured 240.06941

Elemental analysis C 55.24%, H 5.72%, N 5.94%, S 13.09%, Other 20.01% consistent with $^{12}C_{11}{}^{1}H_{14}{}^{14}N_1{}^{16}O_3{}^{32}S_1$.

Potassium *N*-(benzyloxycarbonyl)-*D,L*-thioalanine

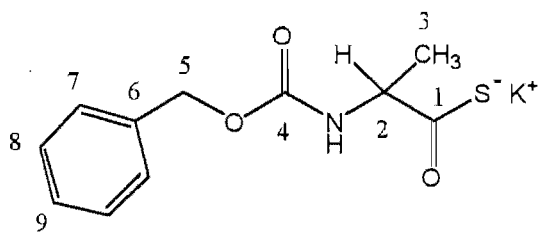

N-(Benzyloxycarbonyl)-*D,L*-thioalanine (183.5 mg, 768 μmol) was added to water (4 mL). Potassium hydroxide (1 M) was added dropwise until the pH was 6.5. The resulting mixture was filtered and the solvent was removed by freeze-drying. The white residue was recrystallised from ethyl acetate and pet ether to yield a white precipitate of potassium *N*-(benzyloxycarbonyl)-*D,L*-thioalanine(155.5 mg, 73.1%) with a melting point of 109-114°C.

δ_H (D_2O, 300 MHz) 1.22 (3H, d, CH_3), 4.13 (1H, t, CH), 4.99 (2H, s, CH_2), 7.30 (5H, m, Ph).

_L_-Alanine methyl ester

(_L_-Alanine methyl ester was prepared by the general method outlined by Bodanszky & Bodanszky[4]).

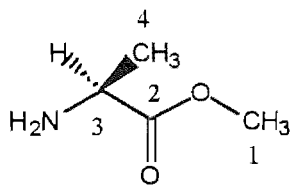

_L_-Alanine (1 g, 11 mmol) was dissolved in methanol (10 mL) and cooled at 0°C. Thionyl chloride (1.14 mL, 16 mmol) was added dropwise and the resulting solution was allowed to warm to room temperature and stirred for 48 hours. The solvent was removed at reduced pressure to yield a colourless oil that crystallised upon standing at room temperature. The needle like crystals were recrystallised from methanol and ether to yield _L_-Alanine methyl ester hydrochloride (1.26 g, 80.84%) with a melting point of 105-107°C.

δ_H (D_2O, 300 MHz) 1.31 (3H, d, CH_3), 3.59 (3H, s, OCH_3), 3.95 (1H, q, CH).

Trial extraction of potassium _N_-(benzyloxycarbonyl)-_D,L_-thioalanine, _L_-alanine methyl ester and _N_-(benzyloxycarbonyl)-_D,L_-alanyl-_L_-alanine methyl ester.

A solution of potassium _N_-(benzyloxycarbonyl)-_D,L_ -thioalanine (4.2 mg, 15.2 μmol), _L_-alanine methyl ester (1 mg, 7.2 μmol) and _N_-(benzyloxycarbonyl)-_D,L_-alanyl-_L_-alanine methyl ester (1 mg, 3.2 μmol) in deuterium oxide (300 μL) was prepared. The pH was

adjusted to 10 with sodium hydroxide and the solution was extracted with deuterated chloroform (300 μL). Both phases were analysed by ^{1}H NMR spectroscopy. The aqueous phase was adjusted to pH 1 with hydrochloric acid and extracted with deuterated chloroform. Analysed of these organic and aqueous phases was performed by ^{1}H NMR spectroscopy.

Potassium *N*-(benzyloxycarbonyl)-*D,L*-thioalanine and *L*-alanine methyl ester in the presence and absence of ferrous ions, ferrocyanide and ferrous sulfide at pH=6.5

Milli-Q water was degassed by under going two freeze-pump-thaw cycles under an atmosphere of oxygen-free nitrogen. Solutions of potassium *N*-(benzyloxycarbonyl)-*D,L*-thioalanine (0.025 M) and *L*-alanine methyl ester (0.025 M) were prepared in Wheaton vials. Ferrous ions, ferrocyanide ions or ferrous sulfide (0.125 M) were added as appropriate. The reaction mixtures were heated at 40°C for 18 hours. The reactions containing ferrous ions and ferrous sulfide were treated with cyanide before analysis by HPLC. The samples were centrifuged and filtered before loading (10 μL) on a C_{18} column. The solvent system was 25 % acetonitrile and 75 % water (0.05 % TFA) for 45 minutes.

	% Yield *N*-Z-*D,L*-thioalanine	% Yield *N*-Z-*D,L*-alanine	% Yield *N*-Z-*D,L*-alanyl-*L*-alanine methyl ester	% Yield *N*-Z-*D,L*-alanyl-*L*-alanine
Control	80	11	2	-
Fe^{2+}	12	28	26	1
$Fe(CN)_6^{4-}$	48	17	18	-
FeS	29	7	9	-

5.4.4 Experimental references for chapter four

1 A. H. Blatt, *Organic Synthesis Collective Volume Two*, Wiley (1943).

2 J. P. Greenstein & M. Winitz, *Chemistry of the amino acids*, Wiley (1961).

3 H. A. Smith & G. Gorin, *J. Org. Chem.*, **26**, 820 (1961).

4 M. Bodanszky & A. Bodanszky, *The Practise of Peptide Synthesis*, Springer-Verlag (1984).

5 G. W. Anderson, J. E. Zimmerman & F. M. Callaham, *J. Am. Chem. Soc.*, **86**, 1839 (1964).

6 Y. V. Mitin & N. P. Zapevalova, *Int. J. Peptide Protein Res.*, **35**, 352 (1990).